องค์ประกอบทางเคมีและฤทธิ์ทางชีวภาพของใบและลำต้นสังหยูหอม

นายวงศ์วริศ พาณิชธนานนท์

วิทยานิพนธ์นี้เป็นส่วนหนึ่งของการศึกษาตามหลักสูตรปริญญาวิทยาศาสตรดุษฎีบัณฑิต
สาขาวิชาเภสัชเวท ภาควิชาเภสัชเวทและเภสัชพฤกษศาสตร์
คณะเภสัชศาสตร์ จุฬาลงกรณ์มหาวิทยาลัย
ปีการศึกษา 2560

CHEMICAL CONSTITUENTS AND BIOACTIVITIES OF THE LEAVES AND STEMS OF *PSEUDUVARIA FRAGRANS*

Mr. Wongvarit Panidthananon

A Dissertation Submitted in Partial Fulfillment of the Requirements
for the Degree of Doctor of Philosophy Program in Pharmacognosy
Department of Pharmacognosy and Pharmaceutical Botany
Faculty of Pharmaceutical Sciences
Chulalongkorn University
Academic Year 2017

Thesis Title	CHEMICAL CONSTITUENTS AND BIOACTIVITIES OF THE LEAVES AND STEMS OF *PSEUDUVARIA FRAGRANS*
By	Mr. Wongvarit Panidthananon
Field of Study	Pharmacognosy
Thesis Advisor	Professor Kittisak Likhitwitayawuid, Ph.D.
Thesis Co-Advisor	Associate Professor Boonchoo Sritularak, Ph.D.

Accepted by the Faculty of Pharmaceutical Sciences, Chulalongkorn University in Partial Fulfillment of the Requirements for the Doctoral Degree

.....Dean of the Faculty of Pharmaceutical Sciences

(Assistant Professor Rungpetch Sakulbumrungsil, Ph.D.)

THESIS COMMITTEE

.....Chairman

(Associate Professor Suchada Sukrong, Ph.D.)

.....Thesis Advisor

(Professor Kittisak Likhitwitayawuid, Ph.D.)

.....Thesis Co-Advisor

(Associate Professor Boonchoo Sritularak, Ph.D.)

.....Examiner

(Professor Wanchai De-eknamkul, Ph.D.)

.....Examiner

(Associate Professor Rutt Suttisri, Ph.D.)

.....Examiner

(Assistant Professor Witchuda Thanakijcharoenpath, Ph.D.)

.....Examiner

(Assistant Professor Taksina Chuanasa, Ph.D.)

.....External Examiner

(Tanawat Chaowasku, Ph.D.)

วงศ์วริศ พาณิชธนานนท์ : องค์ประกอบทางเคมีและฤทธิ์ทางชีวภาพของใบและลำต้นสังหยูหอม (CHEMICAL CONSTITUENTS AND BIOACTIVITIES OF THE LEAVES AND STEMS OF *PSEUDUVARIA FRAGRANS*) อ.ที่ปรึกษาวิทยานิพนธ์หลัก: ศ. ภก. ดร.กิตติศักดิ์ ลิขิตวิทยาวุฒิ, อ.ที่ปรึกษาวิทยานิพนธ์ร่วม: รศ. ภก. ดร.บุญชู ศรีตุลารักษ์, หน้า.

จากการศึกษาองค์ประกอบทางเคมีจากใบและลำต้นของสังหยูหอม สามารถแยกสารบริสุทธิ์ได้ 7 ชนิด ได้แก่ สารใหม่ 1 ชนิด คือ pseuduvarioside ซึ่งมีโครงสร้างเป็น benzophenone *C*-glycoside และสารที่เคยมีรายงานมาแล้ว 6 ชนิด คือ (-)-guaiol, (+)-isocorydine, cyathocaline, isoursuline, *N-trans*-feruloyltyramine และ *N-trans*-coumaroyltyramine ซึ่งพิสูจน์โครงสร้างทางเคมีของสารที่แยกได้โดยอาศัยการวิเคราะห์ข้อมูล UV, HRS-ESI-MS และ NMR เปรียบเทียบกับข้อมูลของสารที่เคยรายงานมาแล้ว เมื่อทดสอบฤทธิ์ยับยั้งเอนไซม์แอลฟากลูโคซิเดสของสารที่แยกได้ทั้งหมดพบว่าสาร *N-trans*-feruloyltyramine และ *N-trans*-coumaroyltyramine มีฤทธิ์แรงในการยับยั้งเอนไซม์แอลฟากลูโคซิเดส โดยมีค่าความเข้มข้นที่สามารถยับยั้งเอนไซม์แอลฟากลูโคซิเดสได้ร้อยละ 50 (IC_{50}) คือ 3.58 และ 0.58 ไมโครโมลาร์ ตามลำดับ เมื่อเปรียบเทียบกับยา acarbose เมื่อศึกษาข้อมูลจลนพลศาสตร์ของโดยการวิเคราะห์รูปกราฟตามวิธีการของ Lineweaver-Burk พบว่า *N-trans*-feruloyltyramine และ *N-trans*-coumaroyltyramine เป็นตัวยับยั้งแบบ uncompetitive ต่อเอนไซม์นี้ งานวิจัยนี้เป็นการรายงานองค์ประกอบทางเคมีและฤทธิ์การยับยั้งเอนไซม์แอลฟากลูโคซิเดสของสังหยูหอมเป็นครั้งแรก

ภาควิชา	เภสัชเวทและเภสัชพฤกษศาสตร์	ลายมือชื่อนิสิต	.....
สาขาวิชา	เภสัชเวท	ลายมือชื่อ อ.ที่ปรึกษาหลัก	.....
ปีการศึกษา	2560	ลายมือชื่อ อ.ที่ปรึกษาร่วม	.....

5576453033 : MAJOR PHARMACOGNOSY
KEYWORDS: BENZOPHENONE / GLYCOSIDE / APORPHINE / 4-AZA-9-FLUORENONE / TYRAMINE AMIDE / GLUCOSIDASE / UNCOMPETITIVE INHIBITION

WONGVARIT PANIDTHANANON: CHEMICAL CONSTITUENTS AND BIOACTIVITIES OF THE LEAVES AND STEMS OF *PSEUDUVARIA FRAGRANS*. ADVISOR: PROF. KITTISAK LIKHITWITAYAWUID, Ph.D., CO-ADVISOR: ASSOC. PROF. BOONCHOO SRITULARAK, Ph.D., pp.

Chemical investigation of the leaves and stems of *Pseuduvaria fragrans* resulted in the isolation of seven pure compounds, including a new benzophenone *C*-glycoside named pseuduvarioside and six known compounds comprising (-)-guaiol, (+)-isocorydine, cyathocaline, isoursuline, *N-trans*-feruloyltyramine and *N-trans*-coumaroyltyramine. The structure determination of the isolated compounds was carried out by analysis of their UV, HRS-ESI-MS and NMR data in comparison with previously reported values. All the isolates were evaluated for their **α**-glucosidase inhibitory activity. Only *N-trans*-feruloyltyramine and *N-trans*-coumaroyltyramine exhibited strong activity with IC_{50} values of 3.58 μM and 0.58 μM, respectively, as compared with the drug acarbose (IC_{50} 985.6 μM). Kinetic studies with Lineweaver-Burk plot analysis revealed that *N-trans*-feruloyltyramine and *N-trans*-coumaroyltyramine were uncompetitive inhibitors of this enzyme. This study is the first report of the chemical constituents and **α**-glucosidase inhibitory activity of *P. fragrans*.

Department:	Pharmacognosy and Pharmaceutical Botany	Student's Signature .....
		Advisor's Signature .....
Field of Study:	Pharmacognosy	Co-Advisor's Signature .....
Academic Year:	2017	

ACKNOWLEDGEMENTS

The author would like to express my deepest gratitude to my thesis advisor, Professor Dr. Kittisak Likhitwitayawuid of the Department of Pharmacognosy and Pharmaceutical Botany, Faculty of Pharmaceutical Sciences, Chulalongkorn University, for his helpful advice, kindness, guidance, support, patience and constant encouragement throughout the course of this study.

I am very thankful to my thesis co-advisor, Associate Professor Dr. Boonchoo Sritularak of the Department of Pharmacognosy and Pharmaceutical Botany, Faculty of Pharmaceutical Sciences, Chulalongkorn University, for helpful, constant advice and kindness.

I would like to thank Dr. Tanawat Chaowasku of the Department of Biology, Faculty of Science, Chiang Mai University, for the plant identification and collection, as well as the photographs of the plant materials.

I wish to express my thanks to all members of my thesis committee for their useful advice and critical review of this dissertation.

I would also like to thank all staff members and students of the Department of Pharmacognosy and Pharmaceutical Botany, Faculty of Pharmaceutical Sciences, Chulalongkorn University, for their support on chemicals and research facilities, and friendship.

Finally, I would like to express infinite gratitude to my family for their love, understanding, support and encouragement.

CONTENTS

Page

Page

Page

Page

LIST OF TABLES

Page

LIST OF FIGURES

Page

Page

Page

Page

LIST OF SCHEMES

Page

ABBREVIATIONS & SYMBOLS

$[\alpha]^{25}_{D}$	=	Specific rotation at 25° and sodium D line (589 nm)
α	=	Alpha
β	=	Beta
Acetone-d_6	=	Deuterated acetone
br s	=	Broad singlet (for NMR spectra)
BuOH	=	Butanol
°C	=	Degree celsius
c	=	Concentration
calcd	=	Calculated
CC	=	Column chromatography
$CDCl_3$	=	Deuterated chloroform
CH_2Cl_2	=	Dichloromethane
cm	=	Centimeter
cm^{-1}	=	reciprocal centimeter (unit of wave munber)
^{13}C-NMR	=	Carbon-13 Nuclear Magnetic Resonance
1-D NMR	=	One-dimensional Nuclear Magnetic Resonance
2-D NMR	=	Two-dimensional Nuclear Magnetic Resonance
d	=	Doublet (for NMR spectra)
δ	=	Chemical shift
DEPT	=	Distortionless Enhancement by Polarization Transfer
DMSO	=	Dimethyl sulfoxide
DMSO-d_6	=	Deuterated dimethyl sulfoxide

ε	=	Molar absorptivity
ESI-MS	=	Electrospray Ionization Mass Spectrometry
EtOAc	=	Ethyl acetate
FCC	=	Flash Column Chromatography
g	=	Gram
GF	=	Gel Filtration
^{1}H-NMR	=	Proton Nuclear Magnetic Resonance
HMBC	=	^{1}H-detected Heteronuclear Multiple Bond Correlation
HPLC	=	High Pressure Liquid Chromatography
HR-ESI-MS	=	High Resolution Electrospray Ionization Mass Spectrometry
HSQC	=	^{1}H-detected Heteronuclear Single Quantum Coherence
Hz	=	Hertz
IC_{50}	=	Concentration exhibiting 50% inhibition
IR	=	Infrared
J	=	Coupling constant
KBr	=	Potassium bromide
K_i	=	Inhibition constant
K_m	=	Michaelis-Menten constant
L	=	Liter
λmax	=	Wavelength at maximal absorption
$[M]^+$	=	Molecular ion
$[M+Na]^+$	=	Sodium-adduct molecular ion
$[M-H]^-$	=	Pseudomolecular ion

m	=	Multiplet (for NMR spectra)
MeOH	=	Methanol
CD_3OD	=	Deuterated methanol
mg	=	Milligram
µg	=	Microgram
min	=	Minute
mL	=	Milliliter
µL	=	Microliter
µM	=	Micromolar
mm	=	Millimeter
mM	=	Millimolar
MS	=	Mass spectrum
MW	=	Molecular weight
m/z	=	Mass to charge ratio
nm	=	Nanometer
NMR	=	Nuclear Magnetic Resonance
NOESY	=	Nuclear Overhauser Effect Spectroscopy
ppm	=	Part per million
s	=	Singlet (for NMR spectra)
t	=	Triplet (for NMR spectra)
TLC	=	Thin Layer Chromatography
UV-VIS	=	Ultraviolet and Visible spectrophotometry
VLC	=	Vacuum Liquid Column Chromatography
V_{max}	=	Maximum velocity

CHAPTER I
INTRODUCTION

Diabetes mellitus (DM) is a chronic metabolic disorder characterized by hyperglycemia, which can lead to many diseases such as atherosclerosis, cardiac dysfunction, retinopathy, neuropathy and nephropathy (Hsieh *et al*., 2010) . DM can be classified into 2 types. Type 1 diabetes mellitus is caused by immunological destruction of pancreatic β cells which leads to abnormal insulin secretion. Type 2 diabetes results from insulin resistance. α-Glucosidase can be found in the intestinal lumen and in the brush border membrane. It catalyzes carbohydrates digestion, and its inhibitors can delay the absorption of dietary carbohydrates and have been commonly used in the treatment of patients with type 2 diabetes (Liu *et al*., 2015). Examples of α-glucosidase inhibitors, which are used as oral anti-diabetic drugs, are acarbose, miglitol and voglibose. They can bind to α-glucosidase and competitively inhibit the enzyme in the small intestine to reduce the level of blood glucose (He *et al*., 2013). However, acarbose, miglitol and voglibose can cause side effects including, flatulence, nausea, vomiting and diarrhea (Liu *et al*., 2015). Several plants have been investigated for α-glucosidase inhibitory activity, for example, *Flemingia macrophylla* (Hsieh *et al*., 2010), *Croton menyharthii* (Aderogba *et al*., 2013), *Morus alba* (Liu *et al*., 2015) and *Ziziphus oxyphylla* (Choudhary *et al*., 2011). A number of annonaceous plants also demonstrated α-glucosidase inhibitory activity, for instance, *Annona crassiflora* (Justino *et al*., 2016), *A. muricata* (Justino *et al*., 2018), *A. squamosa* (Ren *et al*., 2017), *Drepananthus philippinensis* (Macabeo *et al*., 2015) and *Xylopia aethiopica* (Mohammed *et al*., 2016). In addition, 1-deoxynojirimycin and derivatives, and stibenoids from the leaves and root bark of *Morus* (mulberry) species (Choudhary *et al*., 2011; Jiang *et al*., 2014; Kimura *et al*., 2004; Liu *et al*., 2015) showed strong α-glucosidase inhibitory activity.

The family Annonaceae consists of approximately 108 genera and 2,400 species (Chatrou *et al*., 2012). Currently, there are about 56 *Pseuduvaria* species that have been classified and reported, but a few have been investigated chemically and

biologically (Su *et al*., 2008). Some *Pseuduvaria* species have been used to treat fever, nausea, headache, and stomach ailment and have been studied for their alkaloids (Taha *et al*., 2014).

In Thailand, 11 species of *Pseuduvaria* have been identified as follows (Forest herbarium, 2014):

P. fragrans	**สังหยูดอกหอม** sang yu dok hom (General)
P. gardneri	**สังหยูห้วยยอด** sang yu huai yot (General)
P. macrophylla (Oliv.). Merr var. *sessilicarpa*	**สังหยูดอกแดง** sang yu dok daeng (General)
P. monticola	**สังหยูเขา** sang yu khao (General)
P. multiovulata	**สังหยูดอกใหญ่** sang yu dok yai (General)
P. phuyensis	**อนุพรหม** anu phrom (General)
P. reticulata	**สังหยูดอกขาว** sang yu dok khao (General)
P. rugosa	**สังหยูดำ** sang yu dam (Trang)
P. setosa	**สังหยูใบขน** sang yu bai khon (General), สังหยูใบเล็ก sang yu bai lek (General)

Pseuduvaria fragrans was reported as a new species in 2010 (Su *et al*., 2010) and known in Thai as sang yu dok hom. This species is distributed in Southern Thailand. The plant has treelets to 4 m tall. Young branches dark brown, subglabrous, indistinctly lenticellate. Leaf laminas 8.5–15.5 cm long, 2.5–6 cm wide, length:width ratio 2.6–3.6, elliptic, apex acuminate, acumen 9–18 mm long, base acute to obtuse, papyraceous to subcoriaceous, glabrous ad- and abaxially; margins not ciliate; midrib ± impressed and glabrous adaxially, prominent and glabrous abaxially; secondary veins 8–14 pairs per leaf, ± arcuate; petioles 4–7 mm long, 0.8–1.9 mm in diameter, subglabrous, narrowly grooved adaxially. Inflorescences solitary on young branches, with up to 7 flowers, only one flower at anthesis per inflorescence. Flowering peduncles 3.5–8 mm long, ca. 0.5 mm in diameter,

subglabrous. Sympodial rachides to ca. 10 mm long; internodes sometimes well developed, with 2–7 bracts. Flowering pedicels 3–10 mm long, ca. 0.2 mm in diameter, sparsely puberulous with appressed hairs; submedian pedicel bract ca. 1 mm long, densely puberulous with appressed hairs. Sepals free, 1–1.3 mm long, 1–1.5 mm wide, length:width ratio 0.9–1.1, broadly ovate, glabrous adaxially, densely puberulous with appressed hairs abaxially, margins puberulous. Outer petals 3–4 mm long, ca. 3 mm wide, length:width ratio 1.1–1.3, broadly ovate, glabrous adaxially, sparsely puberulous with appressed hairs abaxially, cream-colored, without claws. Inner petals 4.5–5.5 mm long, 3–3.5 mm wide, length:width ratio 1.3–1.8, clawed-rhombic, apex acute, base acute, ca. 0.8 mm thick, very densely puberulous with appressed hairs adaxially, sparsely puberulous with appressed hairs abaxially, cream-colored with purple tinge on adaxial surface of the blade; basal claw 1.5–2.5 mm long, claw:inner petal length ratio 0.3–0.5; glands paired on adaxial surface of inner petal, ± round, surface smooth, raised; apical aperture absent. Flowers unisexual. Staminate flowers with androecium ca. 1.5 mm long, ca. 2.2 mm wide; stamens ca. 24 per flower, ca. 0.6 mm long, ca. 0.5 mm wide; pollen exine rugulate, with small surface elements. Pistillate flowers with gynoecium ca. 2.5 mm long, ca. 2.5 mm wide; carpels 1–3 per flower, ca. 2.5 mm long, ca. 1 mm wide; ovules ca. 5 per carpel, uniseriate; staminodes absent. Fruits with 1 (–3) monocarp(s). Fruiting peduncles ca. 13 mm long, ca. 1 mm in diameter, glabrous. Fruiting pedicels ca. 12 mm long, ca. 1 mm in diameter, glabrous. Monocarps (immature) ca. 25 mm long, ca. 8 mm wide, length:width ratio ca. 3.1, ellipsoid, without apicule but with elongated apex (ca. 8 mm long), without suture, smooth, very densely puberulous with erect hairs, pale green; stipes absent. Seeds not seen. The specific epithet reflects the strong fragrance emitted by the flowers (Su *et al*., 2010).

Previous to this study, there were no studies on the chemical constituents and biological activities of *P. fragrans*. In a preliminary study, the methanol crude extracts of leaves and stems of *P. fragrans* were evaluated for α-glucosidase inhibitory activity. The leaves methanol extract and stem methanol extract showed

56.46% and 66.16% inhibition of α-glucosidase inhibitory activity at a concentration of 200 μg/mL, respectively. This study focused on the chemical constituents and α-glucosidase inhibitory activity of *P. fragrans*.

The purposes of this study are as follows:

(1). Isolation and purification of the chemical constituents of leaves and stems of *P. fragrans*.

(2) Determination of the chemical structures of the isolates.

(3) Evaluation of the α-glucosidase inhibitory activity of each isolate.

Figure 1 *Pseuduvaria fragrans* Su, Chaowasku & Saunders

(Phrotograph by K. Aongyong)

CHAPTER II
HISTORICAL

1. Chemical constituents of *Pseuduvaria*

Chemical studies of the genus *Pseuduvaria* have revealed several types of secondary metabolites, which can be classified as aporphinoid alkaloids, protoberberine alkaloids, benzopyran derivatives and diterpenoids.

The biosynthesis of aporphinoid alkaloids (**Figure 2**) begins with the conversion of L-tyrosine to dopamine and 4-hydroxyphenylacetaldehyde, which are then condensed to (*S*)-norcoclaurine. Three methyltransferases [(*S*)-norcoclaurine 6-*O*-methyltransferase (6OMT), (*S*)-coclaurine-*N*-methyltransferase (CNMT) and (*S*)-3′-hydroxy-*N*-methylcoclaurine-4′-*O*-methyltransferase (4′OMT)] and one hydroxylase [(*S*)-*N*-methylcoclaurine 3′-hydroxylase (NMCH)] are required to transform (*S*)-norcoclaurine to (*S*)-reticuline, which is an intermediate of many types of isoquinoline alkaloids such as aporphinoids, protoberberines and protopines (Doncheva *et al*., 2016). The aporphine and protoberberine alkaloids formed in *Pseuduvaria* are summarized in **Figures 3 and 4** and **Tables 1 and 2**, respectively.

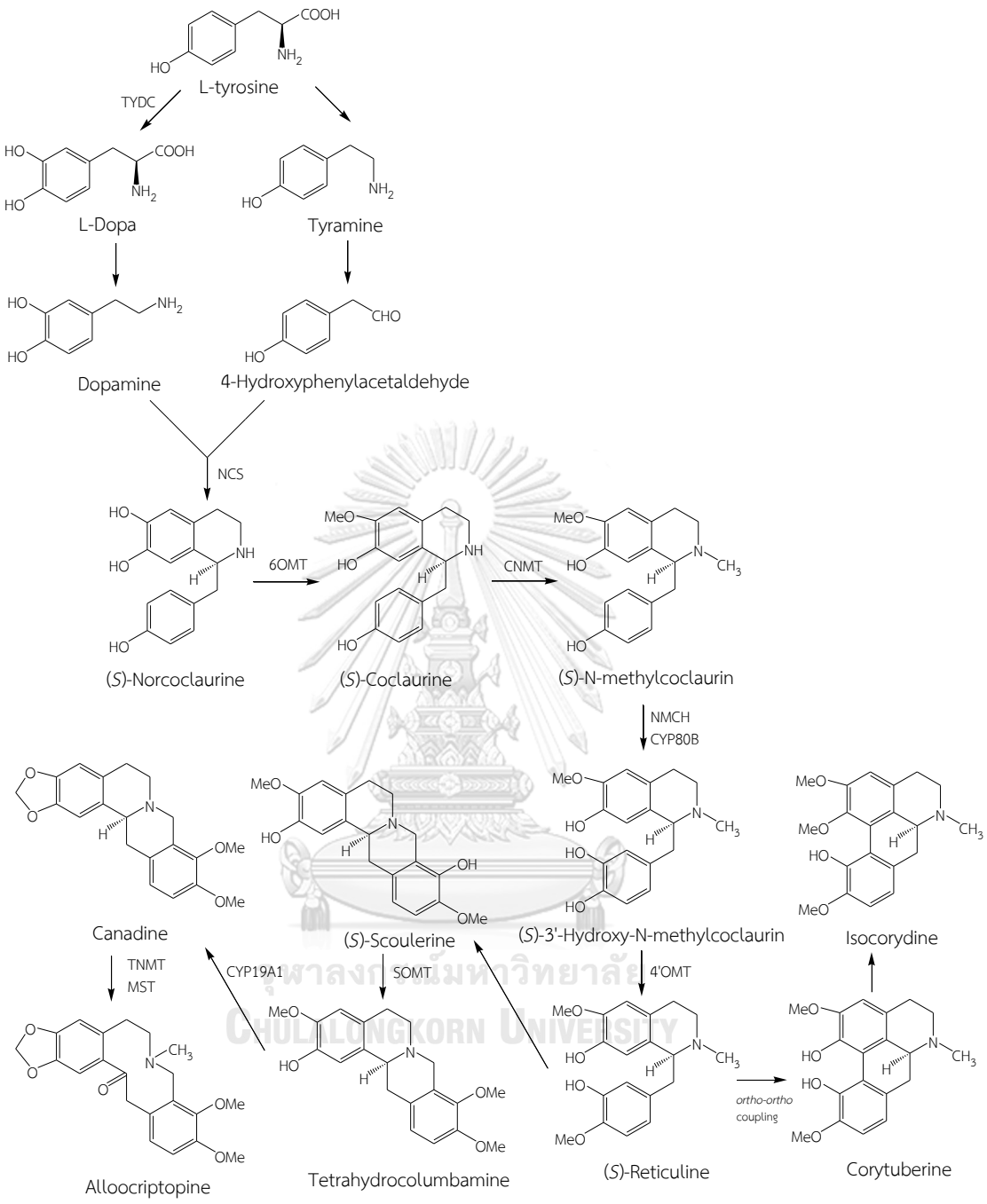

Figure 2 Biosynthetic pathway of aporphinoid alkaloids, protoberberine alkaloids and protopine alkaloids

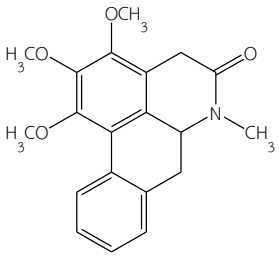

1,2,3-Trimethoxy-5-oxonoraporphine [**1**]

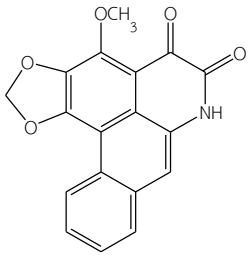

3-Methoxycepharadione-B [**2**]

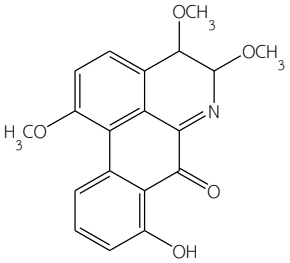

8-Hydroxyartabonatine C [**3**]

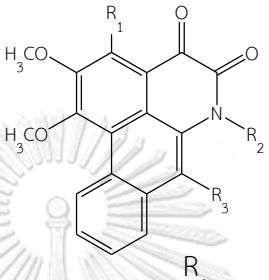

	R_1	R_2	R_3
N-methylouregidione [**4**]	OCH_3	CH_3	H
Ouregidione [**8**]	OCH_3	H	H
Pseuduvarine A [**12**]	H	H	H
Pseuduvarine B [**13**]	H	CH_3	H
Rugosanine [**14**]	OCH_3	H	CHO

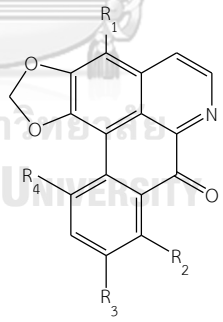

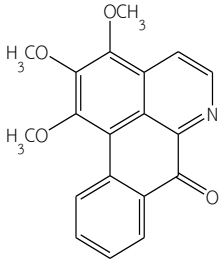

O-Methylmoschatoline [**5**]

	R_1	R_2	R_3	R_4
Atherospermidine [**6**]	OCH_3	H	H	H
Liriodenine [**7**]	H	H	H	H
Oxoanolobine [**9**]	H	H	OH	H
Oxoputerene [**10**]	H	H	H	OCH_3
Oxostephanine [**11**]	H	OCH_3	H	H

Figure 3 Structures of aporphinoid alkaloids previously isolated from *Pseuduvaria* species

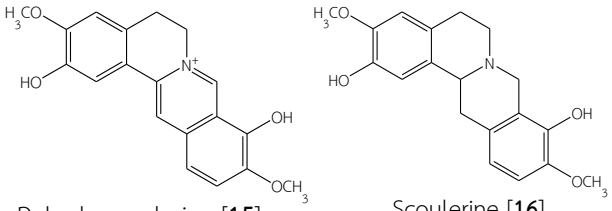

Dehydroscoulerine [**15**] Scoulerine [**16**]

Figure 4 Structures of protoberberine alkaloids previously isolated from *Pseuduvaria* species

Benzopyran derivatives (**Figure 5**) are formed by the fusion of a benzene ring to a pyran ring. It occurs via two pathways. The first is the transformation of *p*-hydroxyphenylpyruvate to homogentisic acid, which is catalyzed by hydroxyphenylpyruvate dioxygenase via the shikimate pathway. The other is the biosynthesis of the isoprenoid side chain, which can occur via two pathways: mevalonate pathway and methylerythritol phosphate pathway (Birringer *et al*., 2018). **Figure 6** and **Table 3** summarize the benzopyrans formed in *Pseuduvaria*.

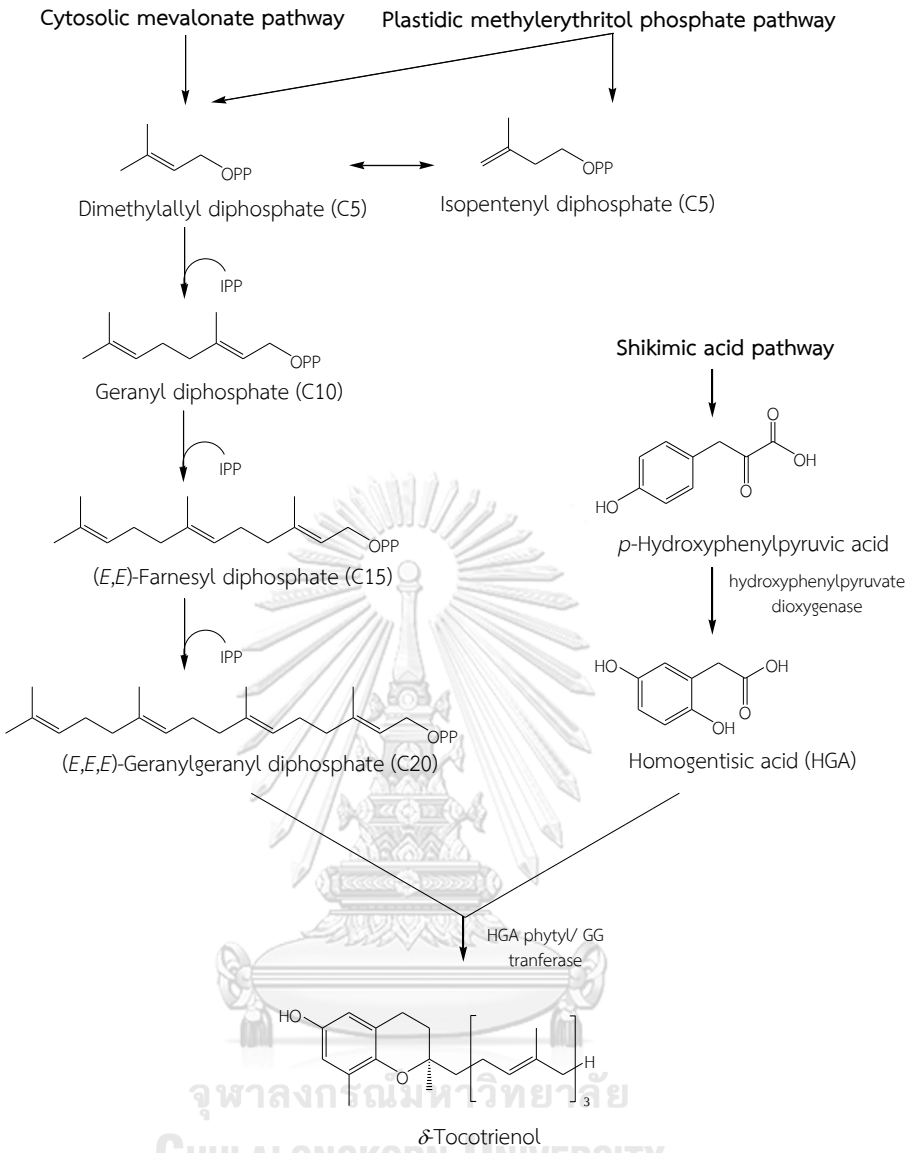

Figure 5 Biosynthetic pathway of benzopyrans

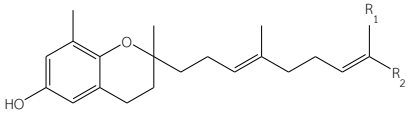

	R_1	R_2
(6*E*,10*E*)-Isopolycerasoidol [**17**]	CH_3	COOH
(6*E*,10*E*)-Isopolycerasoidol methyl ester [**18**]	CH_3	$COOCH_3$
Oligandrol [**19**]	CH_3	CH_3
Polycerasoidol [**20**]	COOH	CH_3
Pseudindochin [**21**]	$COOCH_3$	CH_2OH

Figure 6 Structures of benzopyran derivatives previously isolated from *Pseuduvaria* species

In terpenoids, the biosynthesis (**Figure 7**) can occur via two pathways, the mevalonate (MVA) pathway and the methylerythritol phosphate (MEP) pathway, which leads to the formation of isoprenes (C5), monoterpenes (C10), sesquiterpenes (C15), diterpenes (C20), sesterterpenes (C25), triterpenes (C30) and tetraterpenes (C40) (Okada, 2011). For diterpenes, the biosynthesis starts with the five-carbon (C5) units, isopentenyl pyrophosphate (IPP) and dimethylallyl pyrophosphate (DMAPP). Geranylgeranylpyrophosphate (GGPP) is formed and becomes a common precursor for other diterpenes (Zerbe *et al*., 2015). **Figure 8** and **Table 4** summarize the diterpenoids in *Pseuduvaria*.

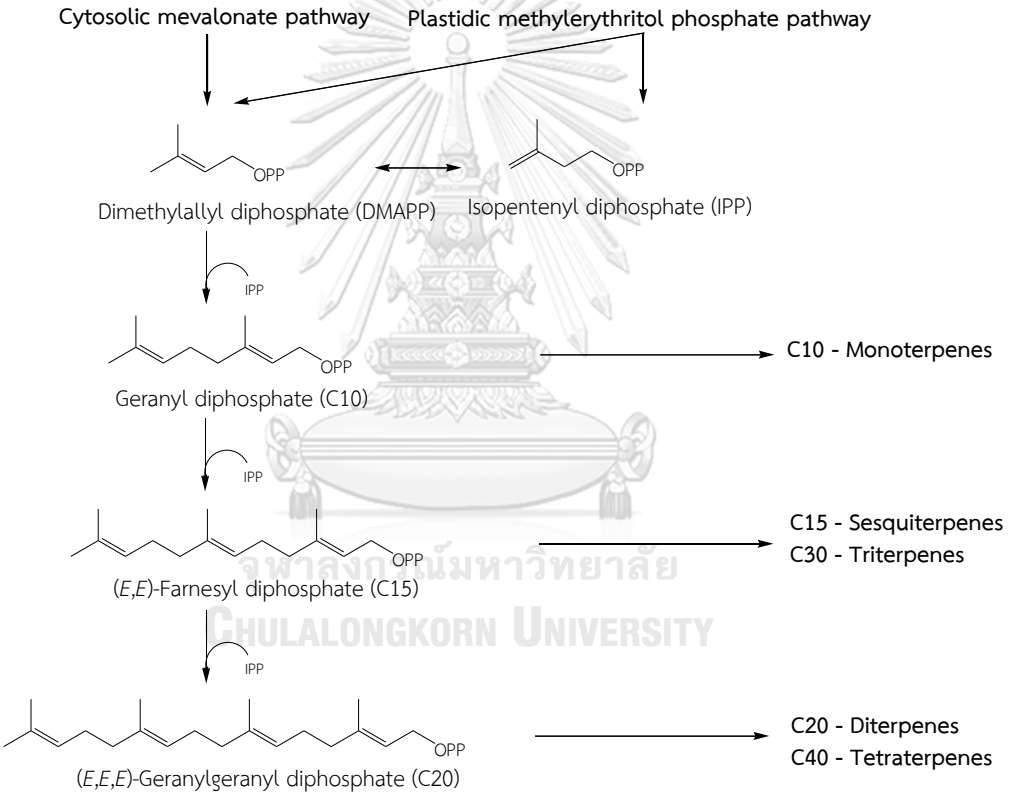

Figure 7 Biosynthetic pathway of terpenoids

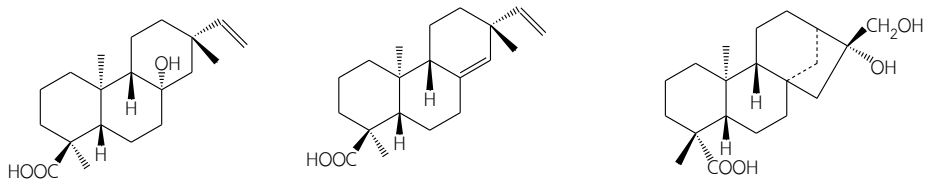

ent-8α-Hydroxypimar-15-en-18-oic acid (**22**)

ent-Pimaric acid (**23**)

ent-16α,17-Dihydroxykauran-19-oic acid (**24**)

Figure 8 Structures of diterpenoids previously isolated from *Pseuduvaria* species

Table 1 Distribution of aporphinoid alkaloids in the genus *Pseuduvaria*

Compounds	**Plant**	**Plant part**	**Reference**
1,2,3-Trimethoxy-5-oxonoraporphine [**1**]	*P. rugosa*	Leaves and twigs	Uadkla *et al*., 2013
3-Methoxycepharadione-B [**2**]	*P. rugosa*	Stem bark	Jamaludin, 1999
8-Hydroxyartabonatine C [**3**]	*P. trimera*	Leaves and twigs	Sesang *et al*., 2014
N-Methylouregidione [**4**]	*P. macrophylla*	Stem bark	Mahmood *et al*., 1986
	P. setosa	Aerial part	Wirasathien *et al*., 2006
O-Methylmoschatoline [**5**]	*P. macrophylla*	Stem bark	Mahmood *et al*., 1986
Atherospermidine [**6**]	*P. indochinensis*	Stem bark	Shou-Ming *et al*., 1988
	P. rugosa	Stem bark	Jamaludin, 1999
Liriodenine [**7**]	*P. indochinensis*	Stem bark	Shou-Ming *et al*., 1988
	P. rugosa	Stem bark	Jamaludin, 1999
	P. setosa	Aerial part	Wirasathien *et al*., 2006

Table 1 (continued)

Compounds	Plant	Plant part	Reference
Ouregidione [**8**]	*P. rugosa*	Leaves and twigs	Uadkla *et al*., 2013
	P. setosa	Aerial part	Wirasathien *et al*., 2006
	P. setosa	Stem bark	Jamaludin, 1999
	P. trimera	Leaves and twigs	Sesang *et al*., 2014
Oxoanolobine [**9**]	*P. indochinensis*	Stem bark	Shou-Ming *et al*., 1988
	P. rugosa	Stem bark	Jamaludin, 1999
Oxoputerine [**10**]	*P. rugosa*	Stem bark	Jamaludin, 1999
Oxostephanine [**11**]	*P. setosa*	Aerial part	Wirasathien *et al*., 2006
Pseuduvarine A [**12**]	*P. setosa*	Stem bark	Taha *et al*., 2011
Pseuduvarine B [**13**]	*P. setosa*	Stem bark	Taha *et al*., 2011
Rugosanine [**14**]	*P. rugosa*	Stem bark	Jamaludin, 1999

Table 2 Distribution of protoberberine alkaloids in the genus *Pseuduvaria*

Compounds	Plant	Plant part	Reference
Dehydroscoulerine [**15**]	*P. indochinensis*	Stem bark	Shou-Ming *et al*., 1988
Scoulerine [**16**]	*P. indochinensis*	Stem bark	Shou-Ming *et al*., 1988

Table 3 Distribution of benzopyran derivatives in the genus *Pseuduvaria*

Compounds	Plant	Plant part	Reference
(6*E*,10*E*)-Isopolycerasoidol [**17**]	*P. indochinensis* *P. monticola*	Twigs and leaves leaves	Zhao *et al*., 2014 Taha *et al*., 2015
(6*E*,10*E*) Isopolycerasoidol methyl ester [**18**]	*P. monticola*	leaves	Taha *et al*., 2015
Oligandrol [**19**]	*P. indochinensis*	Twigs and leaves	Zhao *et al*., 2014
Polycerasoidol [**20**]	*P. indochinensis*	Twigs and leaves	Zhao *et al*., 2014
Pseudindochin [**21**]	*P. indochinensis*	Twigs and leaves	Zhao *et al*., 2014

Table 4 Distribution of diterpenoids in the genus *Pseuduvaria*

Compounds	Plant	Plant part	Reference
ent-8α-Hydroxypimar-15-en-18-oic acid [**22**]	*P. indochinensis*	Stem bark	Ning *et al*., 1989
ent-16α,17-Dihydroxykauran-19-oic acid [**23**]	*P. indochinensis*	Stem bark	Ning *et al*., 1989
ent-Pimaric acid [**24**]	*P. indochinensis*	Stem bark	Ning *et al*., 1989

2. Traditional uses and biological activities of *Pseuduvaria* species

Several species of *Pseuduvaria* have been used to treat fever, nausea, headache, and stomach ailment and have been studied for their alkaloids (Taha *et al*., 2014). The root of *P. setosa* has been used traditionally as a treatment for coughs and as a rubbing powder on the body to treat fever (Wirasathien *et al*., 2006). Two aporphine alkaloids, 1,2,3-trimethoxy-5-oxonoraporphine [**1**] and ouregidione [**8**] were isolated from the leaves and twigs of this plant. At a concentration of 100 µg/mL, they could reduce the viability of human erythroleukemic (K562) promonocytic leukemic (U937) and promyelocytic (HL-60) cells to 63 and 64, 38 and 66, and 49 and 64%, respectively. In addition, at this concentration the exposed U937 and HL-60 cell lines showed cell cycle arrest (Uadkla *et al*., 2013). 8-Hydroxyartabonatine C [**3**] and ouregidione [**8**], isolated from the ethyl acetate-methanol extract from the leaves and twigs of *Pseuduvaria trimera*, exhibited cytotoxic activity against human hepatocellular carcinoma (HepG2) and human breast cancer (MDA-MB231) cells (Sesang *et al*., 2014). Four alkaloids, *N*-methylouregidione [**4**], liriodenine [**7**], ouregidione [**8**] and oxostephanine [**11**], were isolated from the aerial part of *P. setosa*. These alkaloids exhibited antituberculosis activity against *Mycobacterium tuberculosis* with MIC values of 100, 200, 12.5 and 25 µg/mL, respectively. Liriodenine [**7**] showed antimalarial activity against *Plasmodium falciparum* with an IC_{50} value of 2.8 mg/mL. Liriodenine [**7**] and oxostephanine [**11**] were also strongly cytotoxic against epidermoid carcinoma (KB) and breast cancer (BC) cell lines, whereas *N*-methylouregidione [**4**] and ouregidione [**8**] were active against small cell lung cancer (NCI-H187) cells and were able to stimulate lymphocyte proliferation with stimulation indices (SI) of more than 1 (Wirasathien *et al*., 2006). Pseuduvarines A [**12**] and B [**13**] from the stem bark of *Pseuduvaria rugosa* showed cytotoxicity against human breast adenocarcinoma (MCF-7), human liver carcinoma (HepG2), and human promyelocyctic leukemia cells (HL-60) (Taha *et al*., 2011). Two benzopyran derivatives, (6*E*,10*E*) isopolycerasoidol [**17**] and (6*E*,10*E*) isopolycerasoidol methyl ester [**18**] isolated from the leaves of *Pseuduvaria monticola*, showed cytotoxic activity against human breast adenocarcinoma cells

(MCF-7) with IC_{50} values of 59 and 43 μM, respectively (Taha *et al*., 2015). The diterpenes, *ent*-8 α-hydroxypimar-15-en-18-oic acid [**22**], *ent*-pimaric acid [**23**] and *ent*-16α,17-dihydroxykauran-19-oic acid [**24**] isolated from *Pseuduvaria indochinesis* were found to inhibit DNA topoisomerase activity (Ning *et al*., 1989). The methanolic extract of *Pseuduvaria macrophylla* stem bark could normalize the elevated blood glucose levels by upregulating the insulin and C-peptide levels (Taha *et al*., 2018).

CHAPTER III

EXPERIMENTAL

1. Source of plant materials

The leaves and stems of *Pseuduvaria fragrans* were collected from Nopphitam district, Nakhon Si Thammarat, Thailand. Authentication was performed by Dr. Tanawat Chaowasku (Faculty of Science, Chiang Mai University) through comparison with specimens at the Herbarium of the Department of Biology, Faculty of Science, Chiang Mai University. A voucher specimen (K. Aongyong 1) has been deposited at the Department of Biology, Faculty of Science, Chiang Mai University.

2. General techniques

2.1 Analytical normal-phase thin-layer chromatography (TLC)

Technique	:	One dimensional ascending
Absorbent	:	Silica gel 60 F254 (E. Merck) precoated plate
Layer thickness	:	0.2 mm
Distance	:	6.5 cm
Temperature	:	Laboratory temperature (30-35 °C)
Detection	:	1. Ultraviolet light at wavelengths of 254 and 365 nm. 2. Spraying with anisaldehyde reagent (0.5 ml *p*-anisaldehyde in 50 ml glacial acetic acid and 1 ml 97% sulfuric acid) and heating at 105 °C for 10 min. 3. Spraying with Dragendorff's reagent (Solution A: 0.85 g bismuth subnitrate in 40 ml water and 10 ml glacial acetic acid, solution B: 8 g potassium iodide in 20 ml water. Solution A 5 ml and solution B 5 ml mixed with

20 ml glacial acetic acid and adjusted to 100 ml with water).

2.2 Analytical reverse-phase thin-layer chromatography (Reverse phase-TLC)

Technique : One dimensional ascending

Absorbent : C-18 precoated on aluminum foil (Anal Tech)

Layer thickness : 0.2 mm

Distance : 6.5 cm

Temperature : Laboratory temperature (30-35 ºC)

Detection : Fractions were examined as described in section 2.1

2.3 Column chromatography

2.3.1 Vacuum liquid chromatography (VLC)

Adsorbent : Silica gel 60 (No. 7734) particle size 0.063-0.200 mm (E. Merck)

Packing method : Dry packing

Sample loading : The sample was dissolved in a small amount of organic solvent, mixed with a small quantity of the adsorbent, triturated, dried and then gradually placed on top of the column.

Detection : Each fraction was examined by TLC under UV light at the wavelengths of 254 and 365 nm.

2.3.2 Flash column chromatography (FCC) on silica gel

Adsorbent : Silica gel 60 (No. 9385) particle size 0.040-0.063 mm (E. Merck)

Packing method : Wet packing

Sample loading : The sample was dissolved in a small amount of organic solvent, mixed with a small quantity of the adsorbent, triturated, dried and then gradually placed on top of the column.

Detection : Fractions were examined as described in section 2.3.1

2.3.3 Flash column chromatography (FCC) on Diaion HP-20

Adsorbent : Diaion HP20 lot. No. 41504 (Mitsubishi Chemical)

Packing method : Dry packing, an appropriate mixture of deionized water and methanol was used as the eluent.

Sample loading : The sample was dissolved in a small amount of deionized water and then gradually distributed on top of the column.

Detection : Fractions were examined as described in section 2.3.1

2.3.4 Gel filtration chromatography

Adsorbent : Sephadex LH-20 (GE Healthcare)

Packing method : An appropriate organic solvent was used as the eluent. Gel filter was suspended in the eluent, left standing about 24 hours prior to use and then poured into the column and left to set tightly.

Sample loading : The sample was dissolved in a small amount of the eluent and then gradually distributed on top of the column.

Detection : Fractions were examined as described in section 2.3.1

2.3.5 High pressure liquid chromatography

Column : Shim-pack Prep-ODS No.2025820

Flow rate : 1 ml/min

Mobile phase : Isocratic 50% methanol in water

Sample preparation : The sample was dissolved in small of eluent and filtered through Millipore filter paper before injection.

Injection volumn : 1 ml

Pump : LC-8A (Shimadzu)

Detector : SPD-10A UV-Vis Detector (Shimadzu)

Recorder : C-R6A Chromatopac (Shimadzu)

Temperature : Room temperature

2.4 Spectroscopy

2.4.1 Mass spectra

Mass spectra were recorded on a Bruker micro TOF mass spectrometer (ESI-MS) (Department of Chemistry, Faculty of Science, Mahidol University).

2.4.2 Proton and carbon-13 nuclear magnetic resonance (^{1}H and ^{13}C-NMR) spectra

^{1}H NMR (300 MHz) and ^{13}C NMR (75 MHz) spectra were recorded on a Bruker Avance DPX-300 FT-NMR spectrometer (Faculty of Pharmaceutical Sciences, Chulalongkorn University)

Solvents for NMR spectra were deuterated acetone (acetone-d_6), deuterated chloroform ($CDCl_3$), deuterated dimethylsulfoxide (DMSO-d_6) and deuterated methanol (CD_3OD). Chemical shifts were reported in ppm scale using the chemical shift of the solvent as the reference signal.

2.4.3 Ultraviolet (UV) absorption spectra

UV spectra (in methanol) were obtained on an Agilent Technologies Cary 60 UV-Vis spectrophotometer (Pharmaceutical Research Instrument Center, Faculty of Pharmaceutical Sciences, Chulalongkorn University).

2.4.4 Infrared (IR) spectra

IR spectra were obtained on a Perkin-Elmer FT-IR 1760X spectrophotometer (Scientific and Technology Research Equipment Center, Chulalongkorn University).

2.4.5 Physical property

2.4.5.1 Optical rotation

Optical rotations were measured on a Perkin Elmer Polarimeter 341 (Pharmaceutical Research Instrument Center, Faculty of Pharmaceutical Sciences, Chulalongkorn University).

2.5 Solvents

All organic solvents employed throughout this work were of commercial grade and were redistilled prior to use.

3. Extraction and isolation

3.1 Leaves of *Pseuduvaria fragrans*

3.1.1 Extraction

The dried leaves of *Pseuduvaria fragrans* (252.9 g) were ground and then macerated with methanol (3×5 L) for 24 hours. The filtrates were pooled and evaporated under reduced pressure at temperature not exceeding 40°C to give a methanol extract (64.9 g). The extract exhibited cytotoxicity against small cell lung cancer (NCl-H 187) with 95.13% inhibition at 50 µg/mL and showed α-glucosidase inhibitory activity with 51.56% inhibition at 200 µg/mL. This material was then suspended in water and partitioned with hexane, EtOAc and *n*-butanol, respectively,

to give hexane extract (10.2 g), EtOAc extract (11.4 g), *n*-butanol extract (8.5 g), and aqueous extract (21.9 g) (**Scheme 1**).

All four extracts were tested for α-glucosidase inhibitory activity. The hexane and EtOAc extracts showed 51.56% and 99.71% inhibitory activity, respectively, at the concentration of 200 μg/mL, whereas the *n*-butanol and aqueous extracts were inactive (< 50% inhibition) at this concentration.

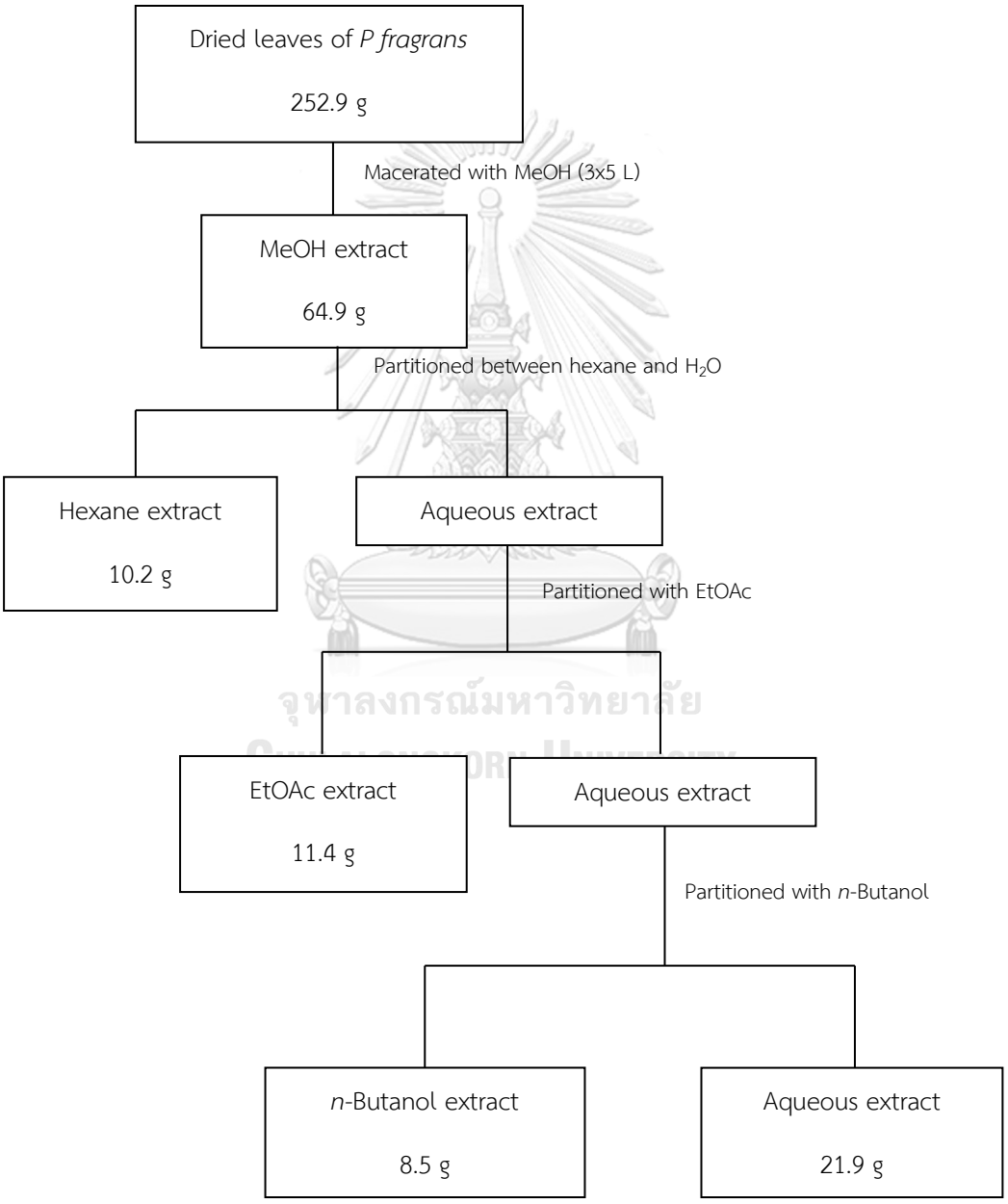

Scheme 1 Separation of the MeOH extract prepared from the leaves of *Pseuduvaria fragrans*

3.1.2 Separation of hexane extract

The hexane extract (10.2 g) was separated by vacuum liquid chromatography (VLC) (**Scheme 2**). Silica gel (No.7734, 330.0 g) was used as the stationary phase, and a step gradient of hexane-EtOAc (1:0 to 0:1) was used as the mobile phase. The eluates 400 mL per fraction were collected and examined by TLC (silica gel, hexane-EtOAc = 9:1). Sixty-four fractions with similar chromatographic patterns were combined to yield 16 fractions: A (376 mg), B (173 mg), C (261 mg), D (158 mg), E (23 mg), F (38 mg), G (209 mg), H (104 mg), I (3.2 g), J (1.3 g), K (405 mg), L (80 mg), M (119 mg), N (112 mg), O (1.3 g), P (1.8 g).

3.1.2.1 Isolation of compound PF-1 [(-)-guaiol]

Fraction I (3.2 g) was further separated by flash column chromatography (FCC). Diaion HP20 was used as the stationary phase with a gradient mixture of methanol-acetone (1:0 to 0:1) as the mobile phase to give 5 fractions: I1 (1.1 g), I2 (1.6 g), I3 (70 mg), I4 (306 mg), I5 (101 mg).

Fraction I1 (1.1 g) was recrystallized from a mixture of EtOAc-acetone (1:1) to give compound PF-1 as white crystals. (43 mg, R_f 0.28, silica gel, hexane-acetone 1:9). It was identified as (-)-guaiol [**25**].

3.1.3 Separation of *n*-butanol extract

The *n*-butanol extract (8.5 g) was fractionated by flash column chromatography (FCC) (**Scheme 3**). Diaion HP20 was used as the stationary phase. Elution was performed in a reverse-polarity gradient (pure water, 25% methanol in water, 50% methanol in water, 75% methanol in water and pure methanol, respectively). The eluates were collected, examined by reverse phase C-18 TLC, MeOH-water 1:4 and combined to give 5 fractions: A (3.7 g), B (1.0 g), C (1.3 g), D (837 mg), E (224 mg).

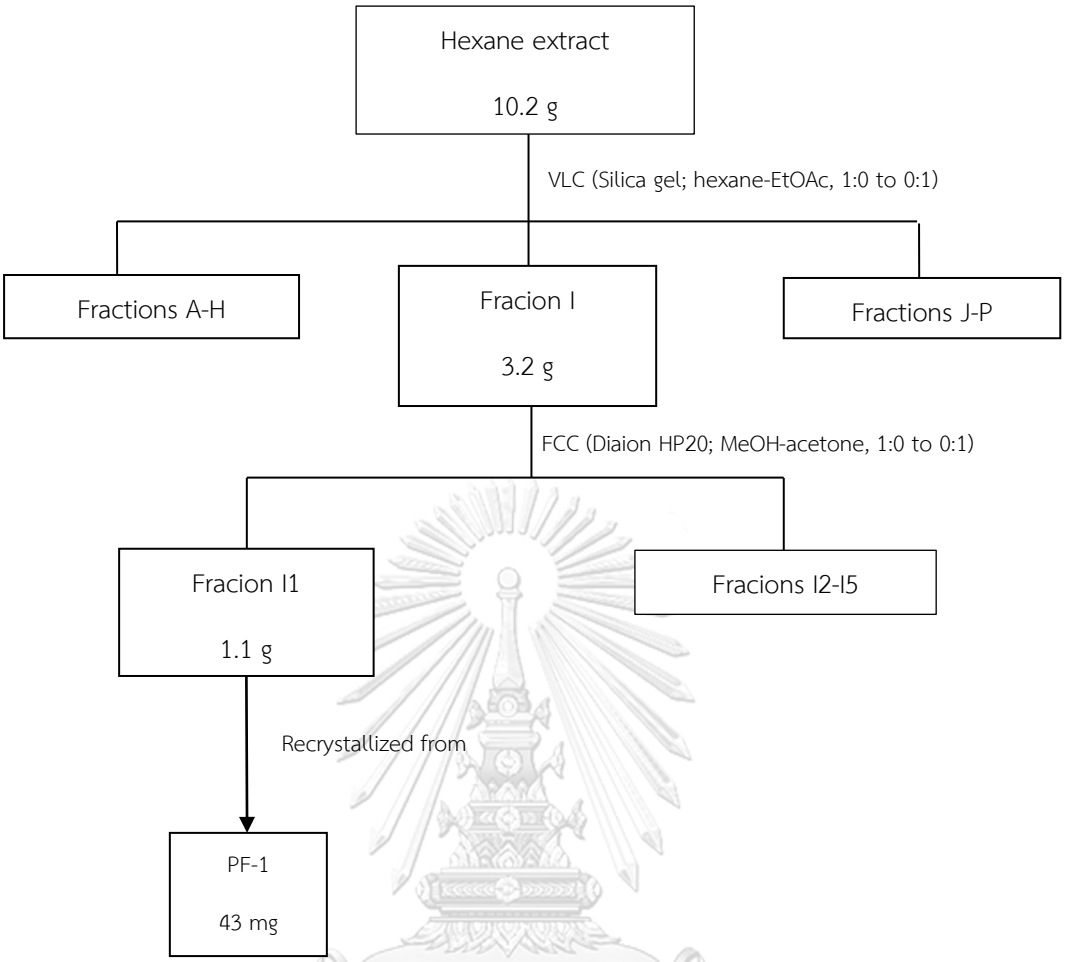

Scheme 2 Separation of the hexane extract prepared from the leaves of *Pseuduvaria fragrans*

3.1.3.1 Isolation of compound PF-2 (pseuduvarioside)

Fraction B (1.0 g) was separated on a Sephadex LH20 column eluting with MeOH. Fractions were combined according to their TLC patterns (silica gel, EtOAc:MeOH = 7:3) to yield 8 fractions: B1 (44 mg), B2 (85 mg), B3 (191 mg), B4 (252 mg), B5 (74 mg), 6 (53 mg), B7 (36 mg), B8 (13 mg).

Fraction B5 (74 mg) was subjected to silica gel column chromatography eluting with a gradient mixture of EtOAc-MeOH (1:0 to 0:1). Twenty-two fractions were collected and combined based on their TLC patterns (solvent system: EtOAc-MeOH = 7:3) to give 6 fractions: B5A (5 mg), B5B (12 mg), B5C (11 mg), B5D (4 mg), B5E (18 mg), B5F (29 mg).

Fraction B5E (18 mg) was further separated by repeated flash column chromatography (FCC) using a gradient mixture of CH_2Cl_2-MeOH (1:0 to 0:1) as the eluent. All fractions were examined and combined according to their TLC (mobile phase: CH_2Cl_2-MeOH = 7:3) to give 4 fractions: B5E1 (8 mg), B5E2 (1 mg), B5E3 (2 mg), B5E4 (9 mg). Compound PF-2 was obtained from fraction B5E4 as a yellow amorphous solid (9 mg, R_f 0.31, silica gel, CH_2Cl_2-MeOH = 7:3). It was characterized as a new compound and named pseuduvarioside [**26**].

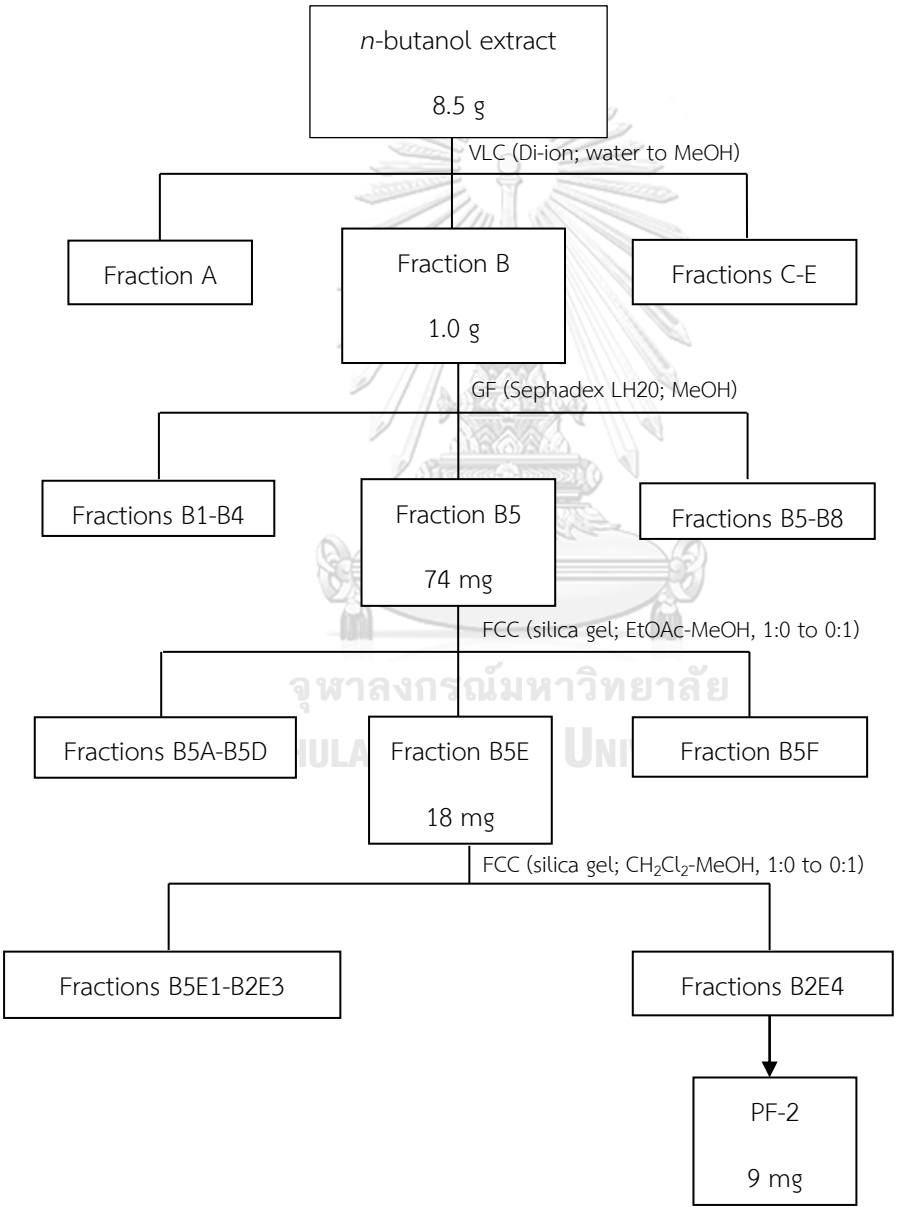

Scheme 3 Separation of the *n*-butanol extract prepared from the leaves of *Pseuduvaria fragrans*

3.1.3.2 Isolation of compound PF-3 [(+)-isocorydine]

Gel filtration chromatography of fraction C (1.3 g) on a Sephadex LH20 column eluted with MeOH (**Scheme 4**) afforded 22 fractions. Each fraction was examined by TLC (solvent system: EtOAc-MeOH = 8:2) under UV light and with Dragendorff's reagent. They were combined into 8 fractions: C1 (108 mg), C2 (720 mg), C3 (192 mg), C4 (105 mg), C5 (38 mg), C6 (13 mg), C7 (18 mg), C8 (15 mg).

Fraction C2 (720 mg) was separated on a silica gel column. Elution was performed in a polarity gradient manner with the mixtures of CH_2Cl_2-MeOH (1:0 to 0:1). A total of 14 fractions were collected. Fractions with similar TLC patterns (mobile phase: CH_2Cl_2-MeOH = 8:2, spraying with Dragendorff's reagent) were combined into 11 fractions: C2A (5 mg), C2B (9 mg), C2C (54 mg), C2D (21 mg), C2E (70 mg), C2F (91 mg), C2G (25 mg), C2H (20 mg), C2I (75 mg), C2J (162 mg), C2K (128 mg).

Fraction C2K (128 mg) was further separated by preparative RP18 HPLC (Shim-pack Prep-ODS) (with MeOH-H_2O = 1:1 as eluent, flow rate 1 ml/min.) to give 3 fractions: C2K1 (46 mg), C2K2 (48 mg), C2K3 (11 mg).

Fraction C2K2 (48 mg) was purified by repeated preparative RP18 HPLC (Shim-pack Prep-ODS) (with MeOH-H_2O = 1:1 as eluent, flow rate 1 ml/min.) to give compound PF3 as a yellow amorphous solid (11 mg, R_f 0.24, C-18 RP18, MeOH-H_2O = 1:1, spraying with Dragendorff's reagent). It was identified as (+)-isocorydine [**27**].

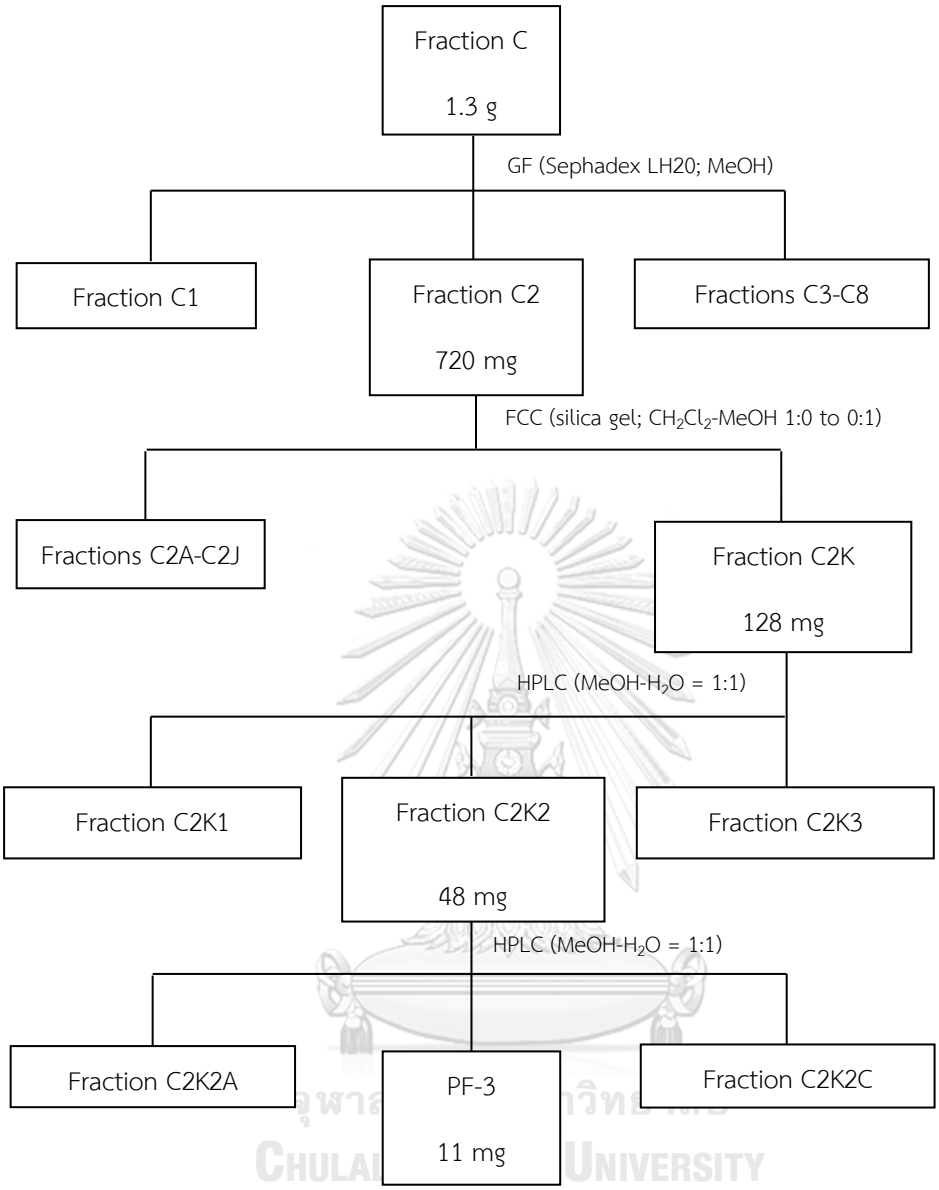

Scheme 4 Separation of fraction C of *n*-butanol extract prepared from the leaves of *Pseuduvaria fragrans*

3.2 Stems of *Pseuduvaria fragrans*

3.2.1 Extraction

The dried stems of *Pseuduvaria fragrans* (898.7 g) were chopped into small pieces and then macerated with methanol (3×5 L) for 24 hours. The filtrates were pooled and evaporated under reduced pressure at temperature not exceeding 40°C to afford a methanolic crude extract (64.5 g). The extract did not exhibit cytotoxic activity at 50 µg/mL but showed 66.16% inhibition α-glucosidase inhibitory

activity at the concentration of 200 μg/mL. This material was then suspended in water and partitioned with hexane, EtOAc and *n*-butanol, respectively, to give hexane extract (3.8 g), EtOAc extract (4.2 g), *n*-butanol extract (18.5 g), and aqueous extract (41.0 g). (**Scheme 5**).

All extracts were tested for α-glucosidase inhibitory activity. The hexane and EtOAc extracts showed high activity with 99.46% and 76.96% inhibition at a concentration of 200 μg/mL, respectively. The *n*-butanol and aqueous extracts were inactive at this concentration.

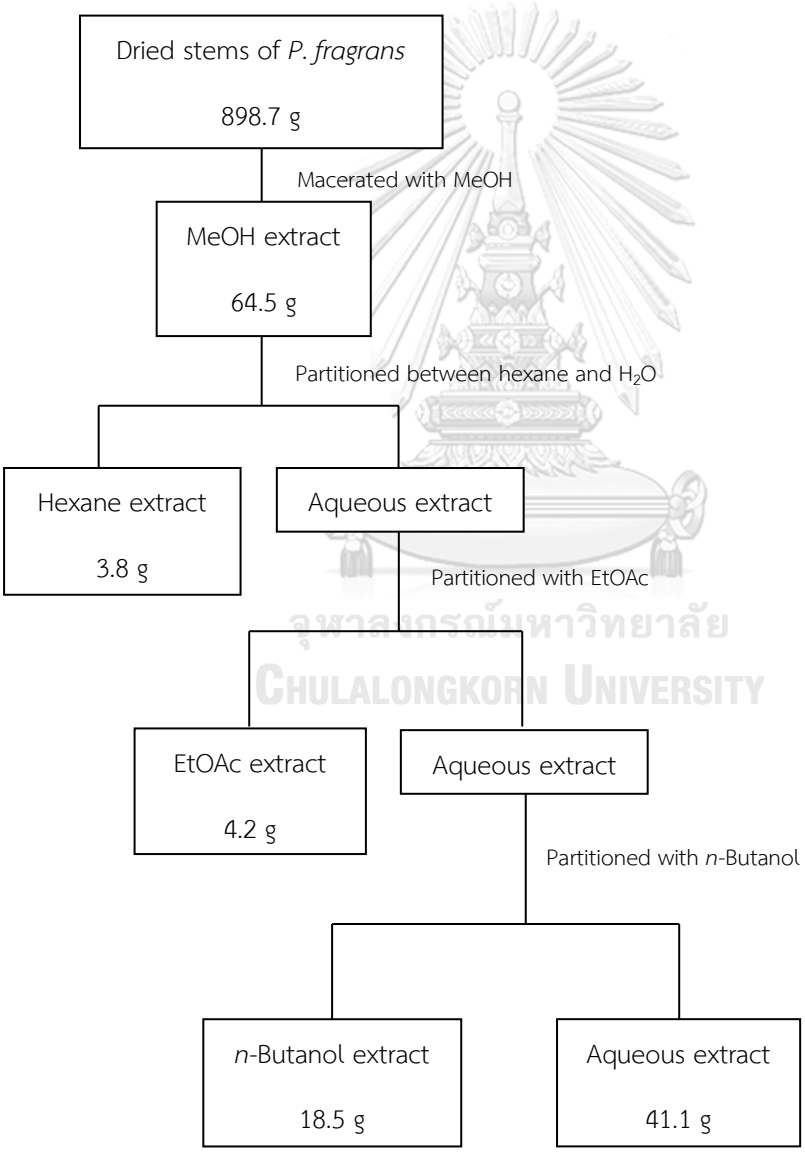

Scheme 5 Separation of the MeOH extract prepared from the stems of *Pseuduvaria fragrans*

3.2.2 Separation of hexane extract

The hexane extract (3.8 g) was separated by silica gel flash column chromatography (FCC) (**Scheme 6**). Elution was performed in a polarity gradient manner with mixtures of hexane-EtOAc (1:0 to 0:1). The eluates were examined by TLC (silica gel, hexane-EtOAc = 8:2). Thirty-three collected fractions with similar chromatographic patterns were combined to yield 16 fractions: A (116 mg), B (816 mg), C (1.0 g), D (439 mg), E (2 mg), F (74 mg), G (320 mg), H (56 mg), I (141 mg), J (509 mg), K (182 mg), L (96 mg), M (78 mg), N (216 mg), O (100 mg), P (210 mg).

3.2.2.1 Isolation of compound PF-4 (cyathocaline)

Fraction I (141 mg) was recrystallized from a mixture of hexane-EtOAc (1:1) to give compound PF-4 as a yellow crystalline solid. (9 mg, R_f 0.31, silica gel, hexane-EtOAc = 1:1, spraying with Dragendorff's reagent). It was identified as cyathocaline [**29**].

3.2.2.2 Isolation of compound PF-5 (isoursuline)

Fraction J (509 mg) was separated on a Sephadex LH20 column, eluted with MeOH. Fractions were combined according to their TLC patterns (silica gel, hexane-EtOAc = 1:1) to yield 9 fractions: J1 (9 mg), J2 (172 mg), J3 (218 mg), J4 (62 mg), J5 (5 mg), J6 (6 mg), J7 (19 mg), J8 (5 mg), J9 (3 mg)

Fraction J7 (19 mg) was subjected to flash column chromatography on a silica gel column. The elution was performed in a polarity manner with mixtures of hexane-EtOAc (1:0 to 0:1) and monitored by TLC (mobile phase: hexane-EtOAc = 8:2) to give compound PF-5 as a yellow crystalline solid (14 mg, R_f 0.45, silica gel, hexane-EtOAc = 8:2, spraying with Dragendorff's reagent) after removal of the solvent. It was identified as isoursuline [**30**].

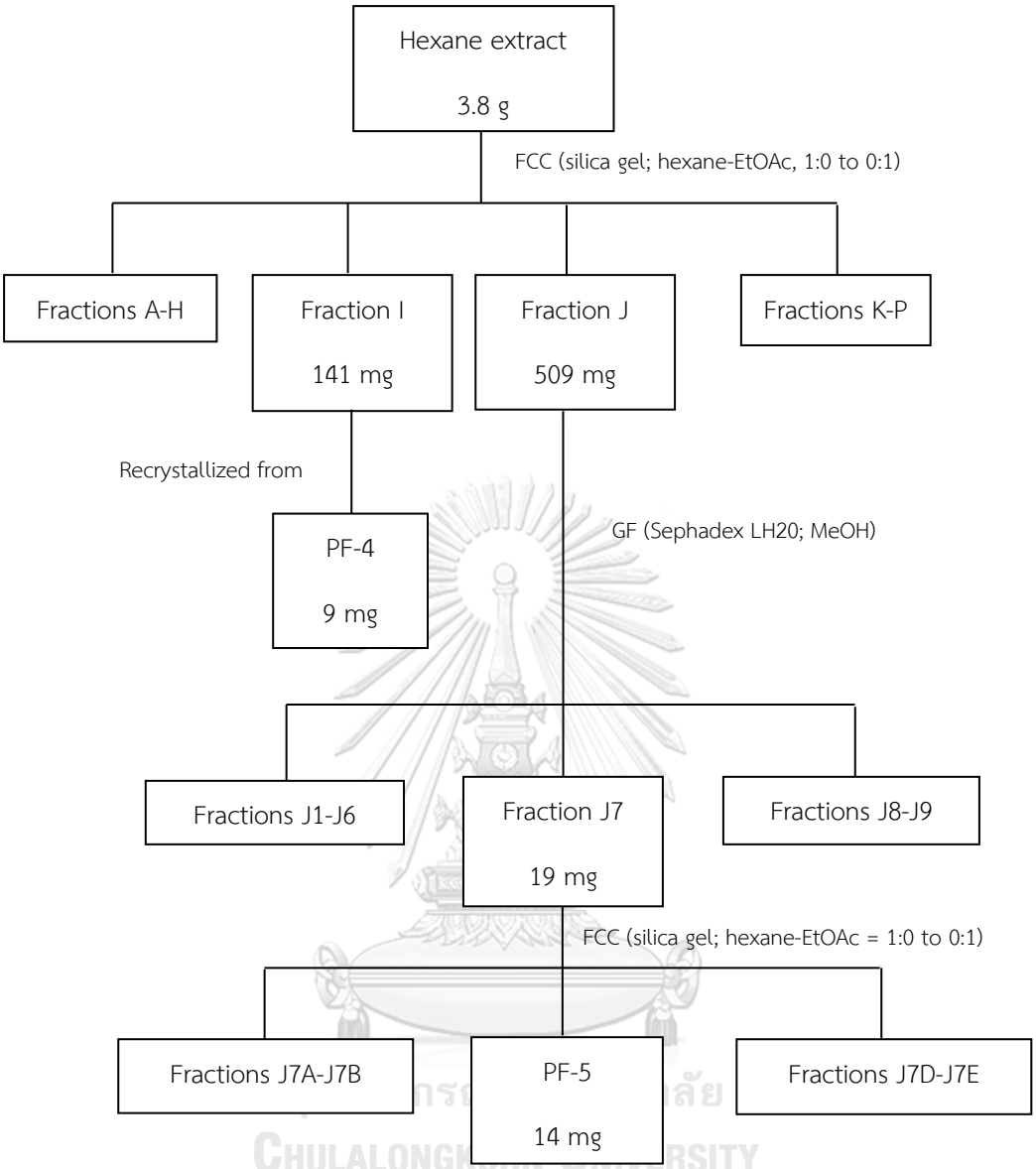

Scheme 6 Separation of the hexane extract prepared from the stems of *Pseuduvaria fragrans*

3.2.3 Separation of EtOAc extract

The EtOAc extract (4.2 g) was fractionated by silica gel flash column chromatography (FCC) (**Scheme 7**). Elution was performed in a polarity gradient manner with mixtures of hexane-EtOAc (1:0 to 0:1). The eluates were examined by TLC (silica gel, hexane-EtOAc = 8:2 and 6:4). Fractions with similar chromatographic patterns were combined to yield 12 fractions: A (40.7 mg), B (14 mg), C (31 mg), D (105 mg), E (250 mg), F (334 mg), G (145 mg), H (223 mg), I (321 mg), J (256 mg), K (128 mg), L (2.1 g).

3.2.3.1 Isolation of compound PF-6 (*N-trans*-feruloyltyramine)

Fraction I (321 mg) was separated on a Sephadex LH20 column, eluted with MeOH. Fractions (28 fractions) were collected and combined according to their TLC patterns (silica gel, hexane-acetone = 6:4) to yield 10 fractions: I1 (61 mg), I2 (89 mg), I3 (67 mg), I4 (23 mg), I5 (24 mg), I6 (14 mg), I7 (0 mg), I8 (2 mg), I9 (1 mg), I10 (1 mg)

Fraction I3 (67 mg) was further separated on a silica gel column using hexane-acetone mixtures (1:0 to 0:1) as the mobile phase. Thirty fractions were collected and combined according to their TLC patterns (solvent system: hexane:acetone = 6:4) into twelve fractions: I3A (4 mg), I3B (1 mg), I3C (2 mg), I3D (2 mg), I3E (3 mg), I3F (10 mg), I3G (5 mg), I3H (5 mg), I3I (4 mg), I3J (31 mg), I3K (4 mg), I3L (13 mg).

Fraction I3J (31 mg) was separated by silica gel flash column chromatography (FCC) using gradient mixtures of hexane-EtOAc (1:0 to 0:1) to afford compound PF-6 as a yellow amorphous solid (9 mg, R_f 0.28, silica gel, hexane-EtOAc = 4:6, spraying with Dragendorff's reagent). It was later identified as *N-trans*-feruloyltyramine [**31**].

3.2.3.2 Isolation of compound PF-7 (*N*-trans-coumaroyltyramine)

Fraction I4 (23 mg) was separated by silica gel flash column chromatography (FFC) (gradient mixture of hexane-acetone 1:0 to 0:1) to give seven fractions: I4A (4 mg), I4B (1 mg), I4C (6 mg), I4D (3 mg), I4E (6 mg), I4F (14 mg), I4G (7 mg).

Fraction I4G (7 mg) was recrystallized from hexane-acetone (1:1) to give compound PF-7 as a white amorphous solid (5 mg, R_f 0.31, silica gel, hexane-acetone = 6:4, spraying with Dragendorff's reagent). It was identified as *N-trans*-coumaroyltyramine [**32**].

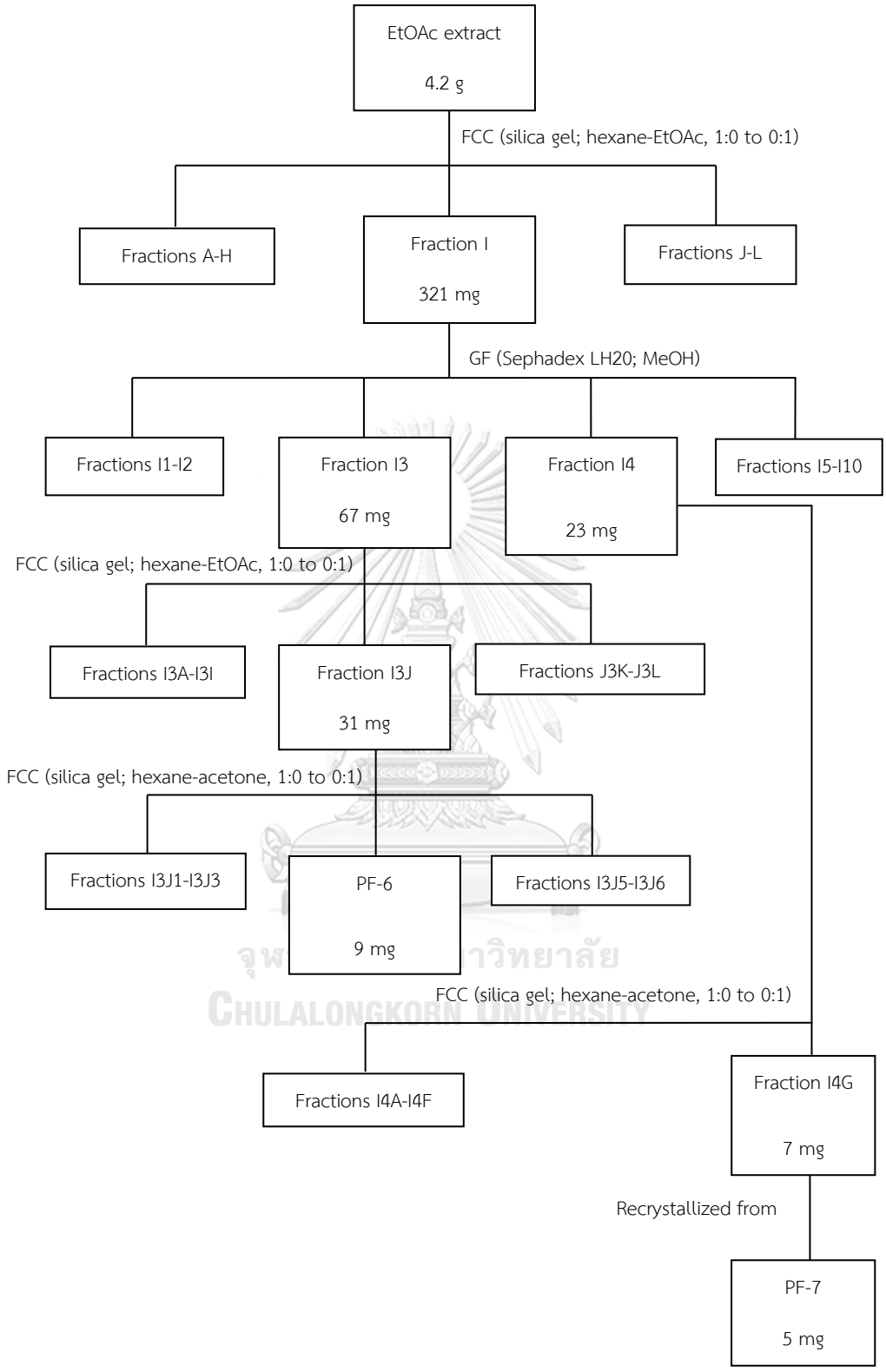

Scheme 7 Separation of the EtOAc extract prepared from the stems of *Pseuduvaria fragrans*

4. Physical and spectral data of isolated compounds

4.1 Compound PF-1 [(-)-guaiol]

Compound PF-1 was obtained as white crystals (43 mg, 0.0168 % based on dried weight of leaves). It was soluble in CH_2Cl_2.

HR-ESI-MS : $[M+Na]^+$ ion at *m/z* 245.1886 ($C_{15}H_{26}ONa$); **Figure 9**

$[\alpha]^{25}_D$: -20.33° (*c* 0.10; MeOH)

^{1}H NMR : δ ppm, 300 MHz, in $CDCl_3$; see **Table 5**, **Figure 10**

^{13}C NMR : δ ppm, 75 MHz, in $CDCl_3$; see **Table 5**, **Figure 11**

4.2 Compound PF-2 (pseuduvarioside)

Compound PF-2 was obtained as a yellow amorphous solid (9 mg, 0.0037 % based on dried weight of leaves). It was soluble in methanol.

HR-ESI-MS : $[M+Na]^+$ ion at *m/z* 593.1485 ($C_{25}H_{30}O_{15}Na$); **Figure 16**

$[\alpha]^{25}_D$: +22.33° (*c* 0.10; MeOH)

UV : λ_{max} (log **ε**), in methanol: 203 (4.19), 230 (3.94), 275 (3.78); **Figure 17**

FT-IR : ν_{max} cm^{-1} (KBr) : 3400, 1731, **Figure 18**

^{1}H NMR : δ ppm, 300 MHz, in CD_3OD; see **Figure 19**, **Table 6**

^{13}C NMR : δ ppm, 75 MHz, in CD_3OD; see **Figure 21**, **Table 6**

4.3 Compound PF-3 [(+)-isocorydine]

Compound PF-3 was obtained as a yellow amorphous solid (11 mg, 0.0043 % based on dried weight of leaves). It was soluble in methanol.

HR-ESI-MS : $[M+H]^+$ ion at *m/z* 342.1702 ($C_{20}H_{24}NO_4$); **Figure 27**

$[\alpha]^{25}_D$: +139.58° (*c* 0.1; MeOH)

UV : λ_{max} (log **ε**), in methanol: 204 (4.20), 230 (4.25), 275 (3.62), 320 (3.55)

Figure 28

^{1}H NMR : δ ppm, 300 MHz, in CD_3OD; see **Table 7**, **Figure 29**

^{13}C NMR : δ ppm, 75 MHz, in CD_3OD; see **Table 7**, **Figure 30**

4.4 Compound PF-4 (cyathocaline)

Compound PF-4 was obtained as a yellow crystalline solid (9 mg, 0.0010 % based on dried weight of stems). It was soluble in methanol.

HR-ESI-MS : $[M+H]^+$ ion at *m/z* 258.0754 ($C_{14}H_{12}NO_4$); **Figure 34**

UV : λ_{max} (log **ε**), in methanol: 210 (4.04), 260 (4.33), 310 (4.01), 355 (3.33); **Figure 35**

^{1}H NMR : δ ppm, 300 MHz, in CD_3OD; see **Table 8**, **Figure 36**

^{13}C NMR : δ ppm, 75 MHz, in CD_3OD; see **Table 8**, **Figure 37**

4.5 Compound PF-5 (isoursuline)

Compound PF-5 was obtained as a yellow crystalline solid (14 mg, 0.0015 % based on dried weight of stems). It was soluble in methanol.

HR-ESI-MS : $[M+H]^+$ ion at *m/z* 242.0824 ($C_{14}H_{12}NO_3$); **Figure 40**

UV : λ_{max} (log **ε**), in methanol: 205 (4.11), 250 (4.38), 290 (3.84), 305 (3.82), 370 (3.58); **Figure 41**

^{1}H NMR : δ ppm, 300 MHz, in $CDCl_3$; see **Table 9**, **Figure 42**

^{13}C NMR : δ ppm, 75 MHz, in $CDCl_3$; see **Table 9**, **Figure 43**

4.6 Compound PF-6 (*N-trans*-feruloyltyramine)

Compound PF-6 was obtained as a yellow amorphous solid (9 mg, 0.0010 % based on dried weight of stems). It was soluble in methanol.

HR-ESI-MS : $[M+Na]^+$ ion at *m/z* 336.1211 ($C_{18}H_{19}NO_4Na$); **Figure 47**

UV : λ_{max} (log **ε**), in methanol: 220 (4.25), 295 (4.10), 315 (4.13); **Figure 48**

^{1}H NMR : δ ppm, 300 MHz, in CD_3OD; see **Table 10**, **Figure 49**

^{13}C NMR : δ ppm, 75 MHz, in CD_3OD; see **Table 10**, **Figure 51**

4.7 Compound PF-7 (*N-trans*-coumaroyltyramine)

Compound PF-7 was obtained as a white amorphous solid (5 mg, 0.0005 % based on dried weight of stems). It was soluble in methanol.

HR-ESI-MS : $[M+Na]^+$ ion at *m/z* 306.1112 ($C_{17}H_{17}NO_3Na$); **Figure 55**

UV : λ_{max} (log **ε**), in methanol: 225 (4.34), 290 (4.39), 310 (4.38); **Figure 56**

^{1}H NMR : δ ppm, 300 MHz, in CD_3OD; see **Table 11**, **Figure 57**

^{13}C NMR : δ ppm, 75 MHz, in CD_3OD; see **Table 11**, **Figure 58**

5. Evaluation of cytotoxicity

The cytotoxicity assays in this study were done at the Bioassay Laboratory, National Center for Genetic Engineering and Biotechnology (BIOTEC).

5.1 Cytotoxicity against primate cell lines

The cytotoxicity assays were performed against three human cancer cell lines, including KB (oral epidermal carcinoma), NCI-H187 (small cell lung carcinoma) and MCF-7 (breast cancer) cells. The test was performed using the resazurin microplate assay method (REMA) (O'Brien *et al*., 2000), with ellipticine, doxorubicin and tamoxifen as positive controls and 0.5% DMSO as negative control. The samples were diluted to 50 µg/mL for the final test concentration. The protocols were as follows:

1. Cells at a logarithmic growth phase were harvested and diluted to $7X10^4$ cells/mL for KB and $9X10^4$ cells/mL for MCF-7 and NCI-H187 cell lines in fresh medium.

2. Successively, 5 µL of test sample was diluted in 5% DMSO, and 45 µL of cell suspension were added, and the mixture was incubated at 37°C in 5% CO_2 incubator.

3. After incubation (3 days for KB and MCF-7, and 5 days for NCI-H187), 12.5 µL of 62.5 µg/mL resazurin solution were added to each well, and the plate was then incubated at 37°C for 4 hours.

4. Fluorescence signal was measured using a SpectraMax M5 multi-detection microplate reader (Molecular Devices, USA) at the excitation and emission wavelengths of 530 nm and 590 nm, respectively. Percent inhibition of cell growth was calculated using the following equation:

$$\% \text{ Inhibition} = [1-(FU_T/FU_C) \times 100]$$

Whereas, FU_T and FU_C are the mean fluorescent unit from treated and untreated conditions, respectively. Dose response curves were plotted from 6 concentrations of 2-fold serially diluted test compounds and the concentrations that inhibited cell growth by 50% (IC_{50}) were derived using the SOFTMax Pro software (Molecular Devices, USA).

The sample was considered active if percent inhibition was more than 50.

6. α-Glucosidase inhibitory activity assay

The enzyme α-glucosidase (α-D-glucoside glucohydrolase) is an exo-type carbohydrase distributed widely in microorganisms, plants and animal tissues, which catalyzes the liberation of α-glucose from the non-reducing end of the substrate (Kumar *et al*., 2011). The clinically useful α-glucosidase inhibitors, including acarbose, miglitol and voglibose, can bind to α-glucosidase and competitively inhibit the enzyme in the small intestine to delay the expeditious generation of blood glucose (He *et al*., 2013). α-Glucosidase inhibitors from plants can be classified as flavonoids, alkaloids, phenolic compounds, quinines and terpinoids (Yin *et al*., 2014).

6.1 Materials and instruments

- Acarbose (Fluka Chemical, USA)
- *p*-Nitrophenyl-α-D-glucopyranoside (*p*NPG) (Sigma-Aldrich, USA)
- α-Glucosidase enzyme (Sigma-Aldrich, USA)

- Sodium carbonate (Na_2CO_3) (Sigma-Aldrich, USA)
- Wallac1420 Multilevel counter, Victor3, Microplate reader (PerkinElmer)
- Transsonic 570/H, Ultrasonic bath (Elma)
- Vortex-Genie2, Vortex mixer (Scientific Industries)

6.2 Determination of α-glucosidase inhibitory activity

The α-glucosidase inhibitory activity was evaluated by monitoring the release of *p*-nitrophenol from *p*-nitrophenyl-α-D-glucopyranoside (*p*NPG). Each test sample was initially prepared in 50% DMSO. Briefly, 10 µL of test sample was mixed in a 96-well plate with 40 µL of the enzyme α-glucosidase (0.1 unit/ml) in 0.1 M phosphate buffer (pH 6.8) in reaction system or 40 µL of the 0.1 M phosphate buffer (pH 6.8) in blank system and pre-incubated at 37 °C for 10 min. Then, 50 µL of 2 mM *p*NPG in 0.1 M phosphate buffer (pH 6.8) as a substrate was added to the mixture to start the reaction, and the mixture was incubated at 37°C for 20 min. The reaction was stopped by adding 100 µL of 0.1 mM Na_2CO_3. The absorbance was then measured at 405 nm using a microplate reader. 5% DMSO was used as a negative control. Acarbose was used as a positive control and treated under the same condition as the samples. The percentage of α-glucosidase inhibitory activity was calculated by the following equation:

$$\% \text{ α-glucosidase inhibitory activity} = [(A_{control} - A_{sample}) / A_{control}] \times 100$$

Where $A_{control}$ is the absorbance of sample without inhibitor, and A_{sample} is the absorbance of sample in the presence of the inhibitor. Each experiment was performed in triplicate. Data were displayed as mean ± SD.

6.3 Kinetic study of α-glucosidase enzyme inhibitory activity

The kinetic studies of enzyme inhibition were done in 96-well plates. The kinetic parameters were obtained by analyzing the Lineweaver-Burk plot (1/V vs. 1/[S]). The experiment was carried out by varying the concentration of *p*NPG [S] (2.0,

1.0, 0.5, 0.25, 0.125 mM) in the absence and presence of different concentrations of test sample. The reaction was monitored at 405 nm using a microplate reader (Wallac1420 Multilevel counter, Victor3, PerkinElmer) every 5 min for a total time of 30 min. The inhibition constant (K_i) was calculated using the secondary plot of the slope of double-reciprocal line versus the inhibitor concentration [I] for acarbose (Chatsumpun *et al*., 2017). For compounds PF-6 and PF7, the secondary plot was obtained by replotting the inverted values of K_m (1/ K_m) versus the inhibitor concentration [I]. The value of K_i was calculated from the intersection on the X axis (Palmer, 1994).

CHAPTER IV
RESULTS AND DISCUSSION

The dried, powdered leaves (252.9 g) and stems (898.7 g) of *Pseuduvaria fragrans* were separately extracted with methanol to yield 64.9 g and 64.5 g of methanol extracts, respectively. The methanol extract of the leaves exhibited cytotoxicity against small cell lung cancer (NCl-H 187) with 95.13% inhibition at 50 µg/mL but the methanol extract of the stem did not exhibit this activity at 50 µg/mL. These methanol extracts were able to inhibit more than 50% inhibition of α-glucosidase activity at the concentration of 200 µg/mL. Each methanol extract was then partitioned with hexane, EtOAc and *n*-butanol, respectively.

The hexane and EtOAc extracts derived from the methanol extract which was obtained from the leaves exhibited approximately 51.56% and 99.71% inhibition of α-glucosidase inhibitory activity at a concentration of 200 µg/mL, respectively. The *n*-butanol extract and aqueous extract did not show α-glucosidase inhibitory activity at concentration 200 µg/mL (< 50%). Chromatographic separation of the hexane extract gave a sesquiterpene (PF-1). The *n*-butanol extract was separated to give 2 compounds, which were characterized as a new benzophenone *C*-glycoside (PF-2) and an aporphine alkaloid (PF-3).

The hexane and EtOAc extracts derived from the methanol extract which was obtained from the stems showed 99.46% and 76.96% inhibition at a concentration of 200 µg/mL, respectively. The *n*-butanol extract and aqueous extract did not show α-glucosidase inhibitory activity at concentration 200 µg/mL. Two 4-aza-9-fluorenone alkaloids (PF-4 and PF-5) were obtained from the hexane extract. The EtOAc extract was separated to give 2 amide alkaloids (PF-6 and PF-7).

The structures of all compounds were determined by analysis of their UV, IR, MS and NMR spectral data. They were then examined for α-glucosidase inhibitory activity.

1. Structure determination of isolated compounds

1.1 Structure determination of compound PF-1

Compound PF-1 was obtained as white crystals. The HR-ESI mass spectrum (**Figure 9**) showed a sodium-adduct molecular ion $[M+Na]^+$ ion at *m/z* 245.1886 (calcd. for $C_{15}H_{26}ONa$; 245.1881), suggesting the molecular formula $C_{15}H_{26}O$.

The ^{1}H-NMR spectrum (**Figure 10** and **Table 5**) of this compound showed aliphatic proton signals at δ_H 0.96-2.53. There were signals for four methyls at δ_H 1.16 (3H, *s*, 13-CH_3), 1.14 (3H, *s*, 12-CH_3), 0.98 (3H, *d*, *J*= 7.2 Hz, 14-CH_3) and 0.96 (3H, *d*, *J*= 6.9 Hz, 15-CH_3).

The ^{13}C-NMR and DEPT spectra (**Figure 11** and **Table 5**) exhibited 15 carbon signals, which could be classified into those of four methyls [δ_C 27.4 (C-13), 26.0 (C-12), 19.8 (C-15) and 19.9 (C-14)], three methines [δ_C 49.6 (C-7), 46.3 (C-4) and 33.7 (C-10)], five methylenes [δ_C 35.4 (C-2), 33.8 (C-9), 30.9 (C-3), 27.9 (C-6) and 27.3 (C-8)], and three quaternary carbons [δ_C 140.0 (C-1), 138.9 (C-5) and 73.6 (C-11)]. These ^{13}C-NMR signals suggested a sesquiterpene structure.

The HSQC spectrum (**Figure 12**) exhibited cross peaks between the methyl protons at δ_H 1.16 (13-CH_3), 1.14 (12-CH_3), 0.98 (14-CH_3) and 0.96 (15-CH_3) and the carbons at δ_C 27.4 (C-13), 26.0 (C-12), 19.9 (C-14) and 19.8 (C-15), respectively. The HMBC correlations (**Figure 13**) from the protons of 14-CH_3 to C-10, C-9 and C-1, and from the protons of 15-CH_3 to C-5, C-4 and C-3 confirmed the positions of the methyl groups at C-10 and C-4, respectively. The protons of 12-CH_3 and 13-CH_3 were correlated to C-11, C-7. Moreover, the protons at δ_H 1.55 (*m*, H-9) and 1.68 (*m*, H-9) were correlated with the carbons at C-1 and C-8. The proton at δ_H 1.52 (*m*, H-7) was correlated with the carbons at C-5, C-6, C-9 and C-11. The proton at δ_H 2.27 (*m*, H-10) was correlated with the carbons at C-1, C-9 and 14-CH_3. The HMBC NMR data confirmed the guaiane skeleton of sesquiterpene.

Through comparison with previously reported data (Benovit *et al*., 2015), compound PF-1 was identified as (-)-guaiol [**25**].

(-)-Guaiol [**25**], a sesquiterpene alcohol, has been found in the essential oils of many plants such as *Callitris neocaledonica*, *C. sulcata* (Waikedre *et al*., 2012), *Helietta longifoliata* (Moura *et al*., 2002), *Aloysia* gratissima (Benovit *et al*., 2015), *Ocotea quixos* (Noriega *et al*., 2018) and *Nectandra lanceolate* (Costa *et al*., 2017). In Annonaceae, (-)-guaiol [**25**] was found in essential oils of *Xylopia elliptica* and *X. malayana* (Ghani *et al*., 2016), *Desmopsis bibracteata* and *Unonopsis costaricensis* (Palazzo *et al*., 2009) and in the genus *Alphonsea* (Bakri *et al*., 2017). This compound showed several bioactivities, for example, antibacterial activity against *Escherichia coli, Bacillus subtilis, Shigella flexneri, Pseudomonas aeruginosa,* and *Salmonella typhi* (Choudhary *et al*., 2007) and antiproliferation of non-small-cell lung cancer cells (Yang *et al*., 2018).

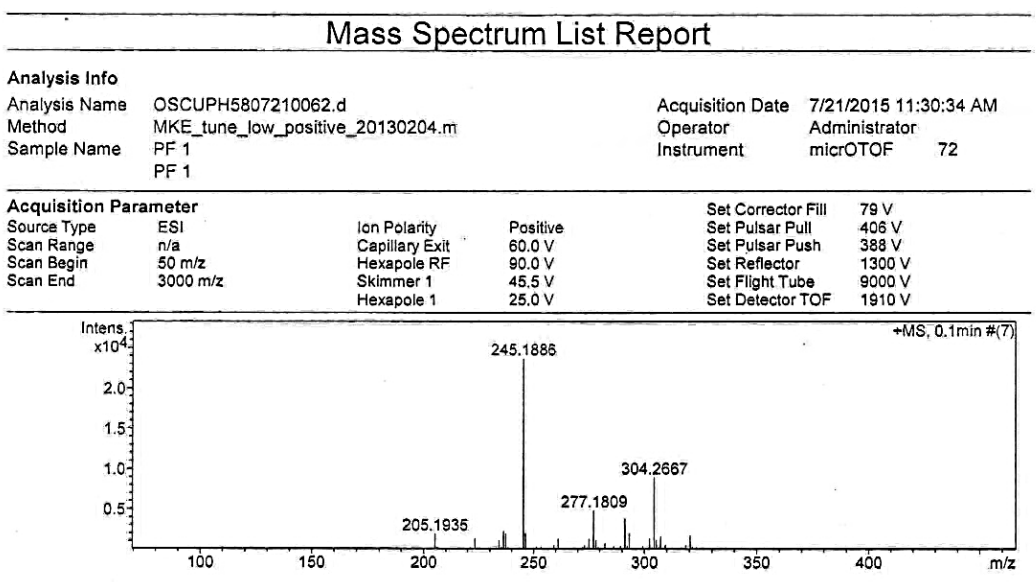

Figure 9 Mass spectrum of compound PF-1

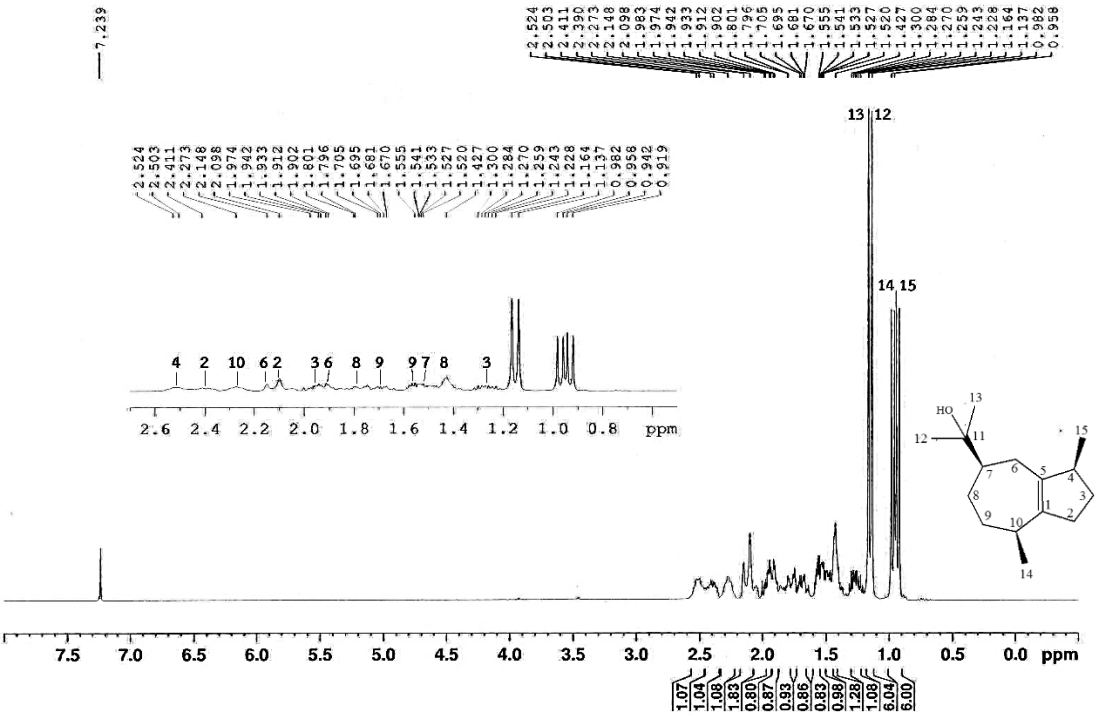

Figure 10 ^{1}H-NMR (300 MHz) Spectrum of compound PF-1 (in $CDCl_3$)

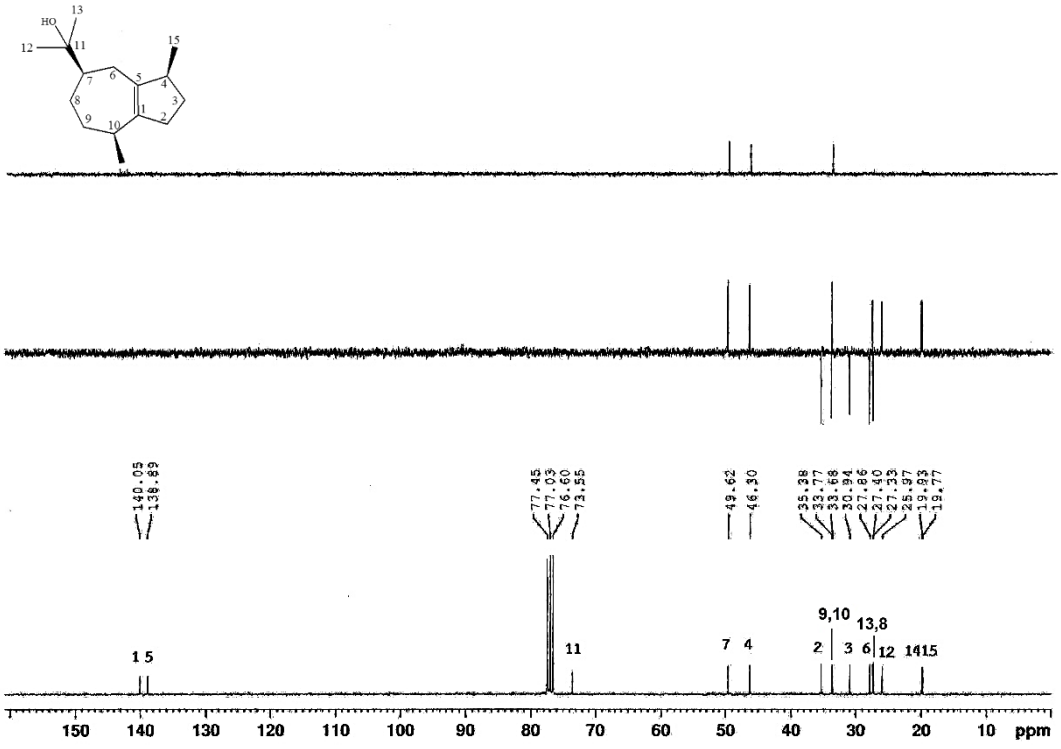

Figure 11 ^{13}C-NMR, DEPT135, DEPT90 (75 MHz) Spectra of compound PF-1 (in $CDCl_3$)

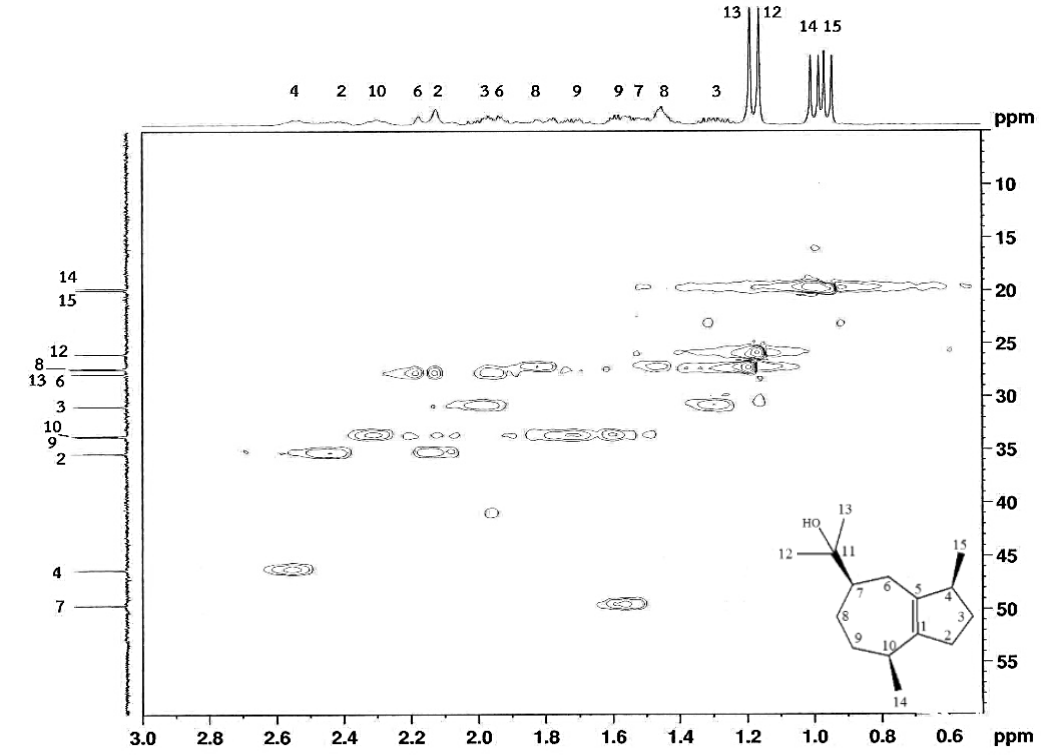

Figure 12 HSQC Spectrum of compound PF-1 (in $CDCl_3$)

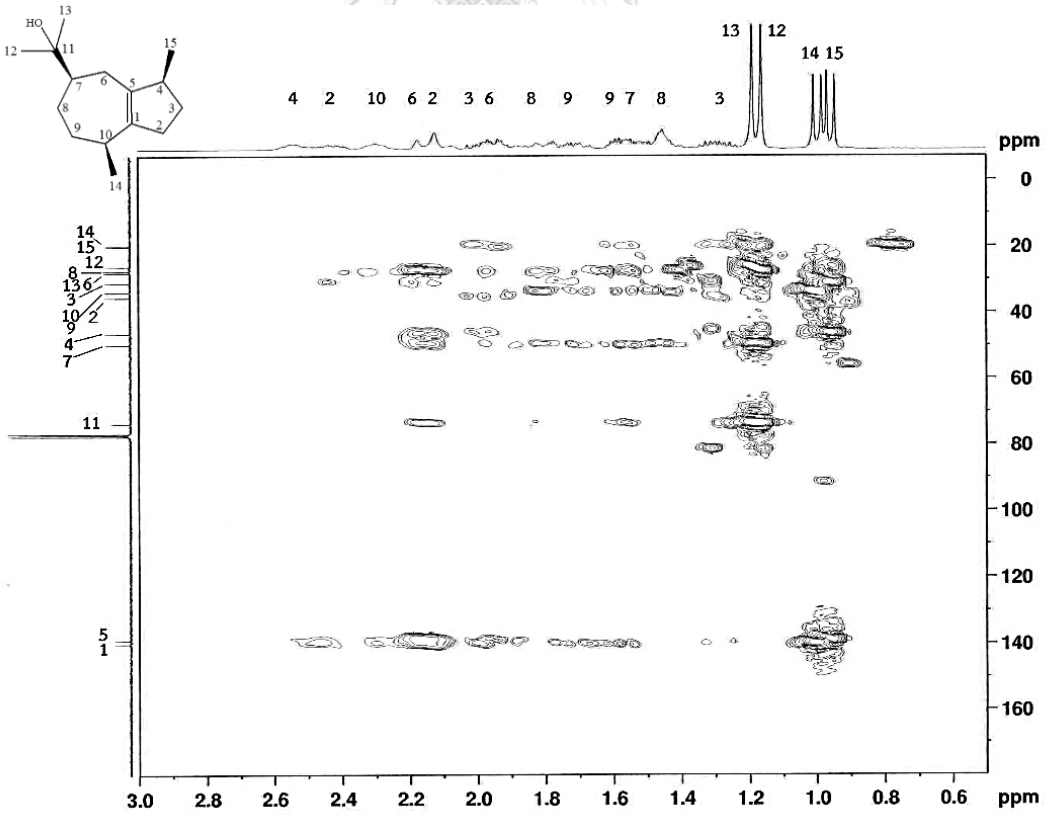

Figure 13 HMBC Spectrum of compound PF-1 (in $CDCl_3$)

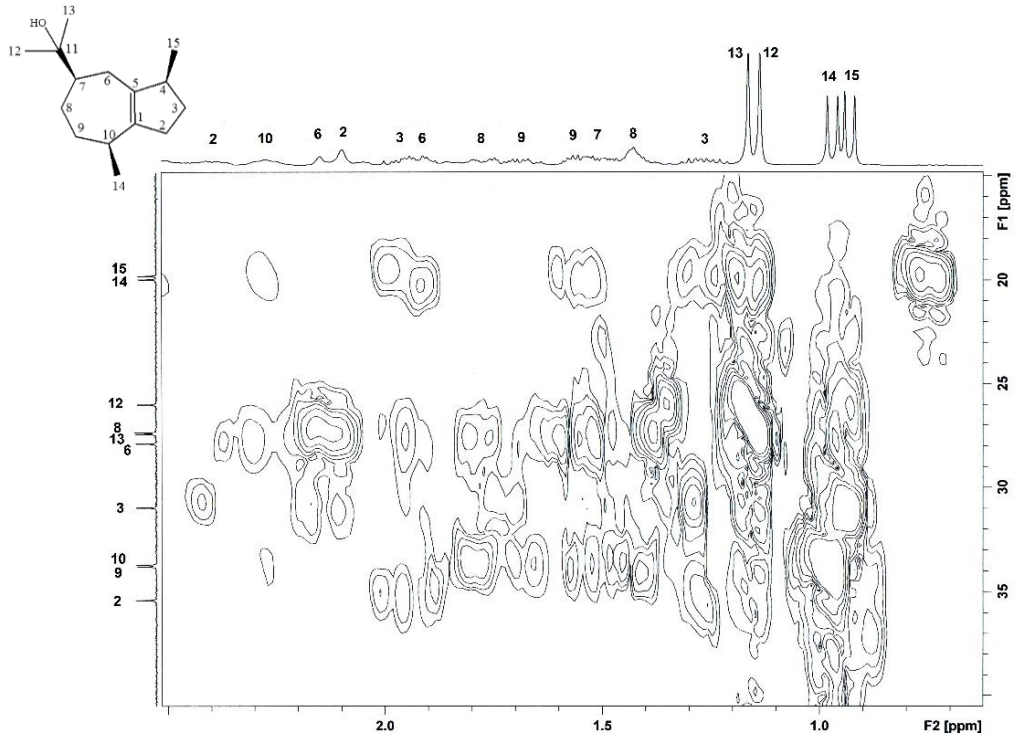

Figure 14 HMBC Spectrum of compound PF-1 (in $CDCl_3$)
[δ_H 0.0-3.0 ppm, δ_C 10-40 ppm]

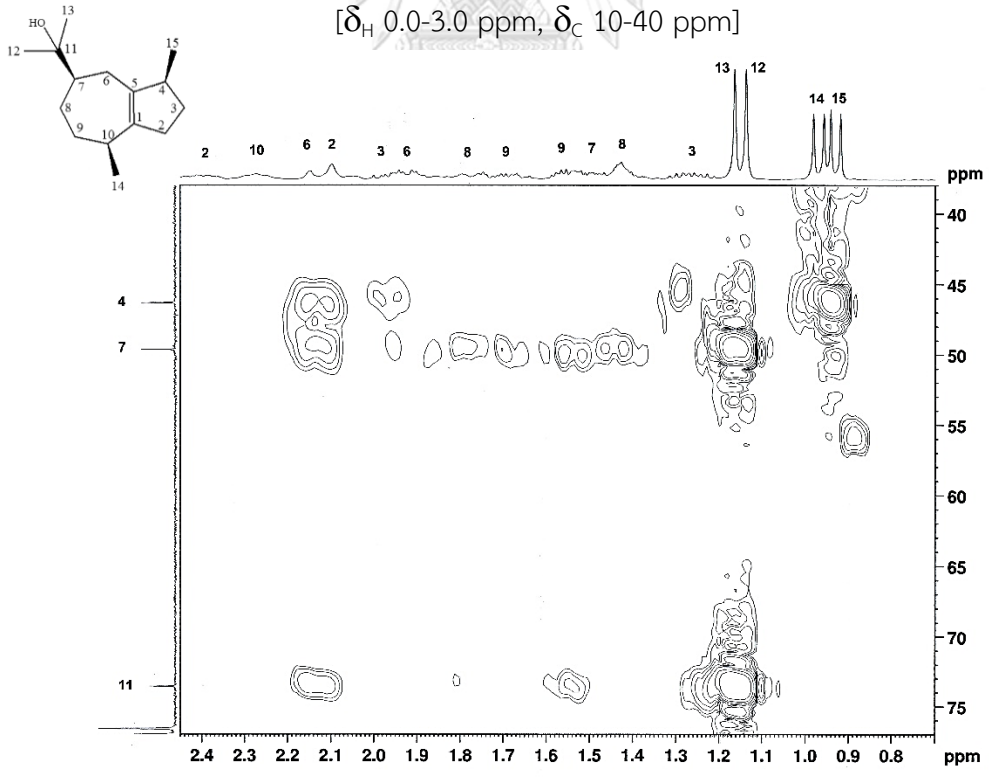

Figure 15 HMBC Spectrum of compound PF-1 (in $CDCl_3$)
[δ_H 0.7-2.5 ppm, δ_C 38-77 ppm]

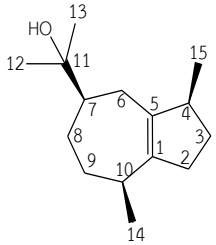

(-)-Guaiol (PF-1) [**25**]

Table 5 NMR Spectral data of compound PF-1 (in $CDCl_3$) and (-)-guaiol (in $CDCl_3$)

Position	Compound PF-1		(-)-Guaiol [25][a]	
	δ_H (mult., *J* in Hz)	δ_C	δ_H (mult., *J* in Hz)	δ_C
1	-	140.0	-	140.07
2	2.10 (*m*), 2.41 (*m*)	35.4	2.05, 2.41 (both *m*)	35.34
3	1.27 (*m*), 1.97 (*m*)	30.9	1.27, 1.95 (both *m*)	30.91
4	2.52 (*m*)	46.3	2.52 (*dd*)	46.27
5	-	138.9	-	138.69
6	1.91 (*m*), 2.15 (*m*)	27.9	1.87, 2.13 (*dd*, m)	27.80
7	1.52 (*m*)	49.6	1.52 (*m*)	49.59
8	1.43 (*m*), 1.80 (*m*)	27.3	1.44 ,1.80 (both *m*)	27.26
9	1.55 (*m*), 1.68 (*m*)	33.8	1.55, 1.70, (both *m*)	33.73
10	2.27 (*m*)	33.7	2.28 (*m*)	33.64
11	-	73.6	-	73.48
12	1.14 (*s*)	26.0	1.14 (*s*)	25.93
13	1.16 (*s*)	27.4	1.17 (*s*)	27.31
14	0.98 (*d*, 7.2)	19.9	0.97 (*d*)	19.69
15	0.96 (*d*, 6.9)	19.8	0.93 (*d*)	19.88

[a]Benovit *et al*., 2015

1.2 Structure determination of compound PF-2

Compound PF-2 was obtained as a yellow amorphous solid. The HR-ESI mass spectrum (**Figure 16**) showed a sodium-adduct molecular ion $[M+Na]^+$ ion at *m/z* 593.1485 (calcd. for $C_{25}H_{30}O_{15}Na$; 593.1482), suggesting the molecular formula $C_{25}H_{30}O_{15}$. Its UV spectrum (**Figure 17**) showed λ_{max} at 203, 230, 275 nm. The IR spectrum (**Figure 18**) displayed absorption bands for hydroxyl (3400 cm^{-1}) and ketone (1731 cm^{-1}) functionalities.

The ^{1}H-NMR (CD_3OD) spectrum of PF-2 (**Figure 19** and **Table 6**) exhibited *ortho*-coupled signals at δ_H 7.47 (1H, *d*, *J* = 8.1 Hz, H-6) and δ_H 6.65 (1H, *d*, *J* = 8.1 Hz, H-5). In addition, an anomeric proton of a sugar unit was present at δ_H 4.84. However, the splitting pattern was not clear due to the overlapping with the residual water signal. The ^{1}H-NMR spectrum of PF-2 in DMSO-d_6 (**Figure 20**) showed this anomeric proton at δ_H 4.65 (1H, *d*, *J* = 9.6 Hz, H-1′).

The ^{13}C-NMR, DEPT 135 and DEPT 90 spectra (**Figure 21** and **Table 6**) exhibited 13 signals which could be assigned to a keto-carbonyl carbon at δ_C 198.6, four quaternary carbons at δ_C 162.6 (C-4), 160.6 (C-2), 133.9 (C-1) and 105.2 (C-3), seven methines at δ_C 132.5 (C-6), 115.5 (C-5), 82.5 (C-5′), 80.0 (C-3′), 77.3 (C-1′), 74.3 (C-2′) and 71.1 (C-4′) and a methylene at δ_C 62.1 (C-6′). These ^{13}C-NMR data, together with the molecular formula suggested that PF-2 had a symmetrical structure.

The HSQC spectrum (in CD_3OD) (**Figure 22**) showed that the signals of two aromatic protons at δ_H 7.47 (1H, *d*, *J* = 8.1 Hz, H-6) and δ_H 6.65 (1H, *d*, *J* = 8.1 Hz, H-5) were correlated with the carbons at δ_C 132.5 (C-6) and 115.5 (C-5). Six aliphatic protons at δ_H 4.48 (H-1′), 3.70 (1H, *m*, H-2′). 3.68 (2H, *d*, *m*, H-6′), .3.38 (2H, *m*, H-3′ and H-4′) and 3.30 (1H, *s*, H-5′) were correlated with the carbons at δ_C 77.3 (C-1′), 74.3 (C-2′), 62.1 (C-6′),.80.0 (C-3′), 71.1 (C-4′) and 82.5 (C-5′), respectively. The anomeric proton was assigned from the HSQC spectrum in DMSO-d_6 (**Figure 23**) and suggested that compound PF-2 should have two β-D-glucopyranosyl moieties. In the

HMBC spectrum (**Figure 24**) the three-bond correlation of the anomeric proton H-1′ (δ_H 4.84) with the aromatic carbons at C-4, C-3 and C-2 and glucosyl moiety at C-5′, C-3′ and C-2′ indicated that the hexose moiety was connected to the aromatic ring at C-3. The signal of H-6 (δ_H 7.47) was correlated with the carbonyl carbon and C-4 in the HMBC spectrum, and the proton signal at δ_H 7.47 (H-6) showed cross peak with the proton signal at δ_H 6.65 (H-5) in the NOESY spectrum (**Figure 25**).

In nature, benzophenone *C*-glycosides have been found in *Aquilaria sinensis* (Wang *et al*., 2015), *Cyclopia genistoides* (Kokotkiewicz *et al*., 2013) *Mangifera indica* (Abdel-Mageed *et al*., 2014; Zhang *et al*., 2011), *Malania oleifera* (Wu *et al*., 2012) and *Polygala telephioides* (Ting-Jun *et al*., 2008). Many previous studies have reported only one glucose moiety attached to the aglycone. This study has found two glucose moieties connected to the benzophenone structure. This compound showed similarity with known structures with regard to ^{1}H-NMR (CD_3OD) and (DMSO-d_6) and ^{13}C-NMR data (Abdel-Mageed *et al*., 2014; Kokotkiewicz *et al*., 2013; Zhang *et al*., 2011). Compound PF-2 was elucidated as new benzophenone *C*-glycoside and named pseuduvarioside [**28**] based on the above spectral data analysis.

The biosynthetic pathway for benzophenones (**Figure 26**) begins with the conversion of L-phenylalanine to benzoyl-CoA (via the shikimate pathway). Benzoyl-CoA is the preferred starter substrate for two type III polyketide synthases (PKSs), biphenyl synthase (BIS) and benzophenone synthase (BPS). BPS catalyzes the decarboxylative condensation of benzoyl-CoA with three molecules of malonyl-CoA to phlorbenzophenone (Beerhues *et al*., 2009; Joubert *et al*., 2014).

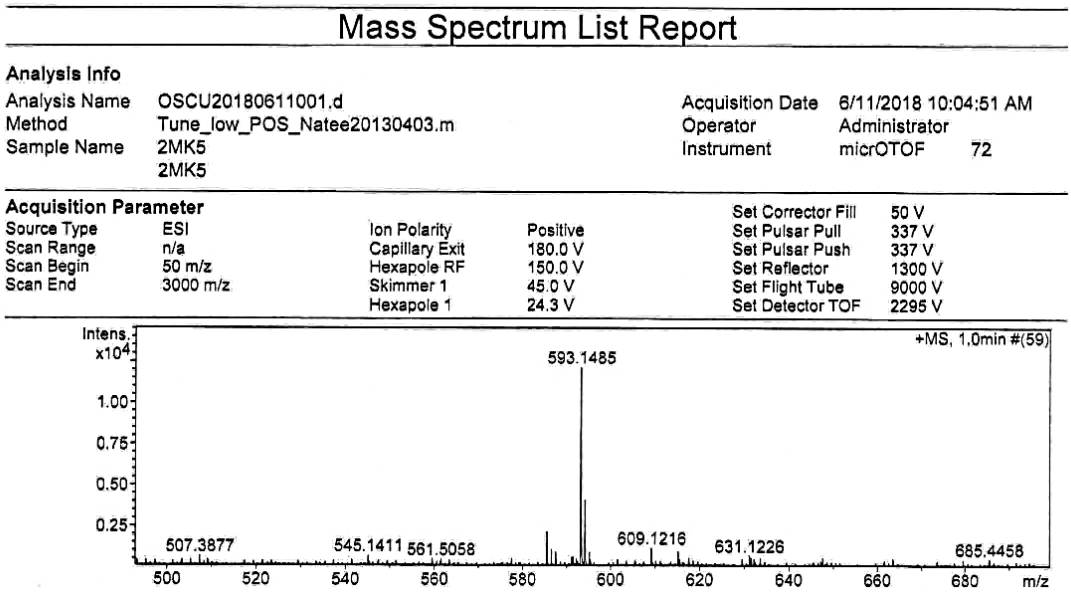

Figure 16 Mass spectrum of compound PF-2

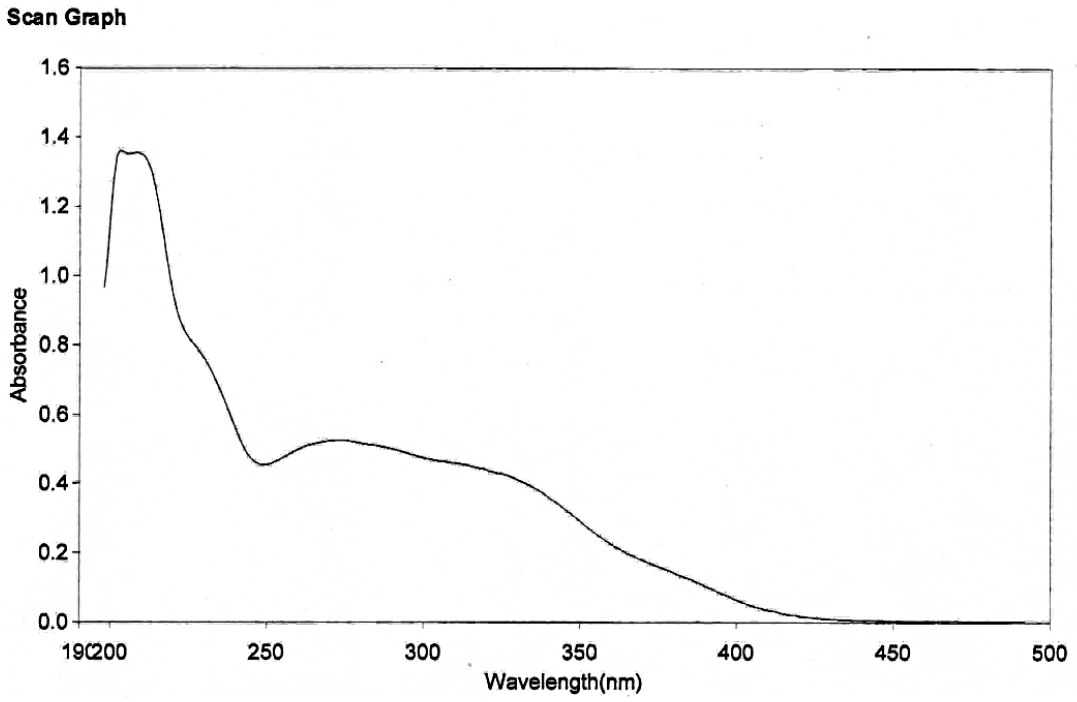

Figure 17 UV Spectrum of compound PF-2

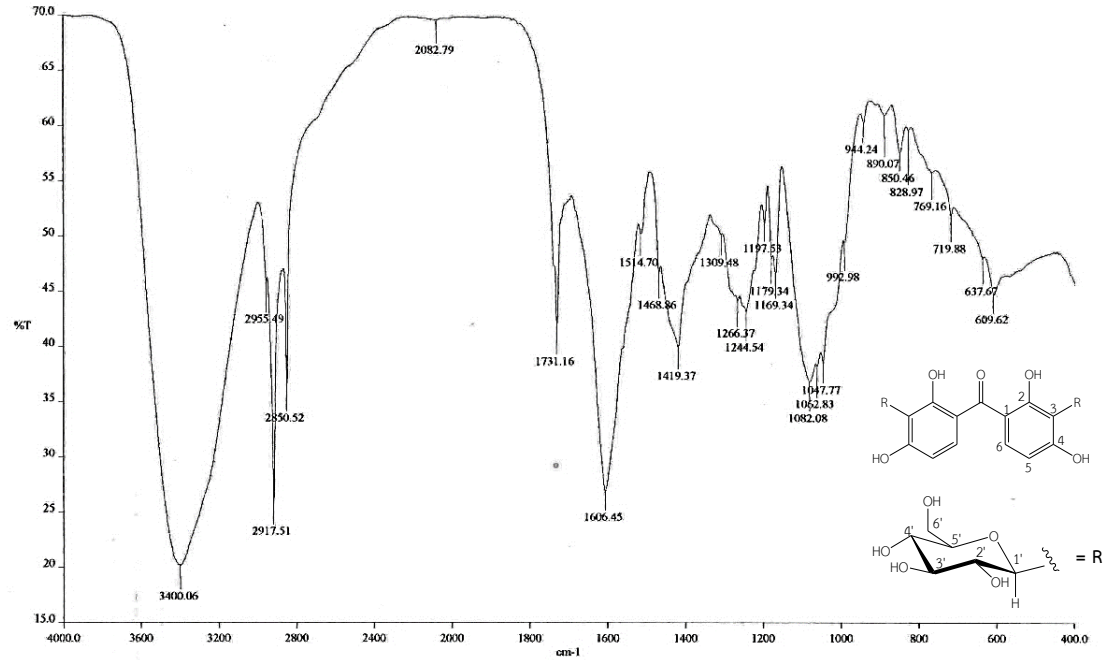

Figure 18 FT-IR Spectrum of compound PF-2

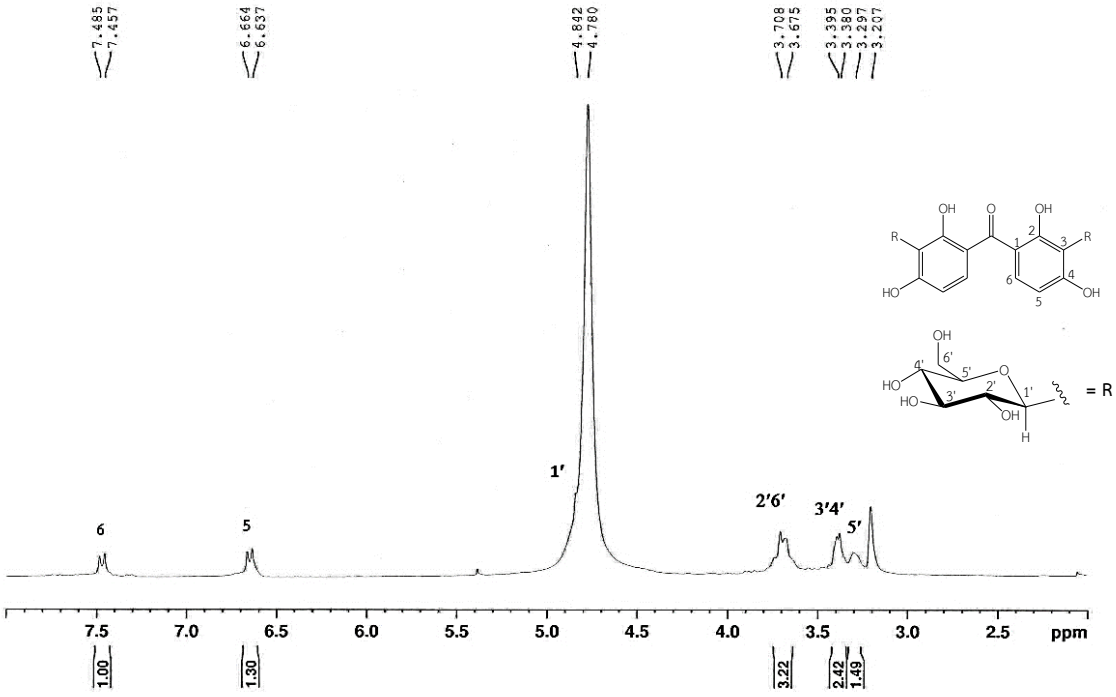

Figure 19 ^{1}H-NMR (300 MHz) Spectrum of compound PF-2 (in CD_3OD)

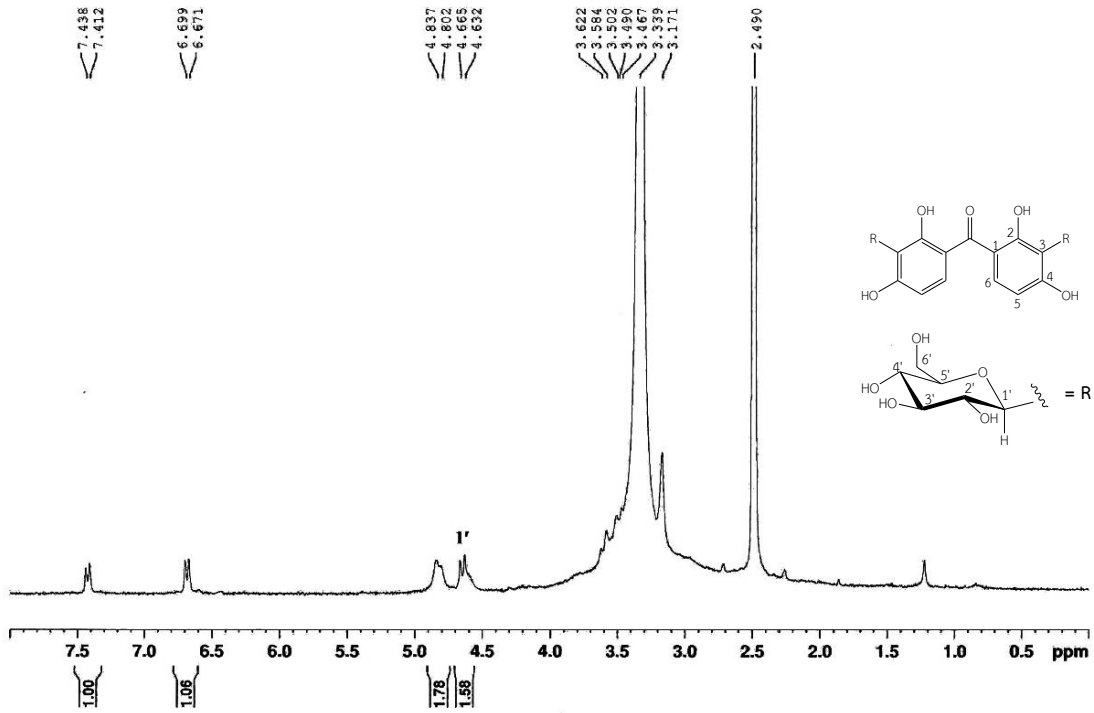

Figure 20 ^{1}H-NMR (300 MHz) Spectrum of compound PF-2 (in DMSO-d_6)

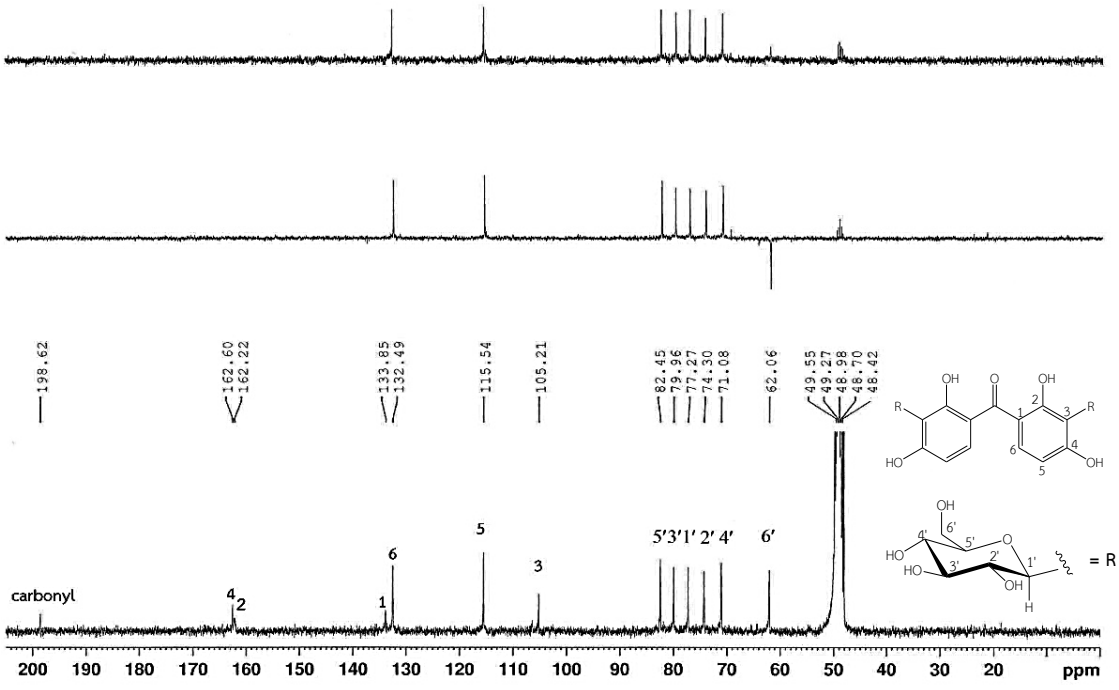

Figure 21 ^{13}C-NMR, DEPT135, DEPT90 (75 MHz) Spectra of compound PF-2 (in CD_3OD)

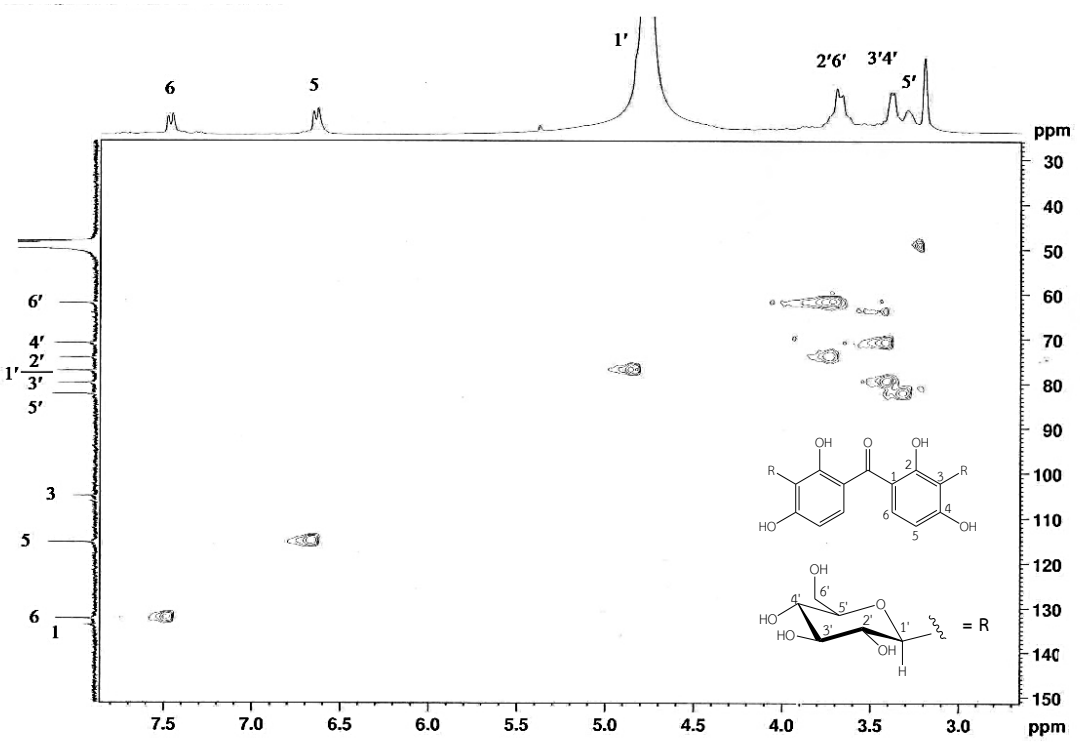

Figure 22 HSQC Spectrum of compound PF-2 (in CD_3OD)

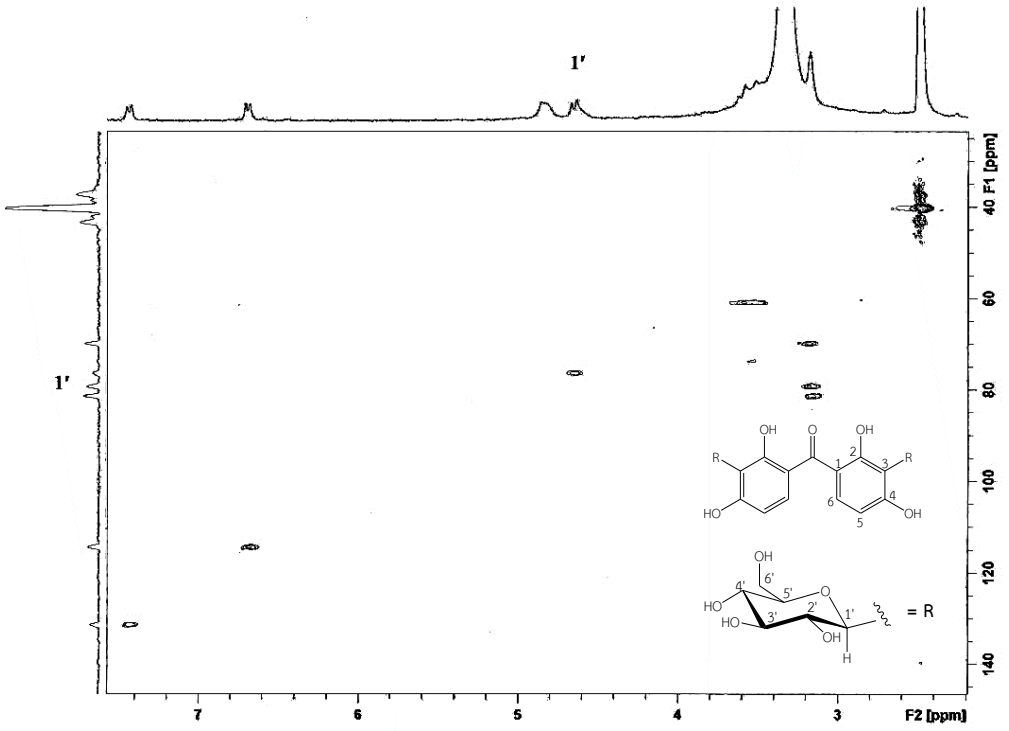

Figure 23 HSQC Spectrum of compound PF-2 (in DMSO-d_6)

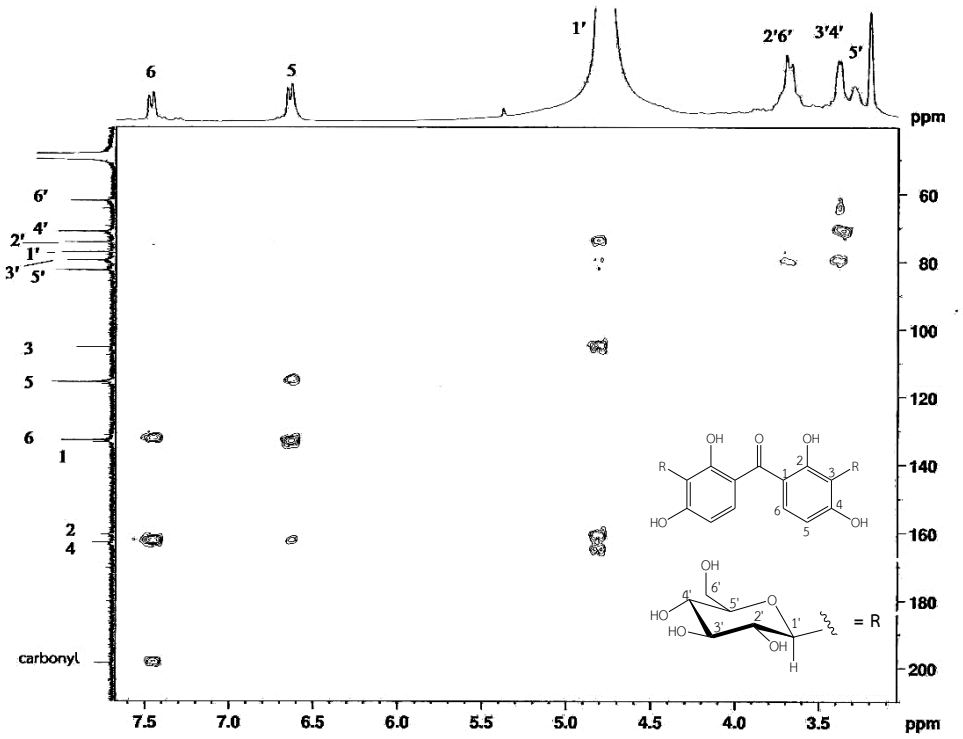

Figure 24 HMBC Spectrum of compound PF-2 (in CD_3OD)

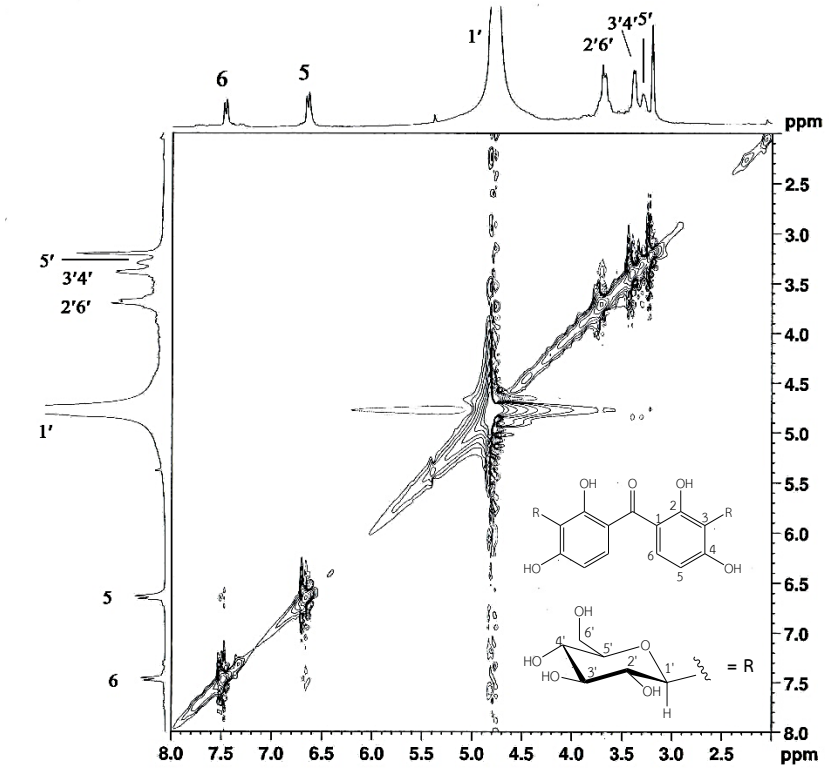

Figure 25 NOESY Spectrum of compound PF-2 (in CD_3OD)

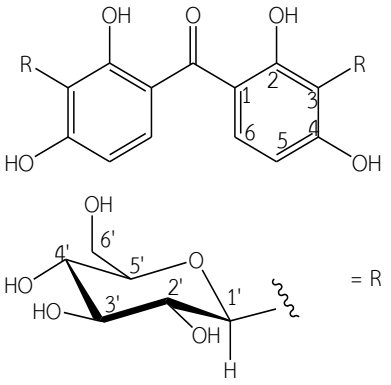

pseuduvarioside [**28**]

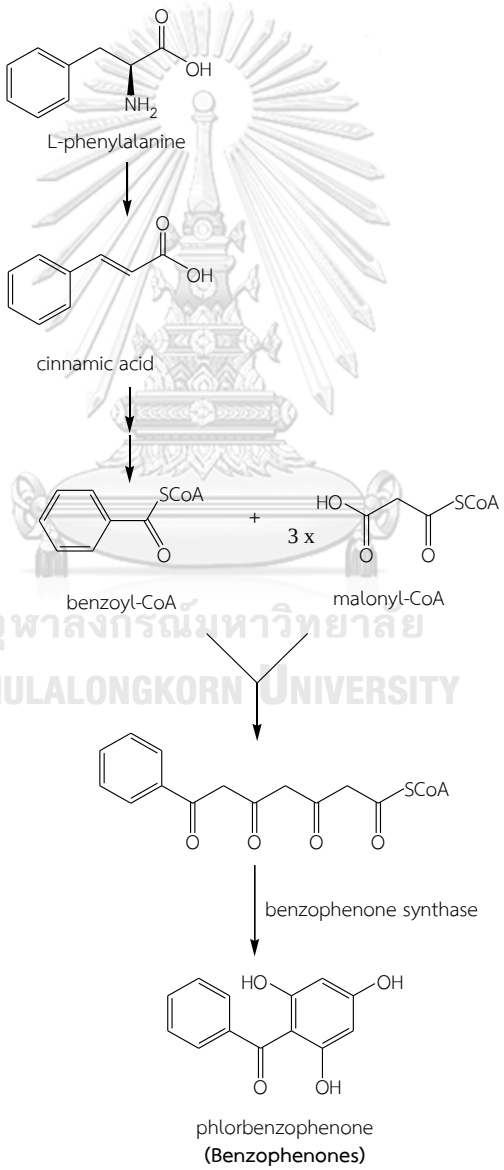

Figure 26 Biosynthetic pathway of benzophenones

Table 6 NMR Spectral data of compound PF-2 (in CD_3OD and DMSO-d_6)

Position	Compound PF-2 [26]		
	δ_H (mult., *J* in Hz) (DMSO-d_6)	**δ_H (mult., *J* in Hz)** (CD_3OD)	**δ_C** (CD_3OD)
1	-	-	133.9
2	-	-	160.6
3	-	-	105.2
4	-	-	162.6
5	6.90 (*d*, 8.1)	6.65 (*d*, 8.1)	115.5
6	7.43 (*d*, 8.1)	7.47 (*d*, 8.1)	132.5
1′	4.65 (*d*, 9.6)	4.84*	77.3
2′	-	3.70 (*m*)	74.3
3′	-	3.38 (*m*)	80.0
4′	-	3.38 (*m*)	71.1
5′	-	3.30 (*m*)	82.5
6′	-	3.68 (*m*)	62.1
Carbonyl	-	-	198.6

*Overlapped with residual water signal

1.3 Structure determination of compound PF-3

Compound PF-3 was obtained as a yellow amorphous solid. The HR-ESI mass spectrum (**Figure 27**) showed a pseudomolecular ion $[M+H]^+$ ion at *m/z* 342.1702 (calcd. for $C_{20}H_{24}NO_4$; 342.1705), suggesting the molecular formula $C_{20}H_{23}NO_4$. Its UV spectrum (**Figure 28**) showed λ_{max} at 204, 230, 275, 320 nm, characteristics of an aporphine structure (Ferreira *et al*., 2010).

The ^{1}H-NMR spectrum (**Figure 29** and **Table 7**) displayed signals for aromatic protons with *ortho*-coupling at δ_H 6.40 (1H, *d*, *J* = 7.8 Hz, H-8) and δ_H 6.59 (1H, *d*, *J* = 7.8 Hz, H-9), an aromatic proton at δ_H 6.40 (1H, *s*, H-3) and aliphatic protons comprising three methoxyl signals at δ_H 3.74 (3H, *s*, 10-OMe), 3.68 (3H, *s*, 2-OMe) and 3.16 (3H, *s*, 1-OMe) and one methyl signal at δ_H 2.71 (3H, *s*, *N*-Me).

The ^{13}C-NMR, DEPT 135 and DEPT 90 spectra (**Figure 30** and **Table 7**) showed 20 carbon peaks assignable to nine quaternary carbons at δ_C 153.1 (C-2), 151.8 (C-10), 150.7 (C-11), 149.8 (C-1), 126.0 (C-7a), 123.5 (3a and 11C), 121.1 (C-11a) and 115.9 (C-11b), four methine carbons at δ_C 117.1 (C-8), 110.6 (C-9), 109.5 (C-3) and 71.1 (C-6a), two methylene carbons at δ_C 31.7 (C-7) and 24.7 (C-4), one *N*-methyl carbon at δ_C 43.5 and three methoxyl carbons at δ_C 56.0 (2-OMe), 56.3 (10-OMe) and 53.9 (1-OMe).

The HSQC spectrum (**Figure 31**) exhibited aromatic protons at δ_H 6.40 (H-8), 6.59 (H-9) and 3.74 (H-6a) which were correlated with the carbons at δ_C 117.1 (C-8), 110.6 (C-9) and 71.1 (C-6a), respectively. In addition, the protons at δ_H 3.68 (10-OMe), 3.74 (2-OMe) and 3.16 (1-OMe) and at δ_H 2.71 (*N*-Me) were correlated with the carbons at δ_C 56.3 (10-OMe), 56.0 (2-OMe), 53.9 (1-OMe) and at δ_C 43.5 (*N*-methyl), respectively. In the HMBC spectrum (**Figure 32**), the aromatic proton at δ_H 6.59 (H-9) was correlated with C-11, C-8, and C-7a. The proton at δ_H 6.40 (H-8) was correlated with the carbons at positions 11a, 10 and 7. The proton at δ_H 6.40 (H-3) was correlated with C-4, C-3a and C-2. The proton at δ_H 2.71 (*N*-Me) was correlated with C-6a and C-5. The methoxy protons at δ_H 3.68 (2-OMe) and 3.74 (10-OMe) were correlated with C-2 and C-10, respectively.

In the NOESY spectrum (**Figure 33**), the methoxy protons at δ_H 3.74 (2-OMe) and 3.68 (10-OMe) revealed correlation peaks with H-3 and H-9, respectively, confirming the locations of the methoxy groups at position 2 and 10.

The ^{1}H and ^{13}C-NMR data of compound PF-3 were compared to previously reported data of two compounds, (+)-isocorydine [**27**] (Cheng *et al*., 2008) and (+)-corydine [**28**] (Ravanelli *et al*., 2016). However, the reported chemical shift and coupling constant of (+)-isocorydine [**27**] were closer to compound PF-3 than (+)-corydine [**28**]. In the ^{13}C-NMR, DEPT 135 and DEPT 90 spectra did not show methylene carbons at δ_C 53.9 (C-5) but this assignment was obtained by analysis of the HMBC spectrum. This study suggested a revision for the ^{13}C-NMR assignments at δ_C 121.1 (C-11a) and 123.5 (C-11b) because the proton at δ_H 6.40 (H-8) was HMBC correlated with the carbons at positions 11a, 10 and 7.

Through comparison of the spectral data of this compound with previously reported data (Cheng *et al*., 2008), compound PF-3 was identified as (+)-isocorydine [**27**].

(+)-isocorydine [**27**] is an aporphine alkaloid previously found in *Aristolochia lagesiana* var. *intermedia* (Ferreira *et al*., 2010), *Alseodaphne corneri* (Nafiah *et al*., 2015), *Dicranostigma leptopodum* (Dang *et al*., 2009), *Sarcocapnos saetabensis* (Blanco *et a*l., 1991) and *Alseodaphne corneri* (Nafiah *et al*., 2016). This compound has been reported as a constituent of Annonaceae such as *Annona squamosa* (Bhakuni *et al*., 1972) and *Guatteria oliviformis* (López *et al*., 1990).

(+)-isocorydine [**27**] has been reported to possess anticancer activity. This compound decreased the percentage of side population cells significantly in hepatocellular carcinoma (HCC) cell lines (SNU-449, SNU-387, Huh-7, and Hep-G2) (Lu *et al*., 2012). It also sensitized cancer cells to doxorubicin, a conventional clinical chemotherapeutic drug for HCC. Additionally, using doxorubicin in combination with (+)-isocorydine [**27**] for chemotherapy against HCC cell lines led to a significant decrease in the IC_{50} for doxorubicin (Pan *et al*., 2018).

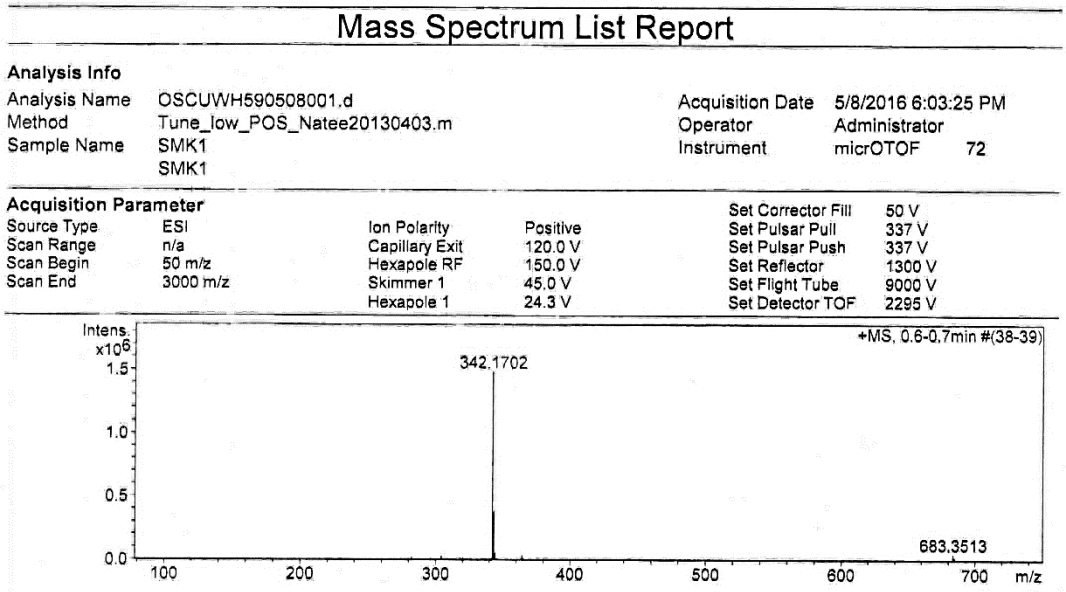

Figure 27 Mass spectrum of compound PF-3

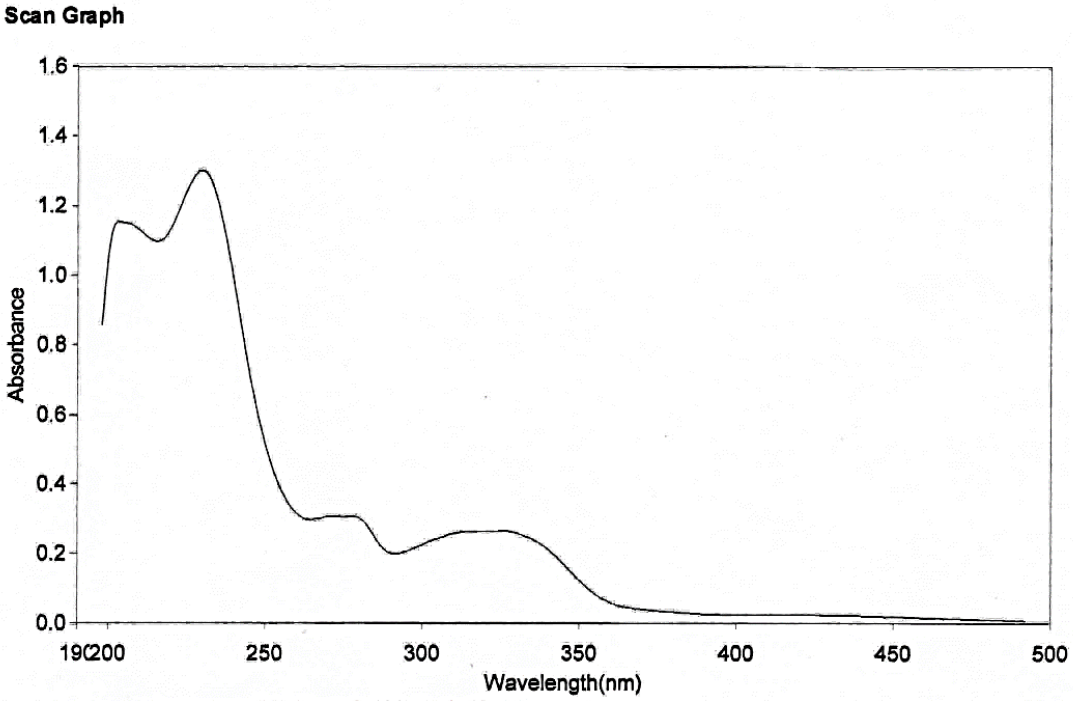

Figure 28 UV Spectrum of compound PF-3

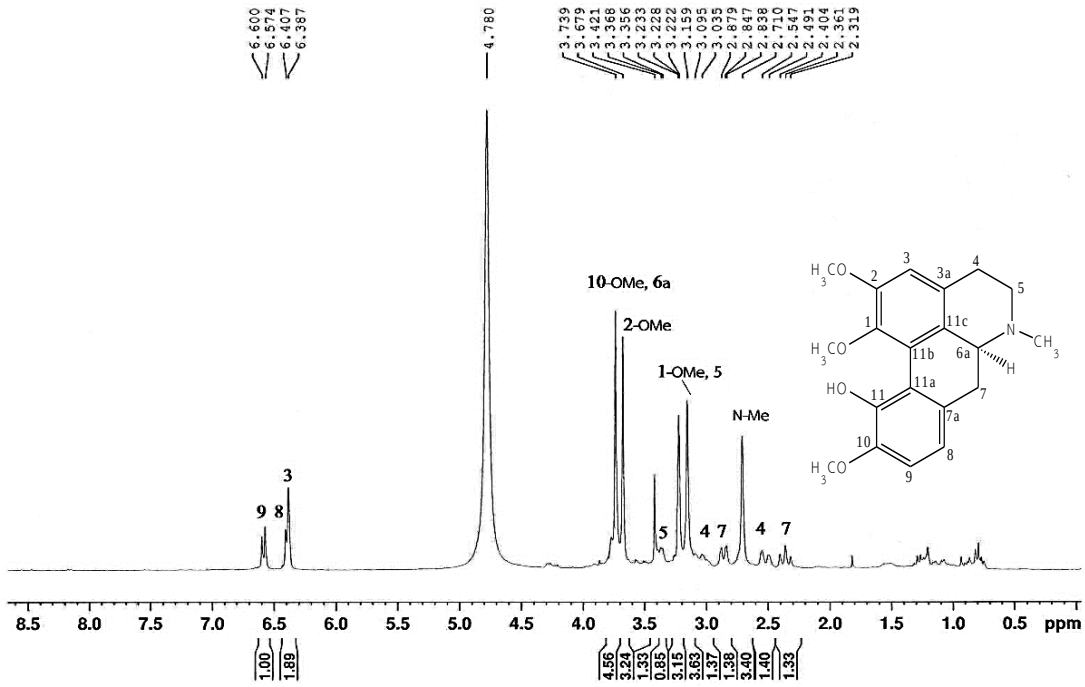

Figure 29 ^{1}H-NMR (300 MHz) Spectrum of compound PF-3 (in CD_3OD)

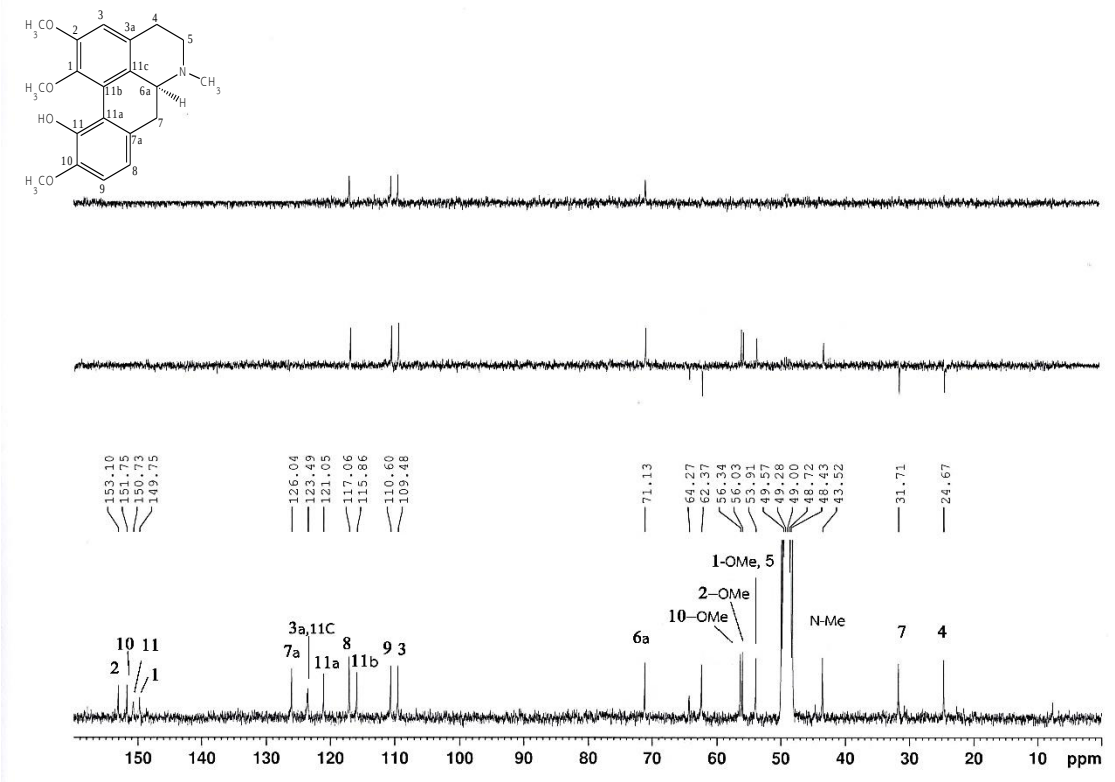

Figure 30 ^{13}C-NMR, DEPT1352, DEPT90 (75 MHz) Spectra of compound PF-3 (in CD_3OD)

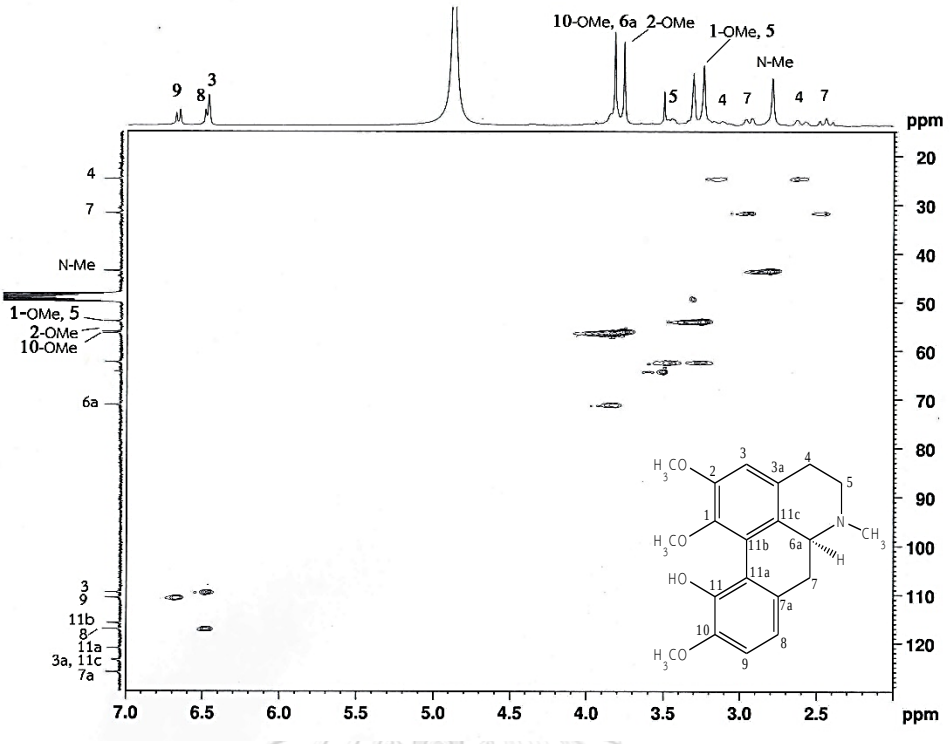

Figure 31 HSQC Spectrum of compound PF-3 (in CD_3OD)

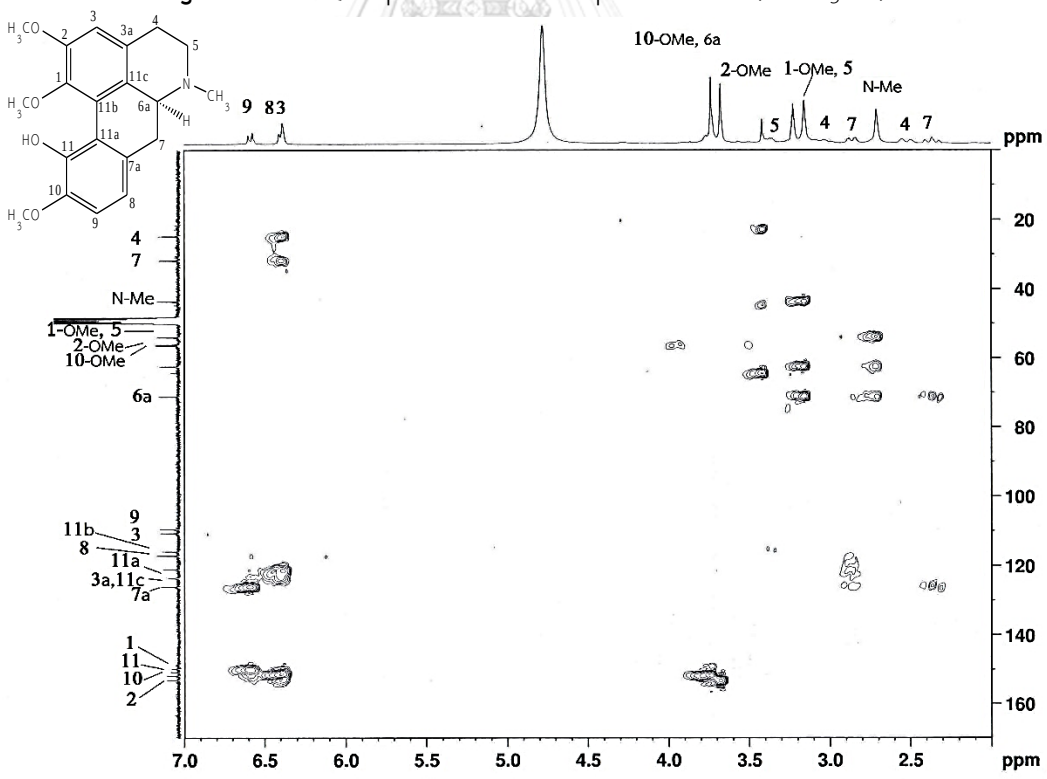

Figure 32 HMBC Spectrum of compound PF-3 (in CD_3OD)

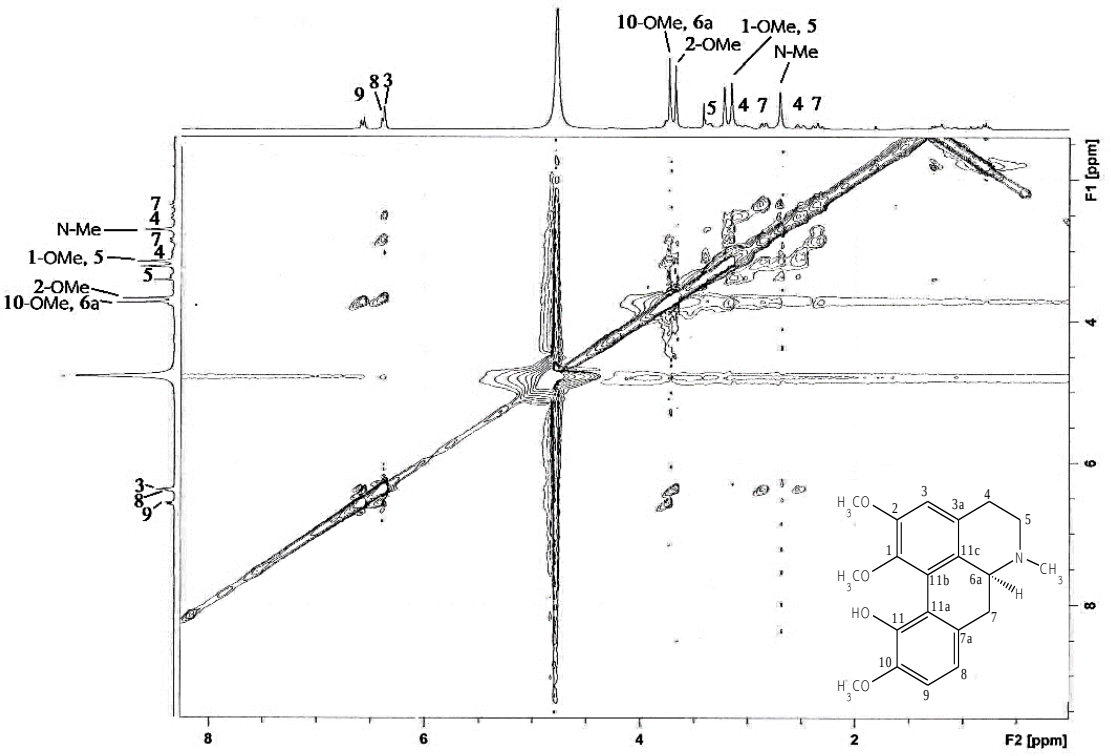

Figure 33 NOESY Spectrum of compound PF-3 (in CD_3OD)

(+)-isocorydine [**27**]

(+)-corydine [**28**]

Table 7 NMR Spectral data of compound PF-3 (in CD_3OD), (+)-isocorydine (in DMSO-d_6) and (+)-corydine (in $CDCl_3$ + drops of CD_3OD)

Position	Compound PF-3		(+)-isocorydine [27][a]		Position	(+)-Corydine [28][b]	
	δ_H (mult., *J* in Hz)	δ_C	δ_H (mult., *J* in Hz)	δ_C		δ_H (mult., *J* in Hz)	δ_C
1	-	149.8	-	150.9	1	-	142.2
2	-	153.1	-	153.0	2	-	149.0
3	6.40 (*s*)	109.5	6.46 (*s*)	109.0	3	6.67 (*s*)	111.2
3a	-	123.5	-	123.3	3a	-	123.7
4	2.52 (*m*)	24.7	2.76 (*d*,16.5)	24.0	4	2.67 (*m*)	28.8
	3.10 (*m*)					3.18 (*m*)	
5	3.16 (*m*)	53.9	3.06 (*d*,11.7)	53.4	5	2.75 (*m*)	52.6
	3.36 (*m*)					3.06 (*m*)	
6a	3.74 (unresolved)	71.1	4.28 (*d*, 13.2)	69.9	6a	3.45 (*m*)	62.6
7	2.36 (*t*, 12.3)	31.7	2.57 (*d*, 13.2)	31.3	7	2.37 (*m*)	35.3
	2.85 (*d*, 12.3)					3.08 (*m*)	
7a	-	126.0	-	125.8	7a	-	130.5
8	6.40 (*d*, 7.8)	117.1	6.33 (*d*, 7.8)	112.4	8	7.05 (*d*, 7.2)	124.2
9	6.59 (*d*, 7.8)	110.6	6.58 (*d*, 7.5)	110.5	9	6.85 (*d*, 7.2)	110.8
10	-	151.8	-	152.6	10	-	151.7
11	-	150.7	-	151.8	11	-	143.7
11a	-	121.1	-	113.2	11a	-	126.3
11b	-	115.9	-	120.7	11b	-	119.1
11c	-	123.5	-	123.7	11c	-	127.8
N-Me	2.71 (*s*)	43.5	2.86 (*s*)	43.4	*N*-Me	2.90 (*s*)	41.2
1-OMe	3.16 (*s*)	53.9	3.37 (*s*)	61.2	2-OMe	3.71 (*s*)	56.3
2-OMe	3.74 (*s*)	56.0	3.67 (*s*)	56.5	10-OMe	3.87 (*s*)	56.3
10-OMe	3.68 (*s*)	56.3	3.65 (*s*)	56.0	11-OMe	3.87 (*s*)	61.7

[a]Cheng *et al*., 2008, [b]Ravanelli *et al*., 2016

1.4 Structure determination of compound PF-4

Compound PF-4 was obtained as a yellow crystalline solid. Its HR-ESI-MS (**Figure 34**) showed a pseudomolecular ion $[M+H]^+$ at *m/z* 258.0754 (calcd. for $C_{14}H_{12}NO_4$; 258.0766), suggesting the molecular formula $C_{14}H_{11}NO_4$. The UV spectrum (**Figure 35**) exhibited λ_{max} at 210, 260, 310 and 355 nm, indicating an 4-aza-9-fluorenone structure (Wijeratne *et al*., 1995).

The ^{1}H-NMR spectrum of compound PF-4 (**Figure 36** and **Table 8**) showed aromatic protons at δ_H 8.06 (1H, *d*, *J* = 4.2 Hz, H-3), δ_H 6.76 (1H, *d*, *J* = 4.2 Hz, H-2) and δ_H 6.58 (1H, *s*, H-8). The ^{1}H-NMR spectrum also exhibited signals for a methoxy group at δ_H 3.85 (3H, *br s*, 6-OMe) and a methyl group at δ_H 2.40 (3H, *br s*, 1-CH_3)

The ^{13}C-NMR and DEPT spectra (**Figure 37** and **Table 8**) displayed fourteen carbon signals representing one carbonyl carbon at δ_C 193.4 (C-9), 8 quaternary carbons at δ_C 167.3 (C-4a), 154.8 (C-7), 148.6 (C-1 and C-5), 142.3 (C-6), 131.7 (C-5a), 126.5 (C-9a) and 120.2 (C-8a), 3 methine carbons at δ_C 152.5 (C-3), 125.1 (C-2) and 105.9 (C-8), one methoxy carbon at δ_C 61.0 (6-OMe) and one methyl carbon at δ_C 17.1 (1-CH_3).

The HSQC spectrum (**Figure 38**) indicated that the aromatic protons at δ_H 8.06 (H-3), δ_H 6.76 (H-2) and δ_H 6.58 (H-8) were correlated to the carbons at δ_C 152.5 (C-3), 125.1 (C-2) and 105.9 (C-8), respectively. Furthermore, the protons of the methoxy group at δ_H 3.85 (6-OMe) and the methyl group at δ_H 2.40 (1-CH_3) were correlated with the carbons at δ_C 61.0 (6-OMe) and 17.1 (1-CH_3), respectively. In the HMBC spectrum (**Figure 39**), the proton at δ_H 8.06 (H-3) was correlated with the carbons at δ_C 167.3 (C-4a), 148.6 (C-1) and 125.1 (C-2). The proton at δ_H 6.58 (H-8) was correlated with the carbons at δ_C 193.4 (C-9), 154.8 (C-7), 142.3 (C-6) and 120.2 (C-8a). The methyl protons at δ_H 2.40 (1-CH_3) were correlated with the carbons at δ_C 148.6 (C-1), 126.5 (C-9a) and 125.1 (C-2). The methoxy protons at δ_H 3.84 (6-OMe) was correlated with the carbon at position 6.

Through analysis of the above spectral data, compound PF-4 was identified as cyathocaline [**29**] (Wijeratne *et al*., 1995).

Cyathocaline [**29**], a 4-aza-9-fluorenone alkaloid, was previously found in *Cyathocalyx zeylanica*. It showed cytotoxicity activity against the A-549 human lung carcinoma cell line (IC_{50} value of 8.5±0.07 μM) (Wijeratne *et al*., 1995).

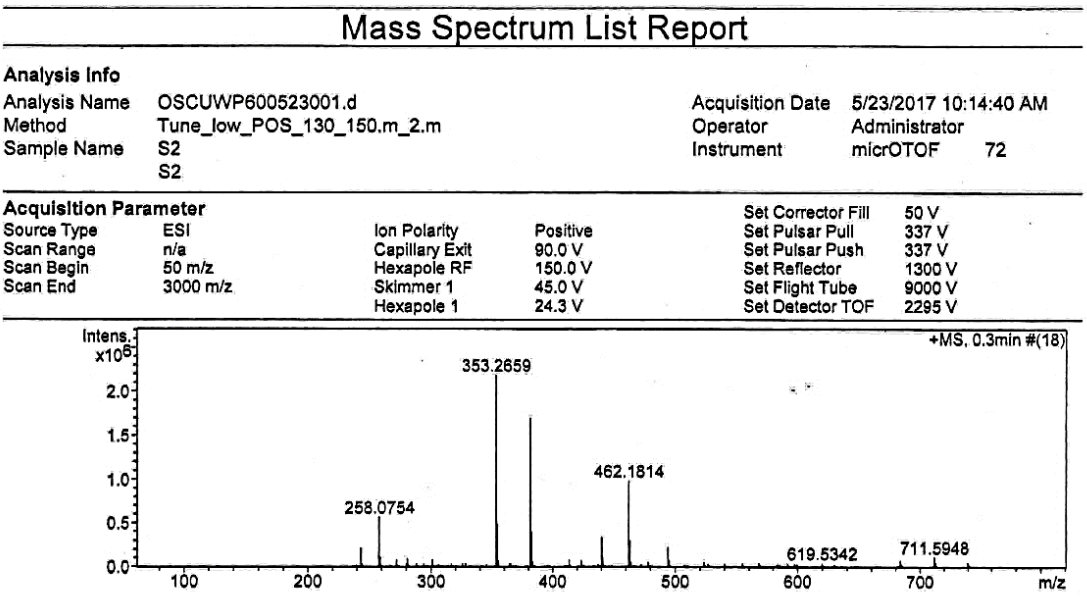

Figure 34 Mass spectrum of compound PF-4

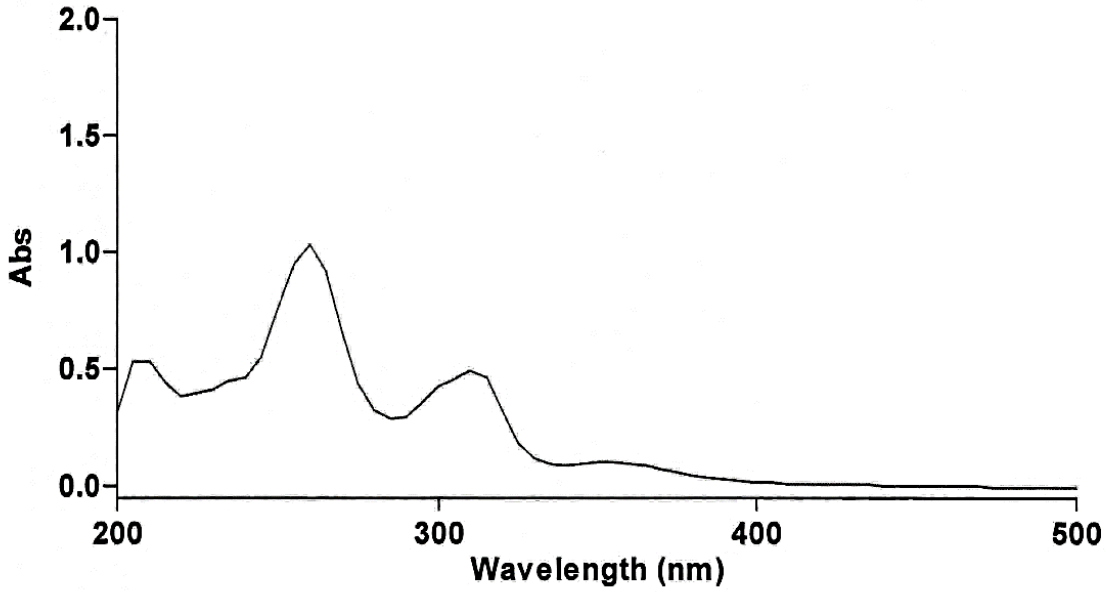

Figure 35 UV Spectrum of compound PF-4

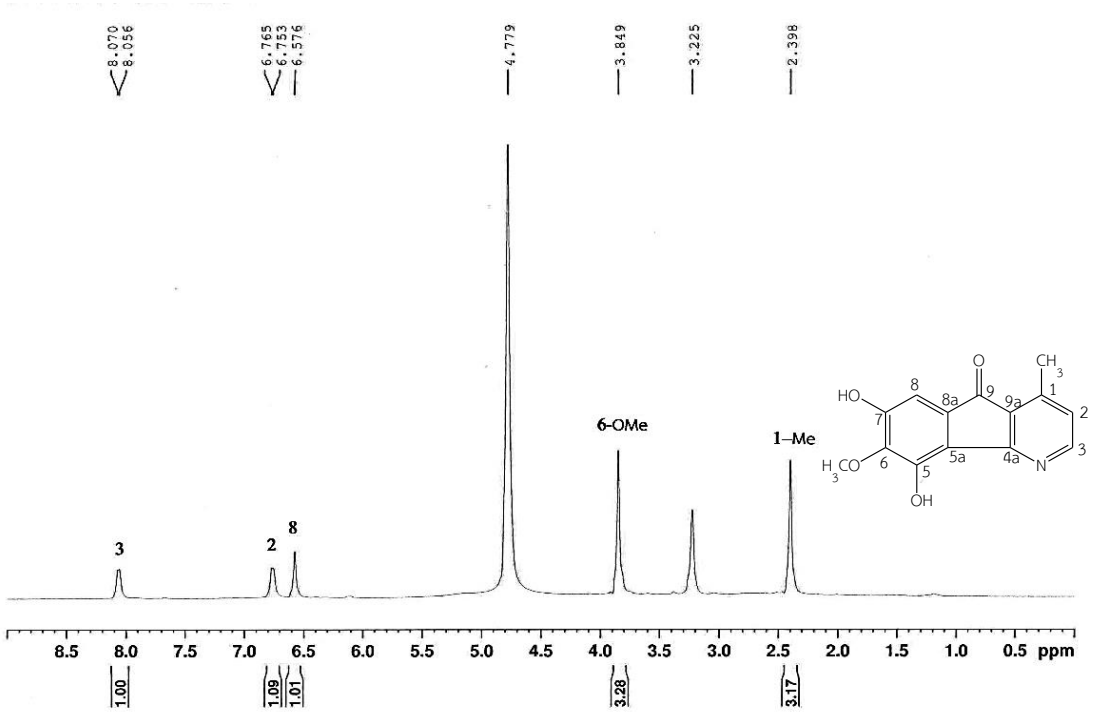

Figure 36 ^{1}H-NMR (300 MHz) Spectrum of compound PF-4 (in CD_3OD)

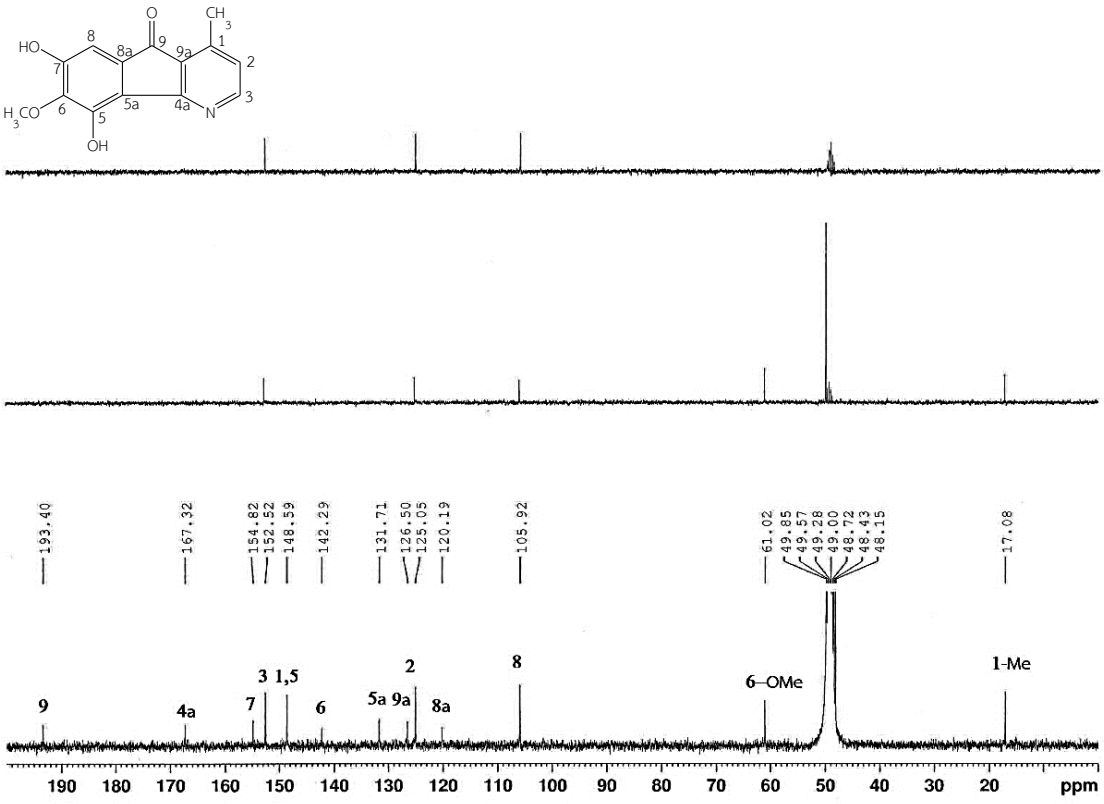

Figure 37 ^{13}C-NMR, DEPT135, DEPT90 (75 MHz) Spectra of compound PF-4 (in CD_3OD)

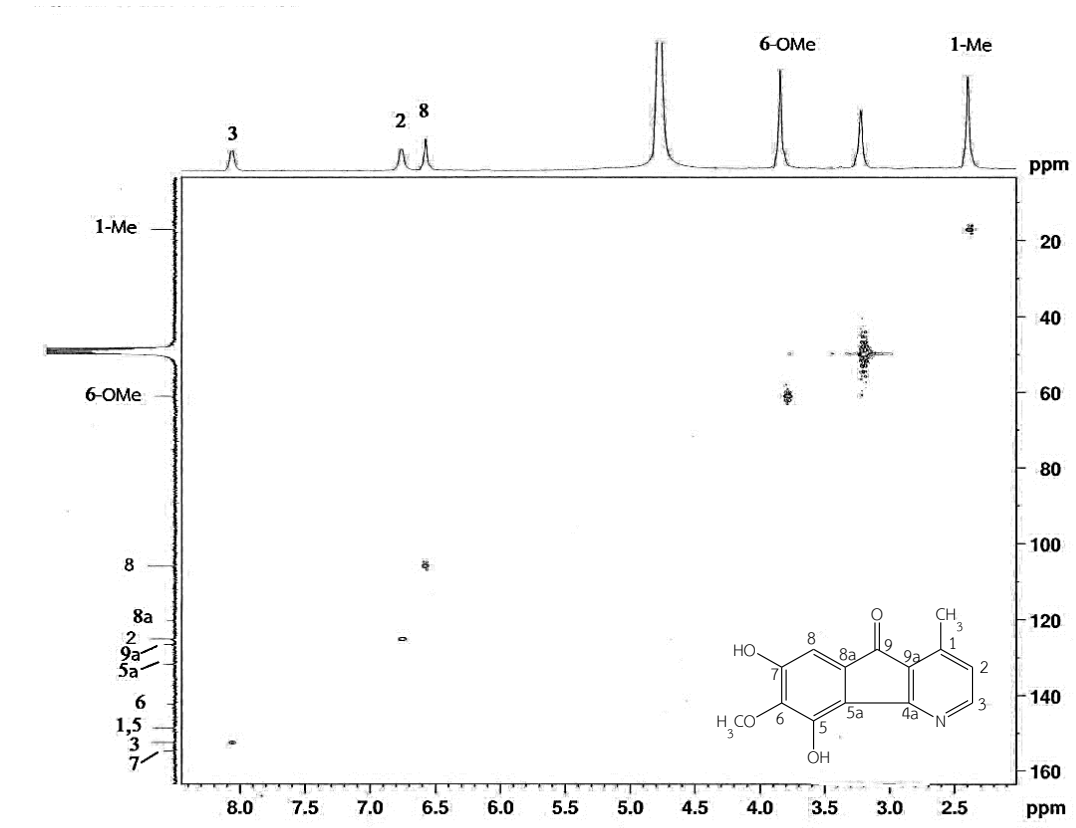

Figure 38 HSQC Spectrum of compound PF-4 (in CD_3OD)

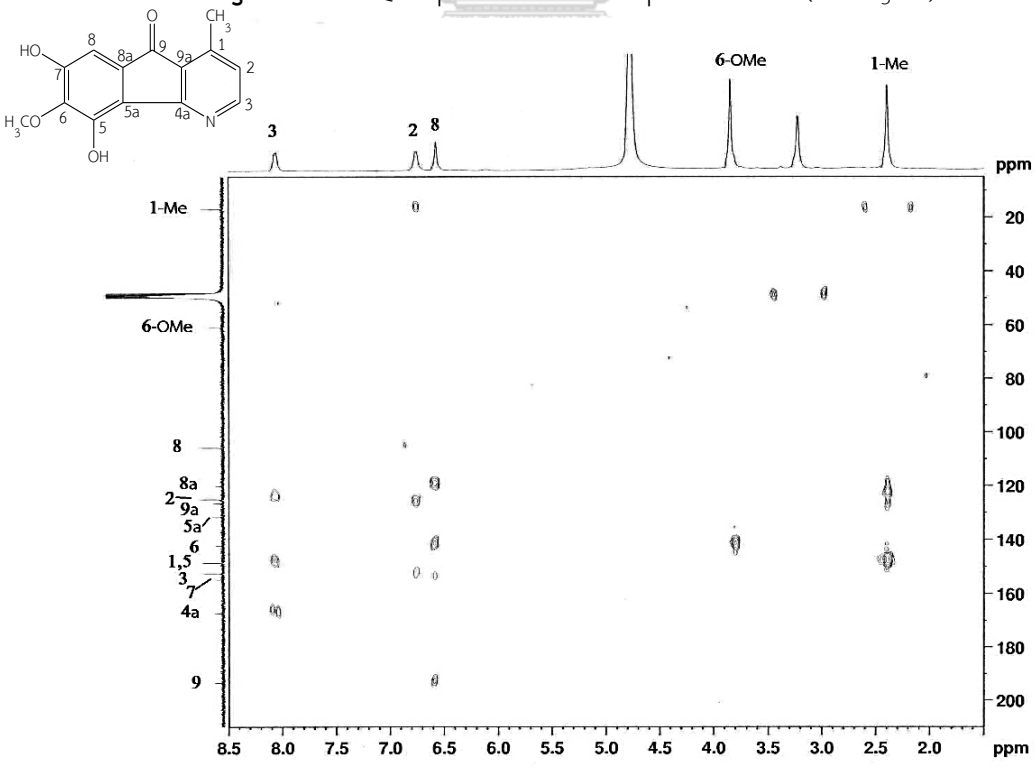

Figure 39 HMBC Spectrum of compound PF-4 (in CD_3OD)

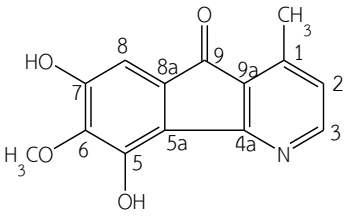

Cyathocaline [**29**]

Table 8 NMR Spectral data of compound PF-4 (in CD_3OD) and cyathocaline

Position	Compound PF-4		Cyathocaline [29][a]	
	δ_H (mult., *J* in Hz)	**δ_C**	**δ_H (mult., *J* in Hz)**	**δ_C**
1	-	148.6	-	148.4
2	6.76 (*d*, 4.2)	125.1	6.97 (*dd*, 5.5, 6.0)	125.5
3	8.06 (*d*, 4.2)	152.5	8.24 (*d*, 5.5)	152.4
4a	-	167.3	-	167.5
5	-	148.6	-	148.6
5a	-	131.7	-	131.2
6	-	142.3	-	141.6
7	-	154.8	-	154.9
8	6.58 (*s*)	105.9	6.75 (*s*)	105.9
8a	-	120.2	-	120.1
9	-	193.4	-	192.3
9a	-	126.5	-	126.4
1-Me	2.40 (*s*)	17.1	2.53 (*s*)	17.4
6-OMe	3.85 (*s*)	61.0	3.98 (*s*)	61.3

[a]Wijeratne *et al*., 1995

1.5 Structure determination of compound PF-5

Compound PF-5 was obtained as a yellow crystalline solid. Its HR-ESI-MS (**Figure 40**) showed a pseudomolecular ion $[M+H]^+$ at *m/z* 242.0824 (calcd. for $C_{14}H_{12}NO_3$; 242.0817), suggesting the molecular formula $C_{14}H_{11}NO_3$. The UV spectrum (**Figure 41**) exhibited maximum absorptions at λ_{max} 205, 250, 290, 305 and 375 nm, suggestive of an 4-aza-9-fluorenone skeleton (Laprévote *et al*, 1988).

The ^{1}H-NMR spectrum (**Figure 42** and **Table 9**) showed two pairs of *ortho*-coupled protons: the first pair at δ_H 8.26 (1H, *d*, *J* = 5.4, H-3) and δ_H 6.89 (1H, *d*, *J* = 5.4, H-2); the second pair at δ_H 7.23 (1H, *d*, *J* = 8.1, H-8) and δ_H 6.78 (1H, *d*, *J* = 8.1, H-7). Other protons appeared at δ_H 2.57 (3H, *s*, 1-CH_3) and δ_H 3.95 (3H, *s*, 6-OMe).

The ^{13}C-NMR and DEPT spectra (**Figure 43** and **Table 9**) exhibited fourteen carbons indicating one carbonyl carbon, seven quaternary carbons, four methine carbons, one methoxy carbon and one methyl carbon.

The HSQC spectrum (**Figure 44**) revealed that the aromatic protons at δ_H 8.26 (H-3), δ_H 6.89 (H-2); 7.23 (H-8) and 6.78 (H-7) were correlated with the carbons at δ_C 151.0 (C-3), 125.1 (C-2), 116.5 (C-8) and 112.5 (C-7) respectively. Furthermore, the protons at δ_H 3.95 (6-OMe). and δ_H 2.57 (1-CH_3) were correlated with the carbons at δ_C 56.4 (6-OMe) and 17.2 (1-Me), respectively. From the HMBC spectrum (**Figure 45**) the protons at δ_H 2.57 (1-CH_3) were correlated to the three carbons of the pyridine ring at δ_C 147.8 (C-1), 126.4 (C-9a) and 125.1 (C-2). The proton at δ_H 6.89 (H-2) was correlated to four carbons at δ_C 151.0 (C-3), 147.8 (C-1), 126.4 (C-9a) and 17.2 (1-CH_3). The aromatic proton at δ_H 7.23 (H-8) was correlated to four carbons at δ_C 191.0 (C-9), 153.8 (C-6), 125.4 (C-5a) and 112.5 (C-7). The methoxy protons at δ_H 3.95 (6-OMe) were correlated with C-6.

Through comparison of the ^{1}H-NMR and ^{13}C-NMR spectra with the previously reported data (Muller *et al*., 2009), compound PF-5 was identified as isoursuline [**29**].

Isoursuline [**30**], a 4-aza-9-fluorenone alkaloid, has been found in *Mitrephora diersifolia* (Muller *et al*., 2009), *Oxandra longipetala* (Ortiz *et al*., 2007) and *Unonopsis spectabilis* (Laprévote *et al*., 1988). It exhibited antimalarial activity against

Plasmodium falciparum (3D7 and Dd2) with IC_{50} values of 9.9 and 11.4 μM, respectively (Muller *et al*., 2009)

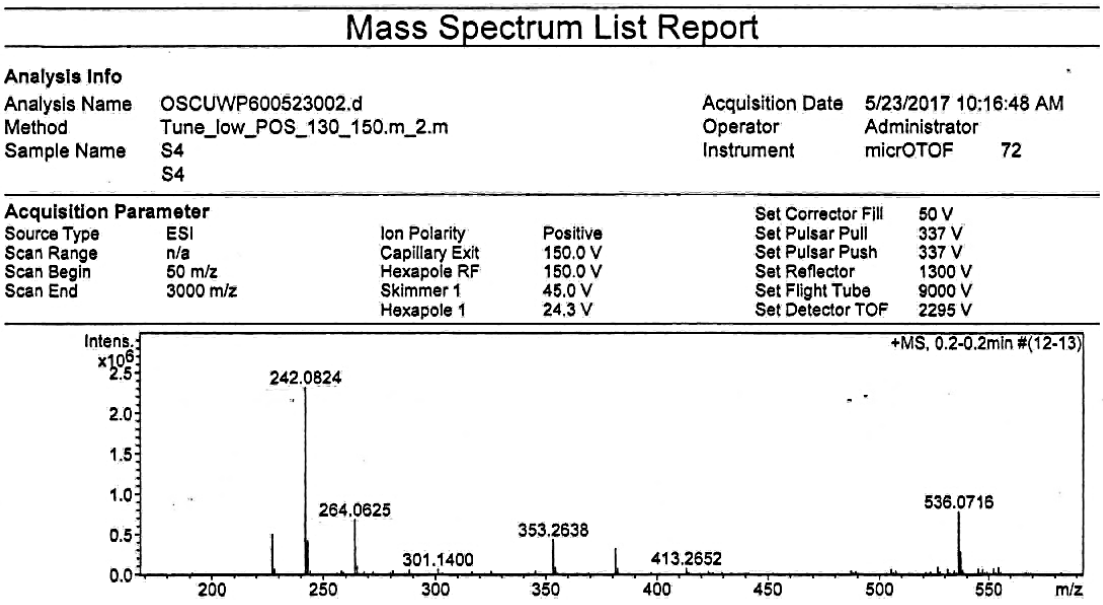

Figure 40 Mass spectrum of compound PF-5

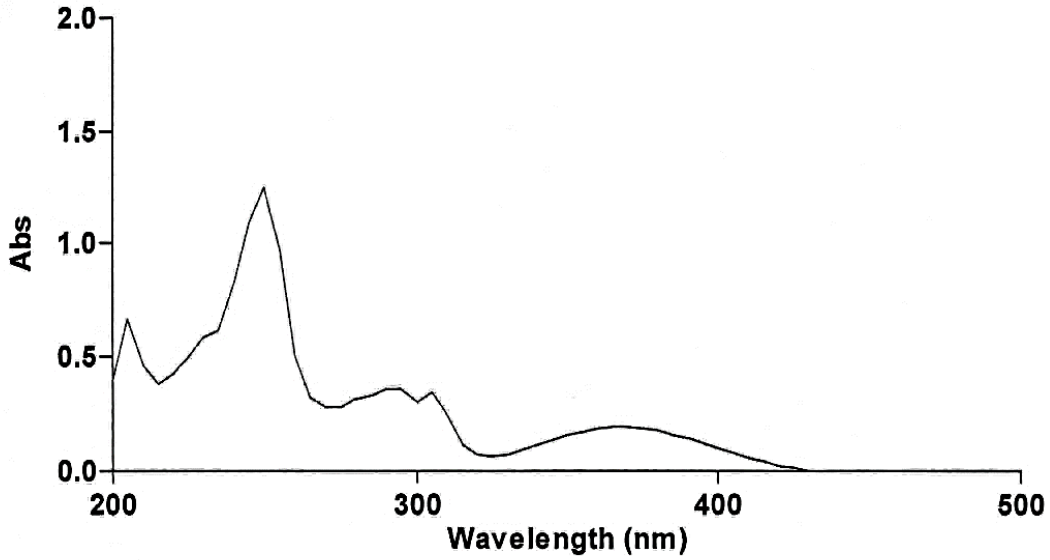

Figure 41 UV Spectrum of compound PF-5

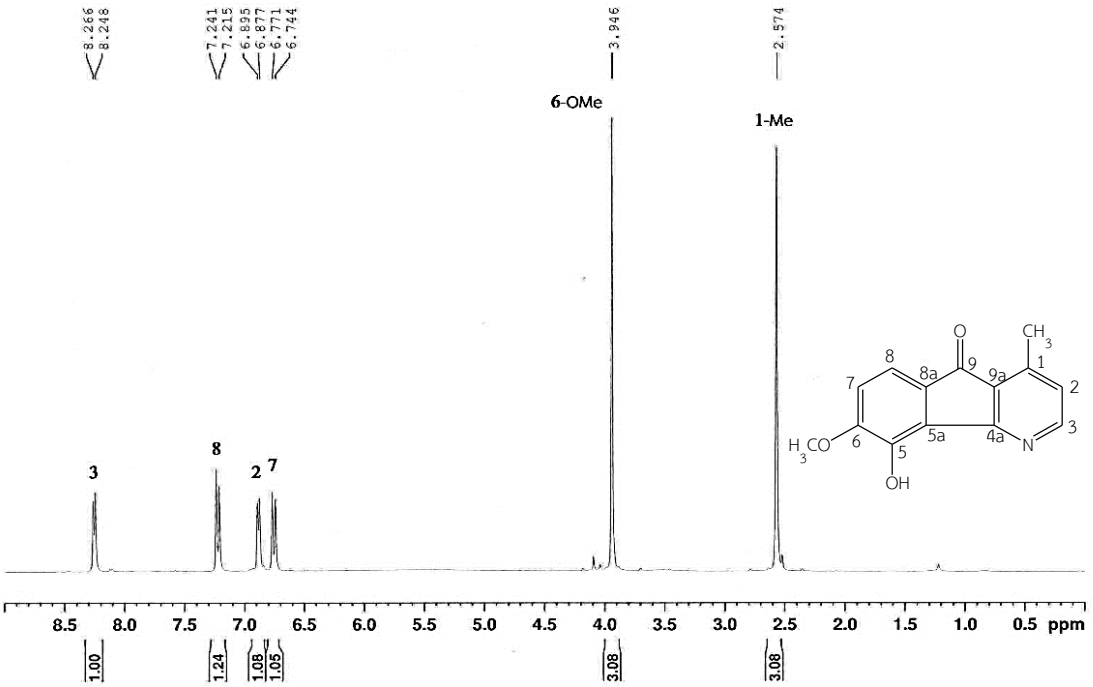

Figure 42 ^{1}H-NMR (300 MHz) Spectrum of compound PF-5 (in $CDCl_3$)

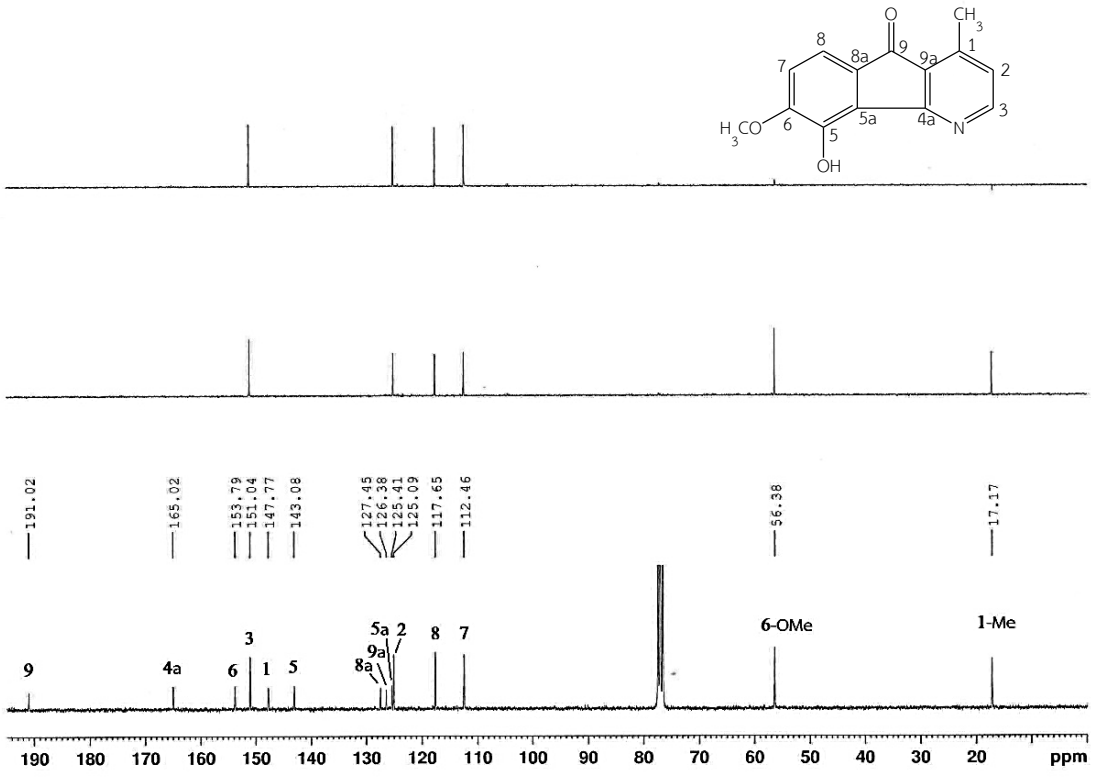

Figure 43 ^{13}C-NMR, DEPT135, DEPT90 (75 MHz) Spectra of compound PF-5 (in $CDCl_3$)

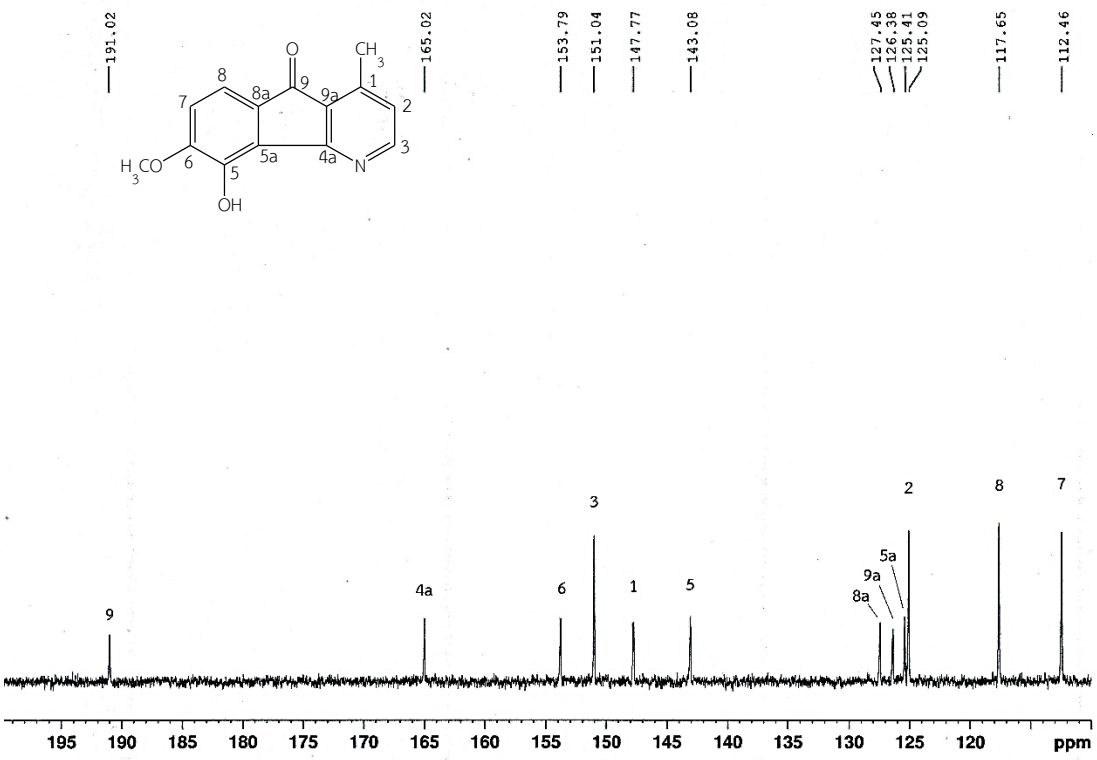

Figure 44 ^{13}C-NMR, DEPT135, DEPT90 (75 MHz) Spectra of compound PF-5 (in $CDCl_3$) [δ_C 100-200 ppm]

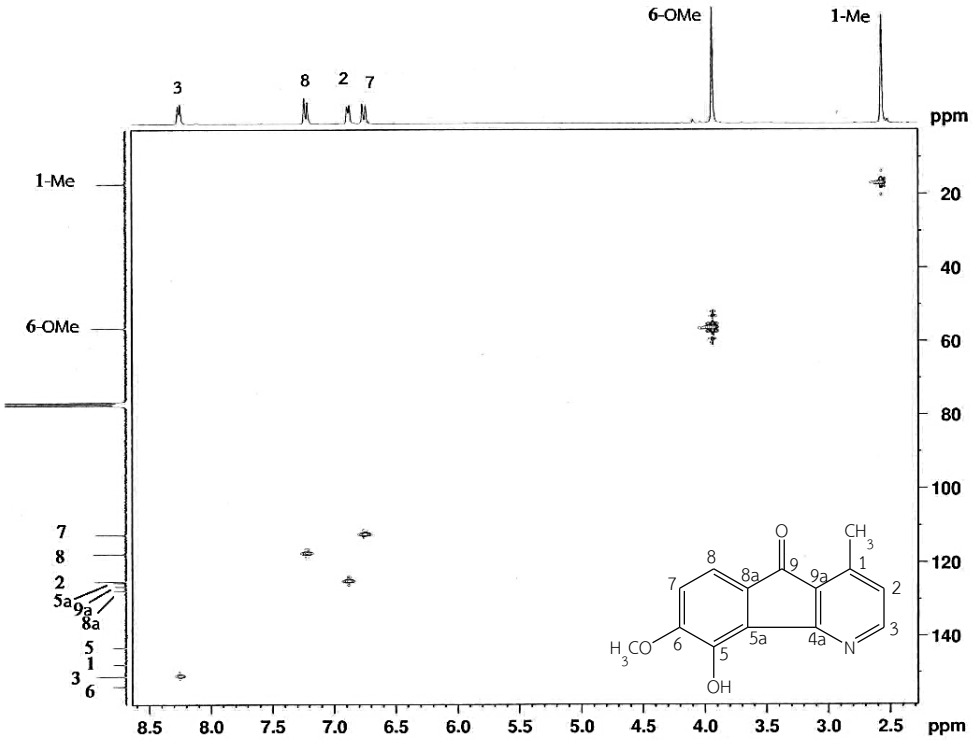

Figure 45 HSQC Spectrum of compound PF-5 (in $CDCl_3$)

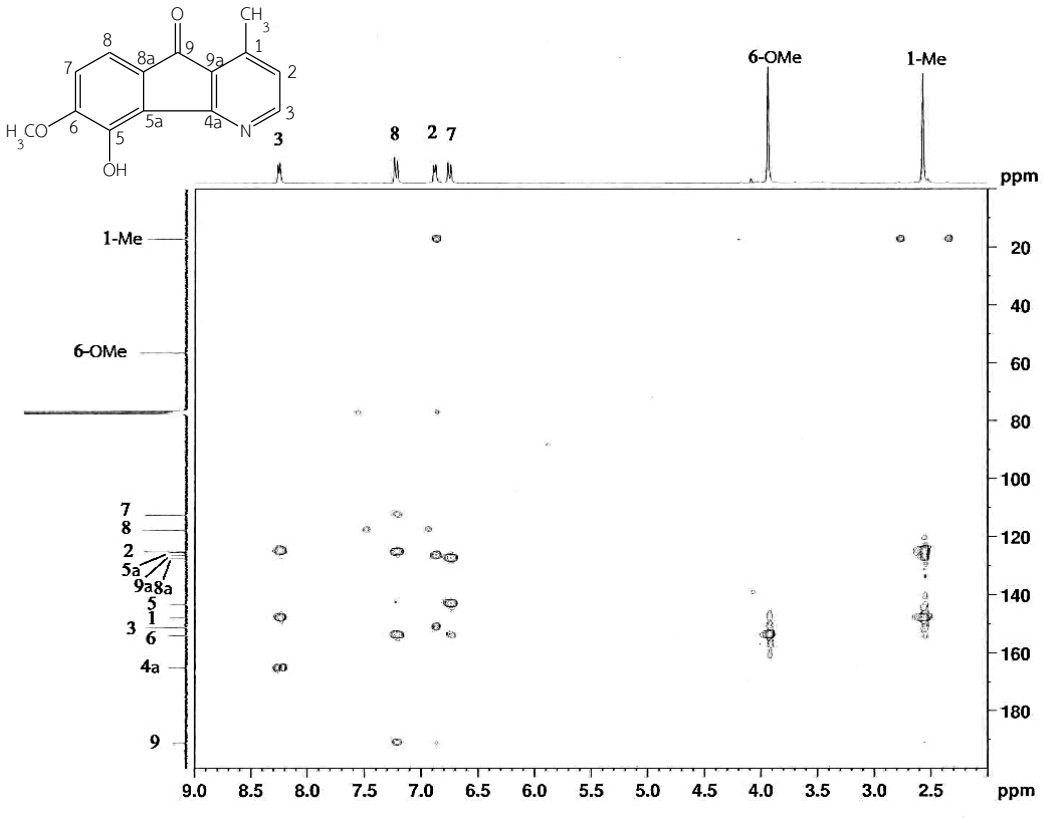

Figure 43 HMBC Spectrum of compound PF-5 (in $CDCl_3$)

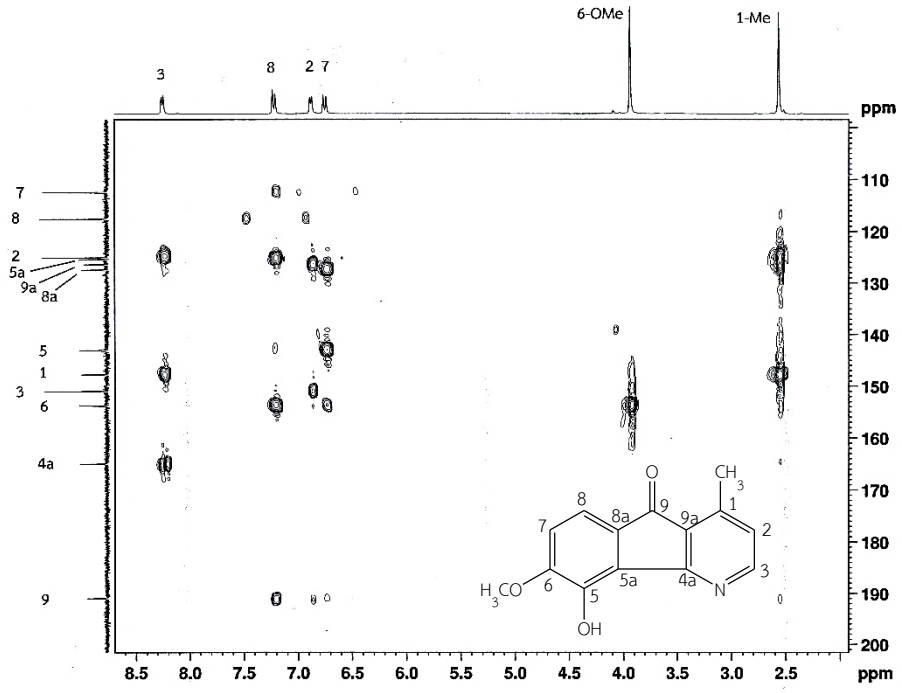

Figure 46 HMBC Spectrum of compound PF-5 (in $CDCl_3$)

[δ_H 2.0-8.7 ppm, δ_C 100-200 ppm]

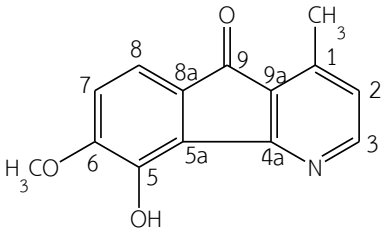

Isoursuline [**30**]

Table 9 NMR Spectral data of compound PF-5 (in $CDCl_3$) and isoursuline (in DMSO-d_6)

Position	Compound PF-5		Isoursuline [30][a]	
	δ_H (mult., *J* in Hz)	δ_C	δ_H (mult., *J* in Hz)	δ_C
1	-	147.8	-	146.6
2	6.89 (*d*, 5.4)	125.1	7.09 (*d*, 5.2)	124.6
3	8.26 (*d*, 5.4)	151.0	8.41 (*d*, 5.2)	151.8
4a	-	165.0	-	164.0
5	-	143.1	-	142.6
5a	-	125.4	-	125.2
6	-	153.8	-	154.3
7	6.78 (*d*, 8.1)	112.5	6.97 (*d*, 8.2)	112.4
8	7.23 (*d*, 8.1)	117.7	7.20 (*d*, 8.2)	116.5
8a	-	127.5	-	127.4
9	-	191.0	-	190.7
9a	-	126.4	-	125.6
1-Me	2.57 (*s*)	17.2	2.53 (*s*)	16.4
6-OMe	3.95 (*s*)	56.4	3.90 (*s*)	56.0

[a]Muller *et al*., 2009

1.6 Structure determination of compound PF-6

Compound PF-6 was obtained as a yellow amorphous solid. Its HR-ESI-MS (**Figure 47**) showed a sodium-adduct molecular ion $[M+Na]^+$ at *m/z* 336.1211 (calcd. for $C_{18}H_{19}NO_4Na$; 336.1212), suggesting the molecular formula $C_{18}H_{19}NO_4$. The UV spectrum (**Figure 48**) exhibited maximal absorptions at λ_{max} 220, 295 and 315 nm., reminiscent of a cinnamoyl tyramide structure (Rajamanickam *et al*., 2016).

The ^{1}H-NMR spectrum of compound PF-6 (**Figure 49** and **Table 10**) showed *ortho*-coupled protons at δ_H 7.05 (2H, *d*, *J* = 8.1 Hz, H-2′ and H-6′) and δ_H 6.72 (2H, *d*, *J* = 8.1 Hz, H-3′ and H-5′), suggesting a *para*-substituted aromatic ring. In addition, the ^{1}H-NMR spectrum exhibited *ortho*-coupled protons at δ_H 7.01 (1H, *d*, *J* = 8.1 Hz, H-6) and δ_H 6.79 (1H, *d*, *J*= 8.1 Hz, H-5). The olefinic protons at δ_H 7.43 and 6.40 (each 1H, *d*, *J* = 15.6 Hz) could be assigned to H-7 and H-8, respectively. The coupling constant of 15.6 Hz indicated a *trans*-configuration between H-7 and H-8. The triplets at δ_H 3.46 (2H, *J* = 6.9 Hz) and 2.75 (2H, *J* = 6.9 Hz) were assigned to the aliphatic protons H-8′ and H-7′, respectively. The signal at δ_H 3.88 (3H, *s*, 3-OMe) represented methoxy protons.

The ^{13}C-NMR and DEPT spectra (**Figure 50** and **Table 10**) exhibited eighteen carbon signals corresponding to one carbonyl carbon at δ_C 169.2 (C-9), five quaternary carbons at δ_C 156.9 (C-4′), 149.8 (C-4), 149.3 (C-3), 131.3 (C-1′) and 128.3 (C-1), nine methine carbons at δ_C 142.0 (C-7), 130.7 (C-2′ and C-6′), 123.2 (C-6), 118.7 (C-8), 116.5 (C-5), 116.3 (C-3′ and C-5′) and 111.5 (C-2), one methoxy carbon at δ_C 56.4 (3-OMe) and two methylene carbons at δ_C 42.6 (C-8′) and 35.8 (C-7′).

The HSQC spectrum (**Figure 51**) showed that the protons at δ_H 7.43 (H-7), 7.11 (H-2), 7.05 (H-2′ and H-6′), 7.01 (H-6), 6.79 (H-5), 6.72 (H-3′ and H-5′) and 6.40 (H-8) were correlated with the carbons at δ_C 142.0 (C-7), 111.5 (C-2), 130.7 (C-2′ and C-6′), 123.2 (C-6), 116.5 (C-5), 116.3 (C-3′ and C-5′) and 118.7 (C-8), respectively. The aliphatic protons at δ_H 3.88 (3-OMe), 3.46 (H-8′) and 2.75 (H-7′) were correlated with the carbons at δ_C 56.4 (3-OMe), 42.6 (C-8′) and 35.8 (C-7′), respectively. In the HMBC

spectrum (**Figure 52**) long-range couplings were observed from the proton at δ_H 7.43 (H-7) to five carbons at δ_C 169.2 (C-9), 128.3 (C-1), 123.2 (C-6), 118.7 (C-8) and 111.5 (C-2). These correlations showed the connectivity between the aromatic ring at C-1 and the substituent at C-7. The proton at δ_H 3.46 (H-8′) was correlated to three carbons at δ_C 169.2 (C-9), 131.3 (C-1′) and 35.8 (C-7′). The carbon at δ_C 35.8 (C-7′) was connected with carbon at position 1′ by 2-bond HMBC correlation. The methoxy protons at δ_H 3.88 (3-OMe) were correlated with the carbon at position 3.

In conclusion, compound PF-6 was identified as *N-trans*-feruloyltyramine [**30**] based on the above analysis of ^{1}H-NMR and ^{13}C-NMR spectra and comparison with previously reported values (Al-Taweel *et al*., 2012)

N-trans-feruloyltyramine [**31**] (amide alkaloid) has been isolated from various plants such as *Cyperus rotundus* (Rajamanickam *et al*., 2016), *Aristolochia gigantea* (Holzbach *et al*., 2010), *Celtis africana* (Al-Taweel *et al*., 2012), a*llium bakeri* (Okuyama *et al*., 1986), *Mucuna birdwoodiana* (Goda *et al*., 1987), *Lycium barbarum* (Forino *et al*., 2016), *Solanum sordidum* (Kanada *et al*., 2012) and *Casearia membranacea* (Chang *et al*., 2003). This compound has been studied for several bioactivities, such as cytotoxicity against the P-388 and the HT-29 cancer cell lines (Chang *et al*., 2003), inhibition of platelet aggregation (Okuyama *et al*., 1986), antioxidant activity and anti-inflammatory activity (Al-Taweel *et al*., 2012).

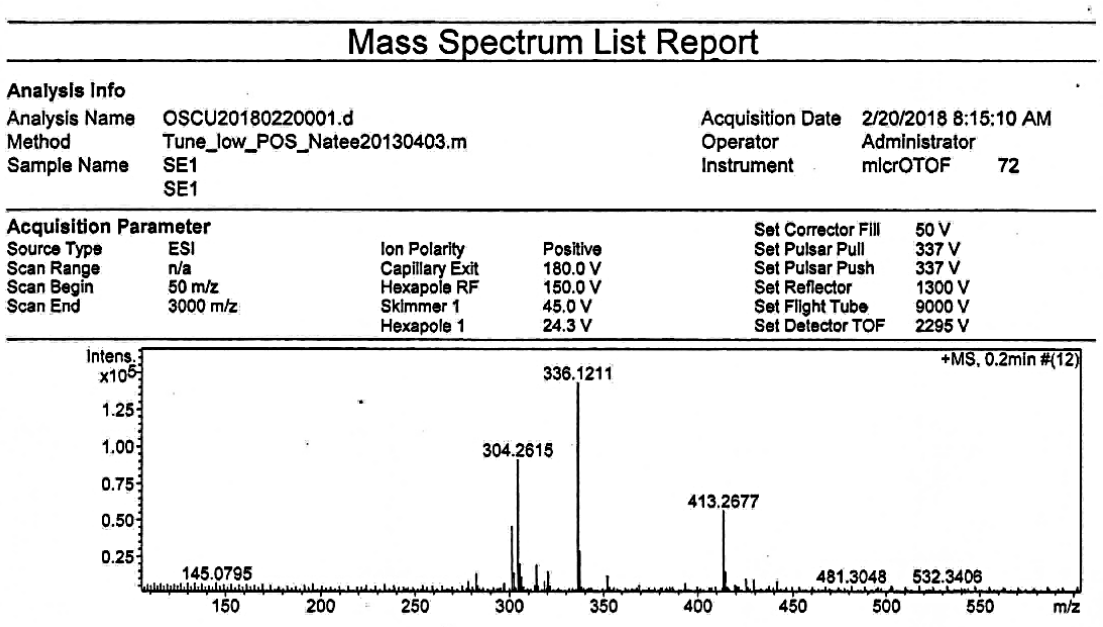

Mass Spectrum List Report

Analysis Info

Analysis Name	OSCU20180220001.d	Acquisition Date	2/20/2018 8:15:10 AM
Method	Tune_low_POS_Natee20130403.m	Operator	Administrator
Sample Name	SE1	Instrument	micrOTOF 72
	SE1		

Acquisition Parameter

Source Type	ESI	Ion Polarity	Positive	Set Corrector Fill	50 V
Scan Range	n/a	Capillary Exit	180.0 V	Set Pulsar Pull	337 V
Scan Begin	50 m/z	Hexapole RF	150.0 V	Set Pulsar Push	337 V
Scan End	3000 m/z	Skimmer 1	45.0 V	Set Reflector	1300 V
		Hexapole 1	24.3 V	Set Flight Tube	9000 V
				Set Detector TOF	2295 V

Figure 47 Mass spectrum of compound PF-6

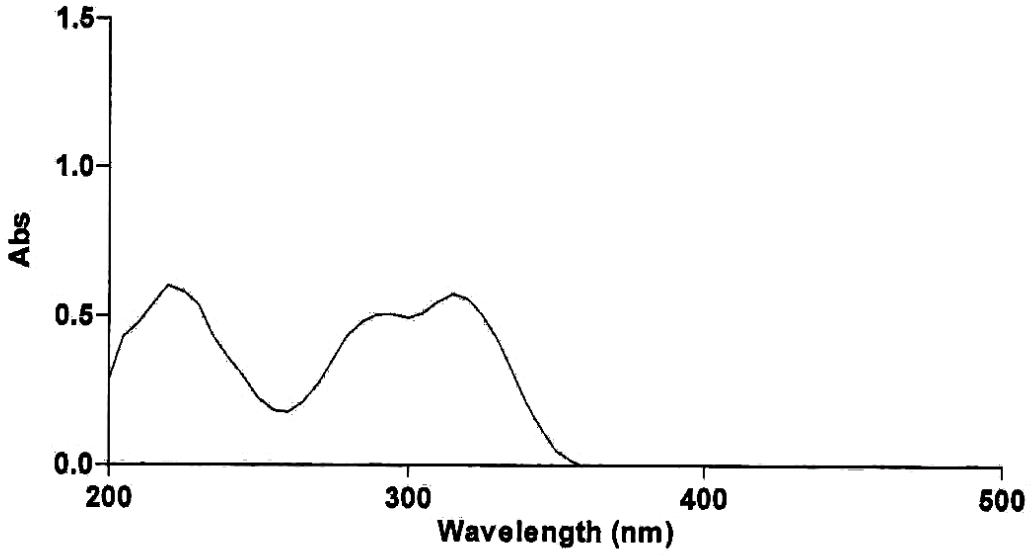

Figure 48 UV Spectrum of compound PF-6

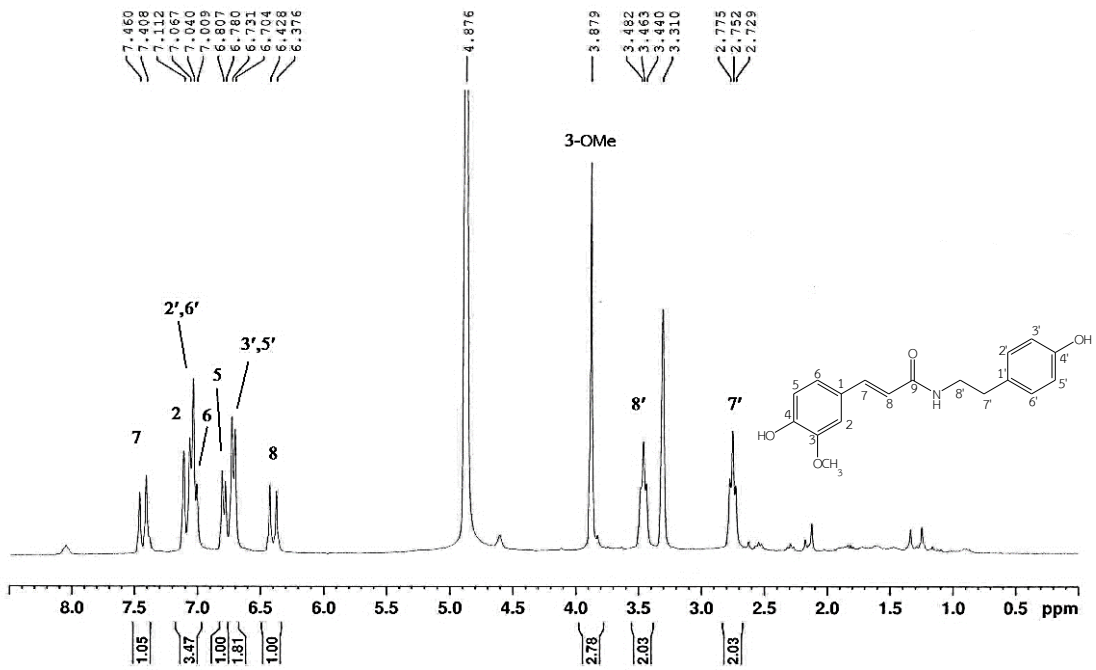

Figure 49 ^{1}H-NMR (300 MHz) Spectrum of compound PF-6 (in CD_3OD)

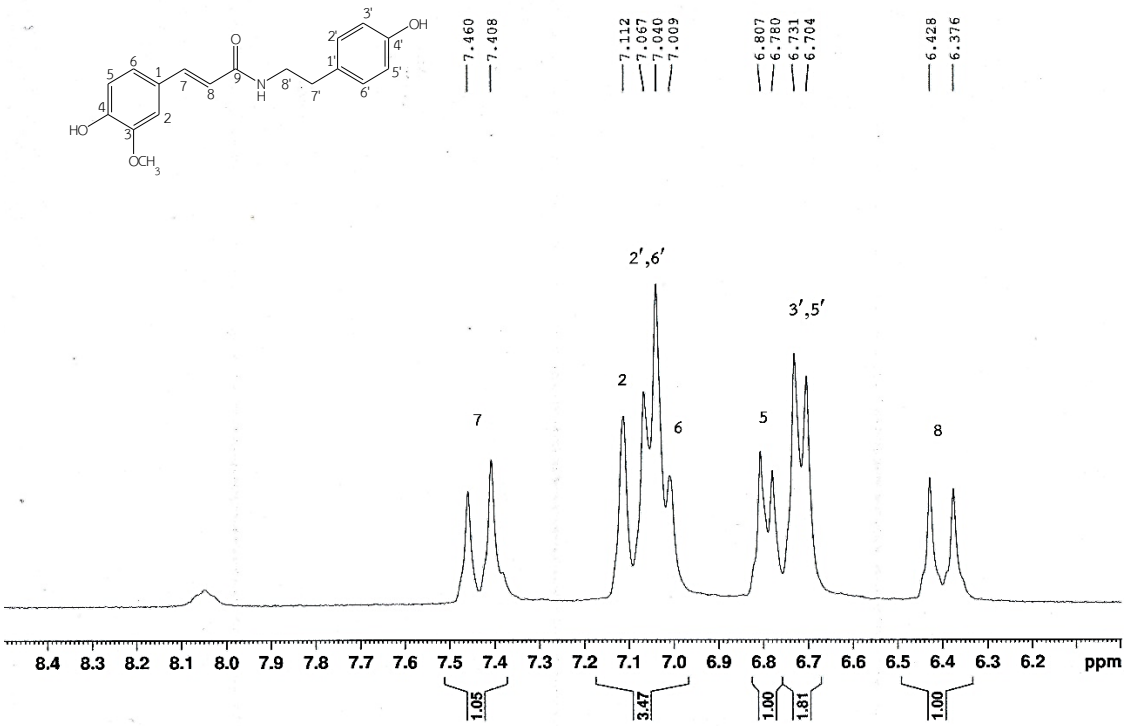

Figure 50 ^{1}H-NMR (300 MHz) Spectrum of compound PF-6 (in CD_3OD)

[δ_H 6.0-8.5 ppm]

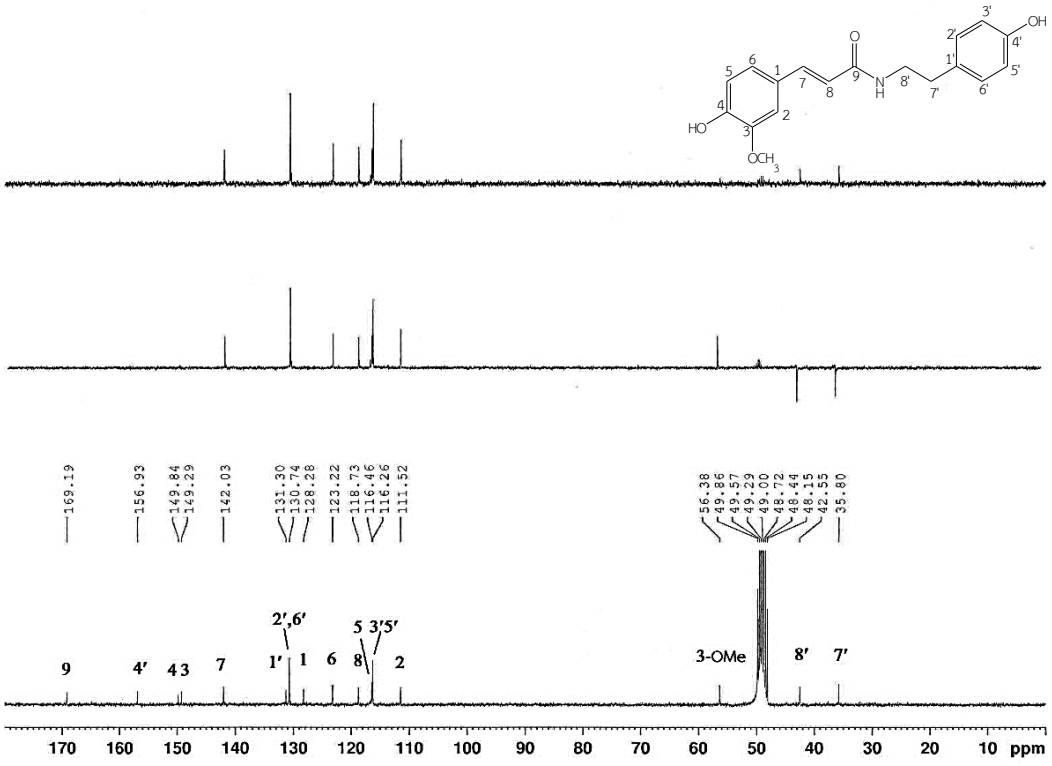

Figure 51 ^{13}C-NMR, DEPT135, DEPT90 (75 MHz) Spectra of compound PF-6 (in CD_3OD)

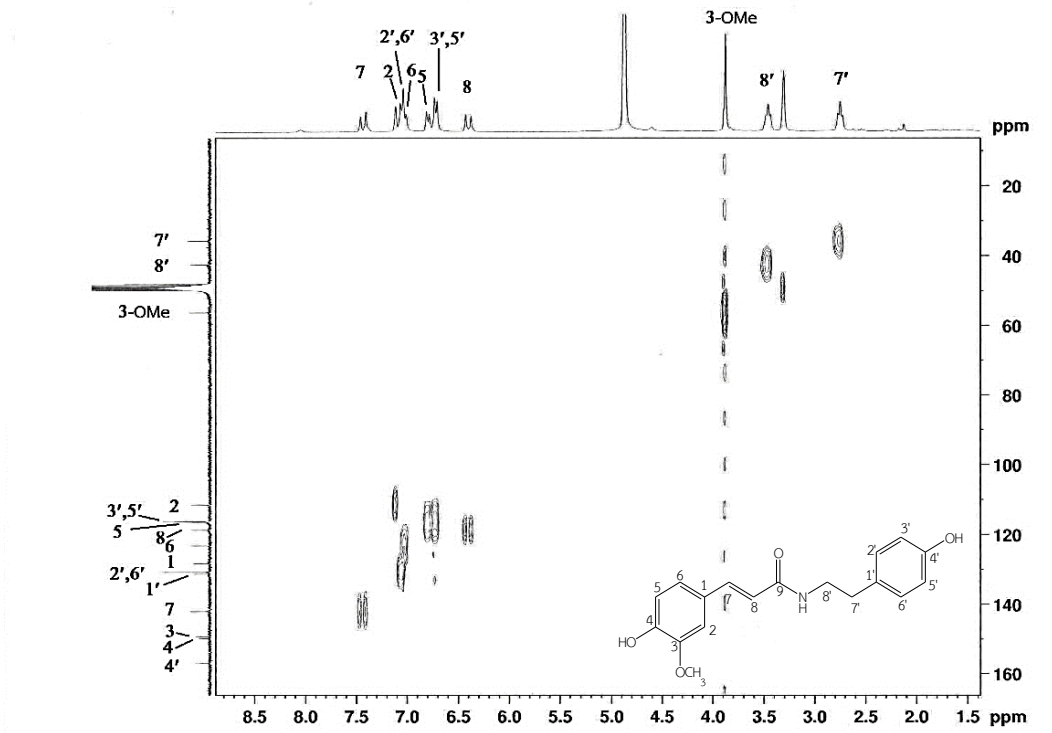

Figure 52 HSQC Spectrum of compound PF-6 (in CD_3OD)

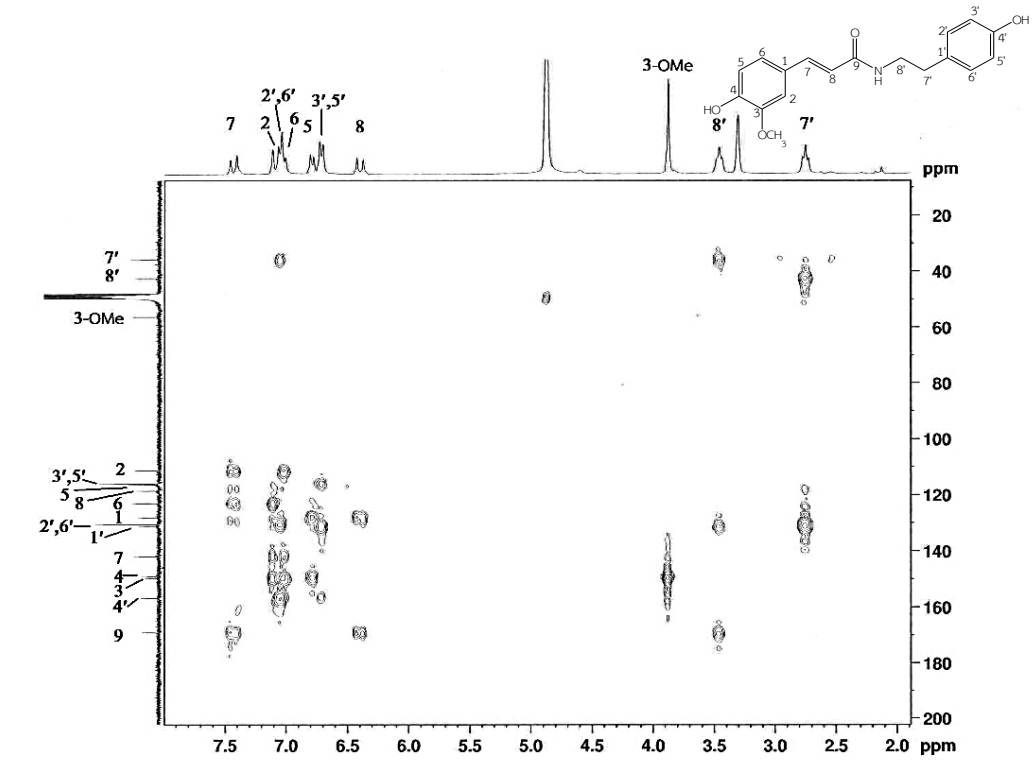

Figure 53 HMBC Spectrum of compound PF-6 (in CD_3OD)

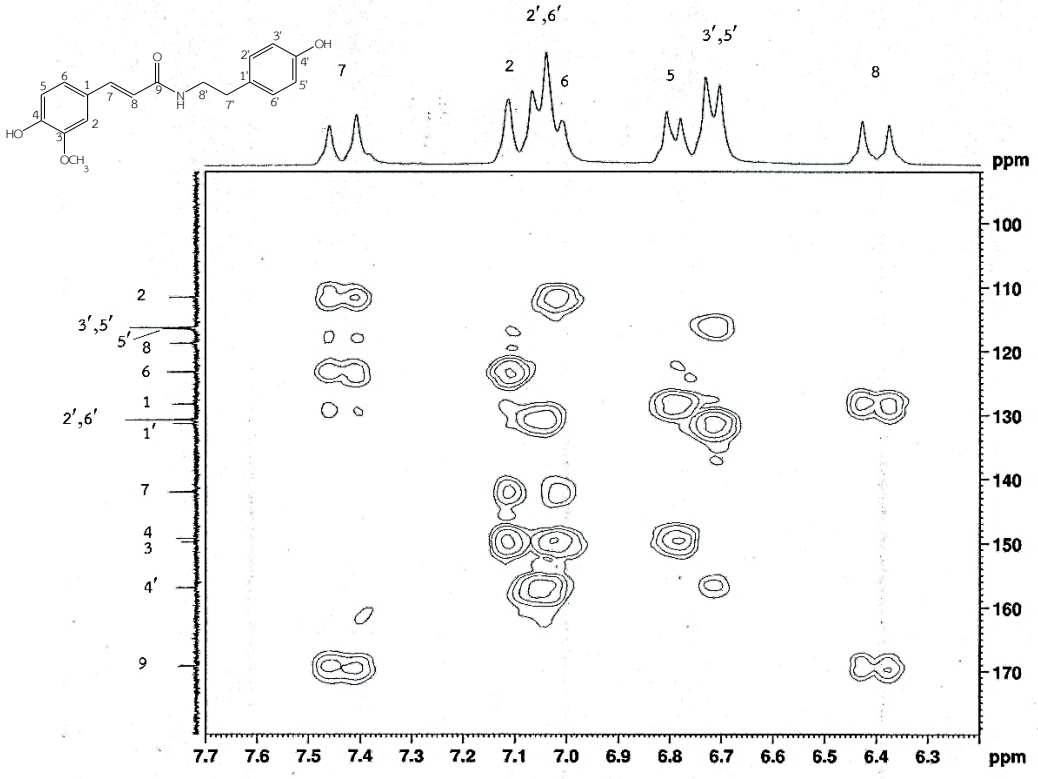

Figure 54 HMBC Spectrum of compound PF-6 (in CD_3OD)

[δ_H 6.2-7.7 ppm, δ_C 90-180 ppm]

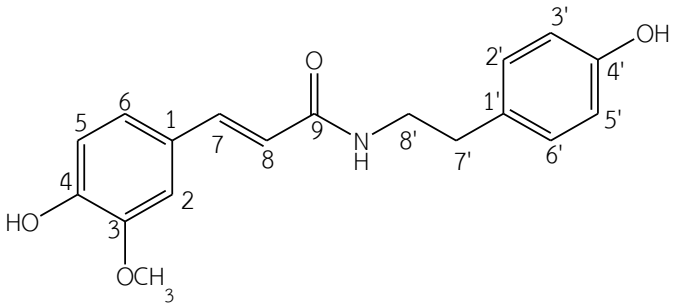

N-trans-feruloyltyramine [**31**]

Table 10 NMR Spectral data of compound PF-6 (in CD_3OD) and *N-trans*-feruloyltyramine (in CD_3OD)

Position	Compound PF-6		*N-trans*-feruloyltyramine [31][a]	
	δ_H (mult., *J* in Hz)	δ_C	δ_H (mult., *J* in Hz)	δ_C
1	-	128.3	-	128.2
2	7.11 (*s*)	111.5	7.13 (*d*; 1.2)	111.5
3	-	149.3	-	149.3
4	-	149.8	-	149.8
5	6.79 (*d*, 8.1)	116.5	6.81 (*d*; 8.5)	116.4
6	7.01 (*d*, 8.1)	123.2	7.05 (*dd*; 8.5 and 1.2)	123.2
7	7.43 (*d*, 15.6)	142.0	7.44 (*d*; 15.5)	142.0
8	6.40 (*d*, 15.6)	118.7	6.41 (*d*; 15.5)	118.7
9	-	169.2	-	169.2
1′	-	131.3	-	131.3
2′	7.05 (*d*, 8.1)	130.7	7.07 (*d*; 8.4)	130.7
3′	6.72 (*d*, 8.1)	116.3	6.73 (*d*; 8.4)	116.2
4′	-	156.9	-	156.9
5′	6.72 (*d*, 8.1)	116.3	6.73 (*d*; 8.4)	116.2
6′	7.05 (*d*, 8.1)	130.7	7.07 (*d*; 8.4)	130.7
7′	2.75 (*t*, 6.9)	35.8	2.76 (*t*; 7.5)	35.8
8′	3.46 (*t*, 6.9)	42.6	3.47 (*t*; 7.5)	42.5
3-OMe	3.88 (*s*)	56.4	3.85 (*s*)	56.4

[a]Al-Taweel *et al*., 2012

1.7 Structure determination of compound PF-7

Compound PF-7 was obtained as a yellow amorphous solid. Its HR-ESI-MS (**Figure 55**) showed a sodium-adduct molecular ion $[M+Na]^+$ at *m/z* 306.1112 (calcd. for $C_{17}H_{17}NO_3Na$; 306.1106), suggesting the molecular formula $C_{17}H_{17}NO_3$. The UV spectrum (**Figure 56**) exhibited maximum absorptions at λ_{max} 225, 290 and 310 nm, similar to those of PF-6.

The ^{1}H-NMR spectrum of compound PF-7 (**Figure 57** and **Table 11**) showed two sets of *ortho*-coupled aromatic protons. The first set appeared at δ_H 7.30 (2H, *d*, *J* = 8.7 Hz, H-6 and H-2) and 6.69 (2H, *d*, *J* = 8.7 Hz, H-5 and H-3). The second set resonated at δ_H 6.96 (2H, *d*, *J* = 8.4 Hz, H-6′ and H-2′) and 6.62 (2H, *d*, *J* = 8.4 Hz, H-5′ and H-3′). Each set indicated *para*-substitution for a benzene ring. The olefinic protons at δ_H 7.37 (1H, *d*, *J* = 15.6 Hz) and 6.28 (1H, *d*, *J* = 15.6 Hz) could be assigned to H-7 and H-8, respectively. The coupling constant of 15.6 Hz indicated a *trans*-configuration between H-7 and H-8. The triplets at δ_H 3.36 (2H, *J* = 7.2 Hz) and 2.65 (2H, *J* = 7.2 Hz) could be assigned to H-8′ and H-7′, respectively.

The ^{13}C-NMR spectrum (**Figure 58** and **Table 11**) displayed seventeen carbon signals, including one carbonyl carbon at δ_C 169.2 (C-9). The other sixteen carbon signals of PF-7 could be classified into two methylene carbons at δ_C 42.5 (C-8′) and 35.8 (C-7′), four quaternary carbons at δ_C 160.5 (C-4), 156.9 (C-4′), 129.8 (C-1′) and 127.6 (C-1), ten methine carbons at δ_C 142.4 (C-7), 131.6 (C-6′ and C-2′), 131.2 (C-6 and C-2), 119.3 (C-8), 117.7 (C-5 and C-3) and 117.2 (C-5′ and C-3′).

The HSQC spectrum (**Figure 59**) showed that the protons at δ_H 7.30 (H-6 and H-2), 6.69 (H-5 and H-3), 6.96 (H-6′ and H-2′), 6.62 (H-5′ and H-3′) 7.37 (H-7) and 6.28 (H-8) were correlated with the carbons at δ_C 131.2 (C-6 and C-2), 117.7 (C-5 and C-3), (C-6′ and C-2′), 117.2 (C-5′ and C-3′), 142.4 (C-7) and 119.3 (C-8), respectively. The aliphatic protons at δ_H 3.36 (H-8′) and 2.65 (H-7′) were correlated with the carbons at δ_C 42.5 (C-8′) and 35.8 (C-7′), respectively. In the HMBC spectrum (**Figure 60**), the olefinic proton at δ_H 7.37 (H-7) was correlated to five carbons at δ_C 169.2 (C-9), 119.3

(C-8), 131.2 (C-6 and C-2) and 127.6 (C-1), and the aliphatic proton at δ_H 2.65 (H-7′) was correlated to four carbons at δ_C 131.6 (C-6′ and C-2′), 129.8 (C-1′) and 42.5 (C-8′). Thus, the carbons at δ_C 142.4 (C-7) and 35.8 (C-7′) were connected with aromatic carbons at positions 1 and 1′, respectively.

Based on these spectral data and comparison with previous reports (Sipowo *et al*., 2017) compound PF-7 was identified as *N-trans*-coumaroyltyramine [**32**].

N-trans-Coumaroyltyramine [**32**], an amide alkaloid, has been found in *Celtis Africana* (Al-Taweel *et al*., 2012), a*llium bakeri* (Okuyama *et al*., 1986), *Allium fistulosum* (Seo *et al*., 2011), *Ochthocosmus africanus* (Sipowo *et al*., 2017). This compound showed effective inhibition against platelet aggregation induced by adenosine 5'-diphosphate (Okuyama *et al*., 1986), antioxidant, anti-inflammatory, acetylcholinestrease inhibitory activity (Al-Taweel *et al*., 2012) and inhibition of α-glucosidase activity (IC_{50} = 0.42 μM) (Song *et al*., 2016).

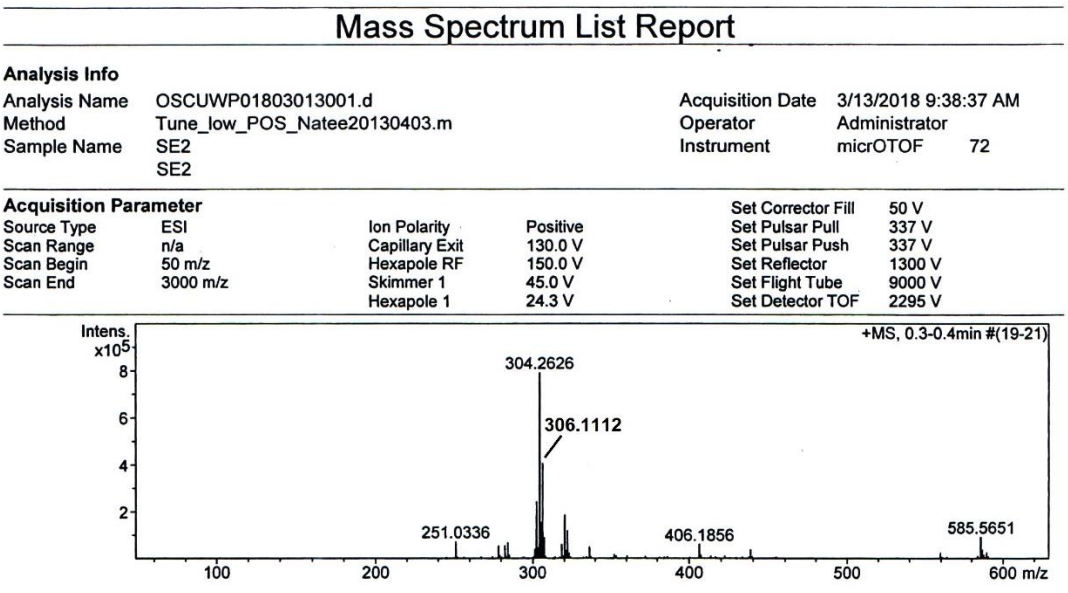

Figure 55 Mass spectrum of compound PF-7

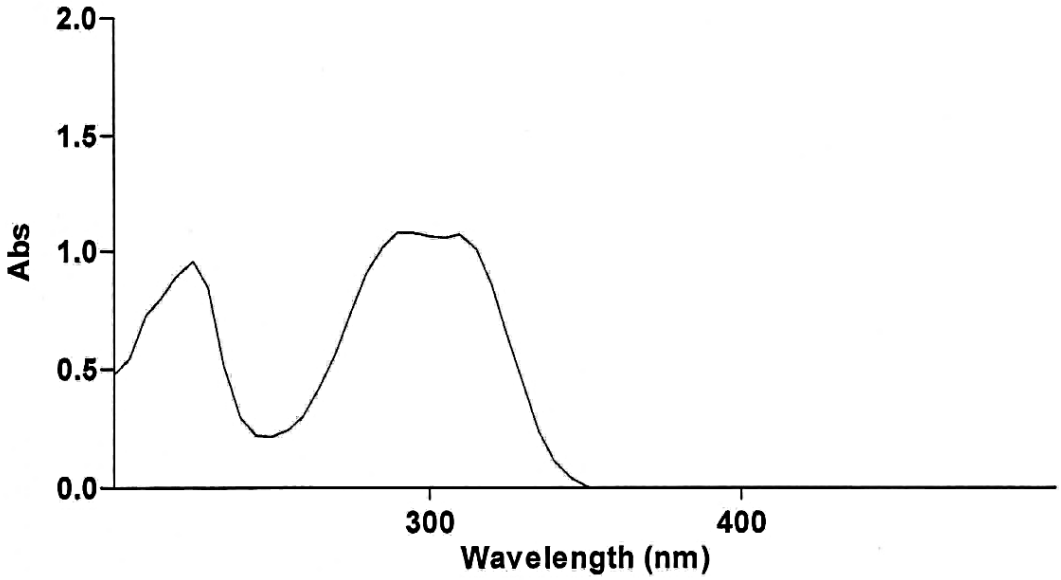

Figure 56 UV Spectrum of compound PF-7

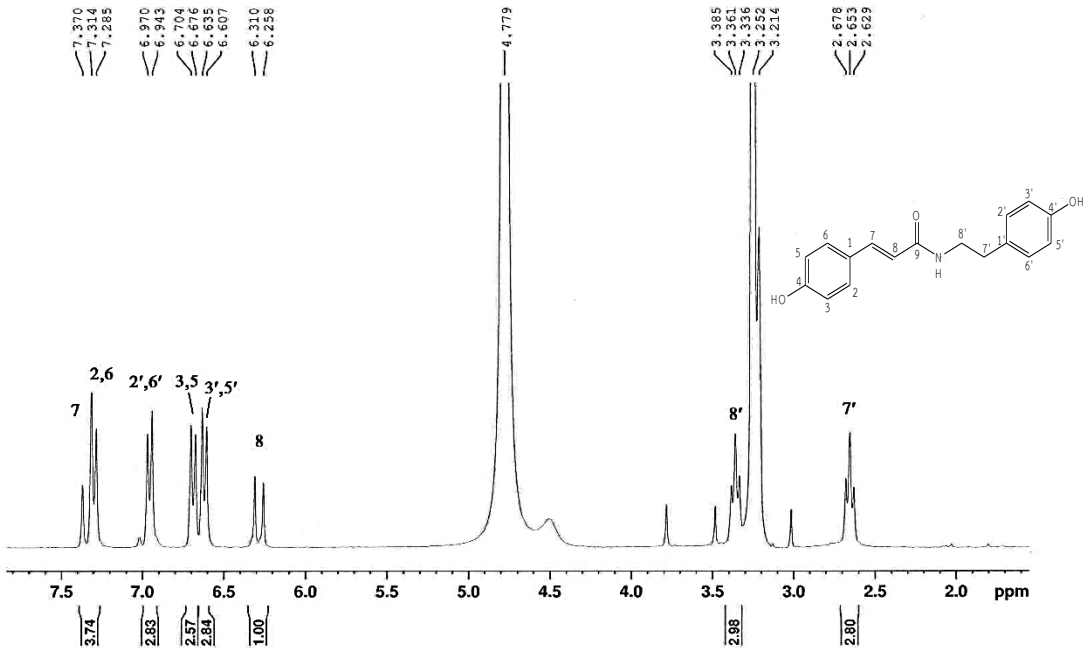

Figure 57 ^{1}H-NMR (300 MHz) Spectrum of compound PF-7 (in CD_3OD)

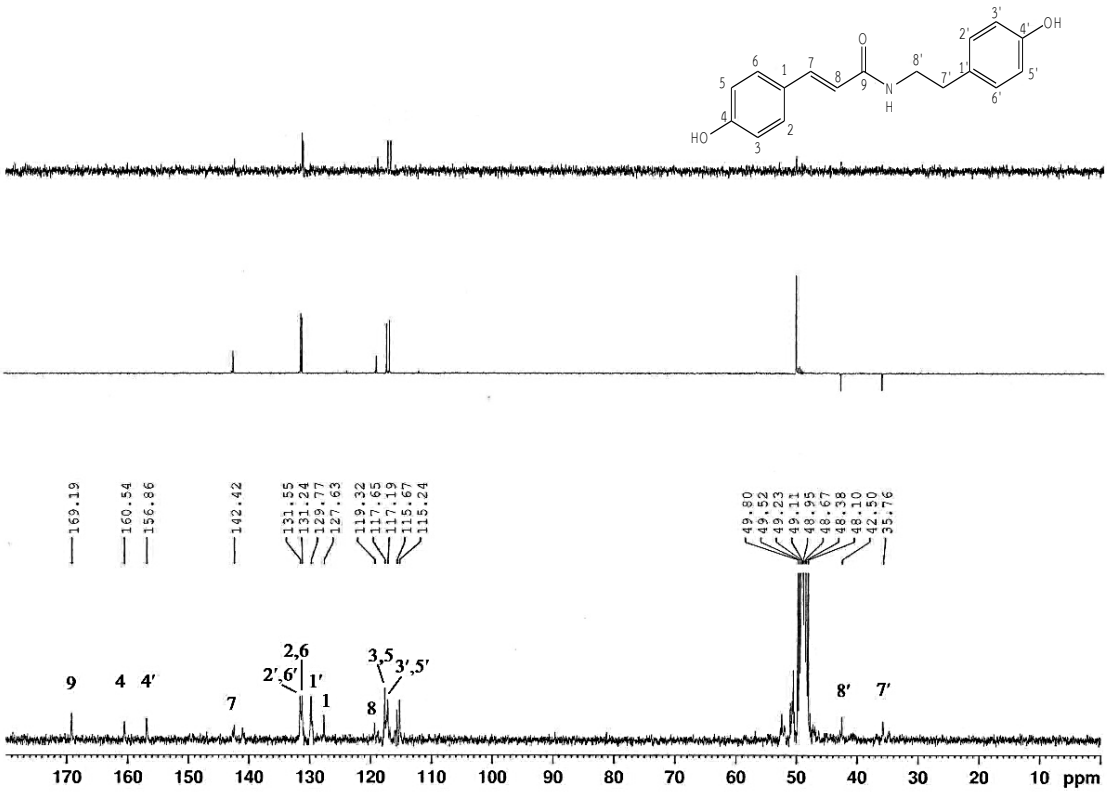

Figure 58 ^{13}C-NMR, DEPT135, DEPT90 (75 MHz) Spectra of compound PF-7 (in CD_3OD)

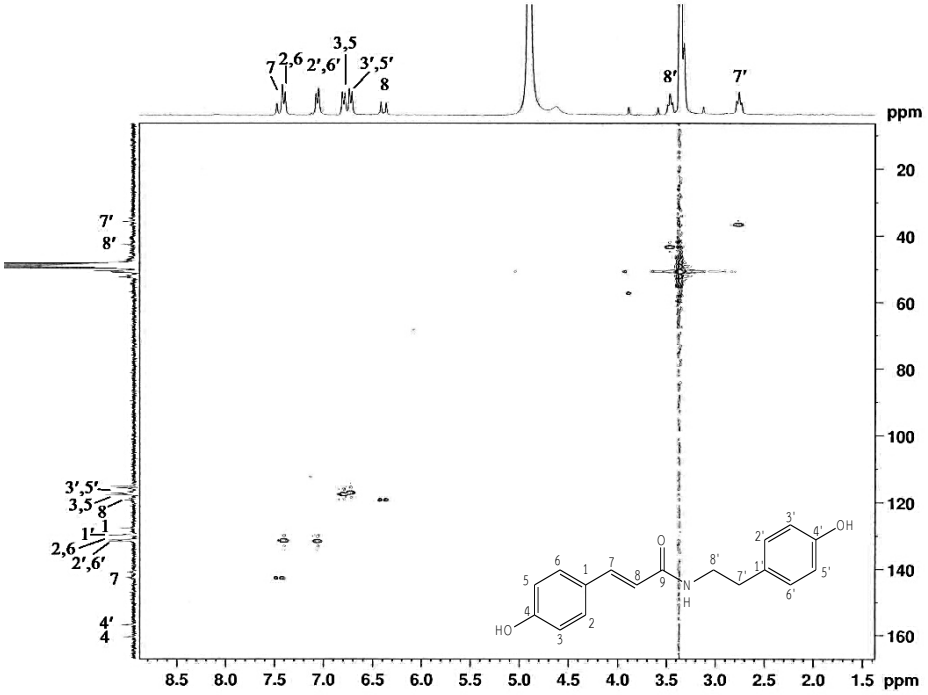

Figure 59 HSQC Spectrum of compound PF-7 (in CD_3OD)

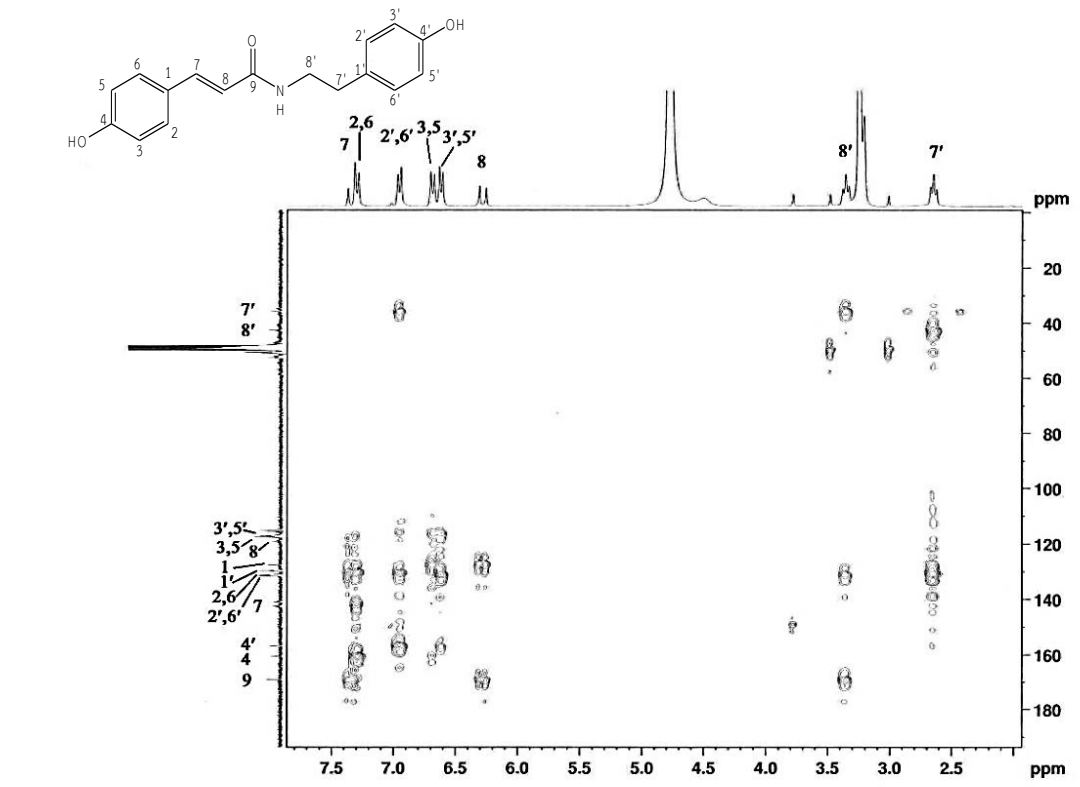

Figure 60 HMBC Spectrum of compound PF-7 (in CD_3OD)

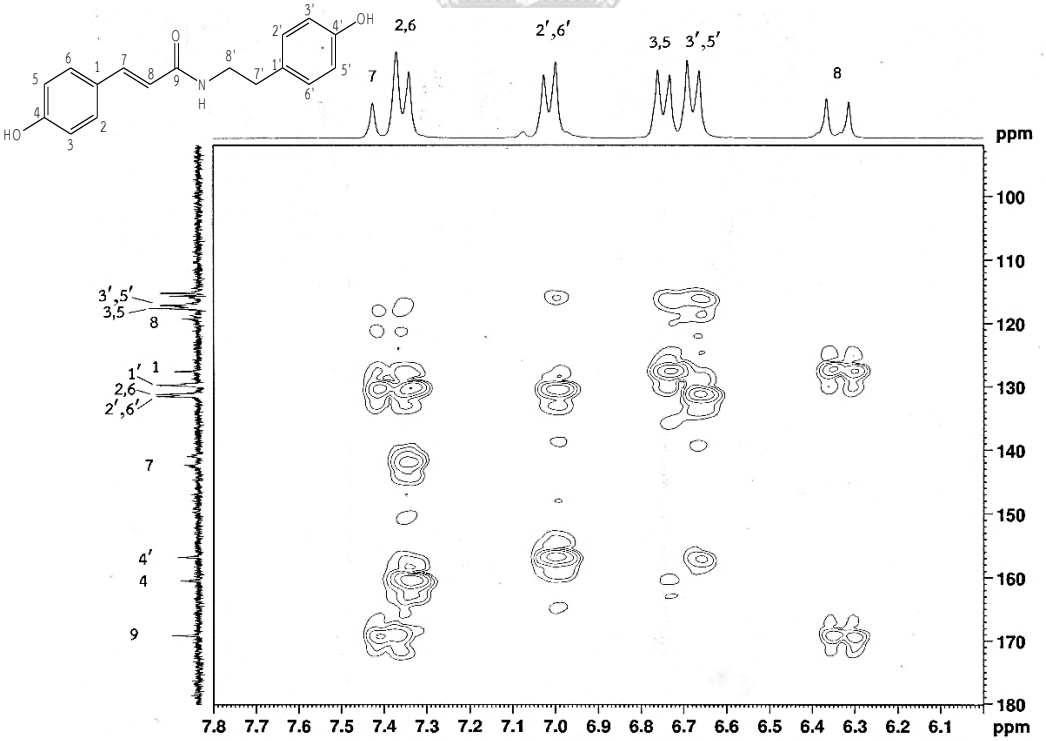

Figure 61 HMBC Spectrum of compound PF-7 (in CD_3OD)

[δ_H 6.0-7.8 ppm, δ_C 90-180 ppm]

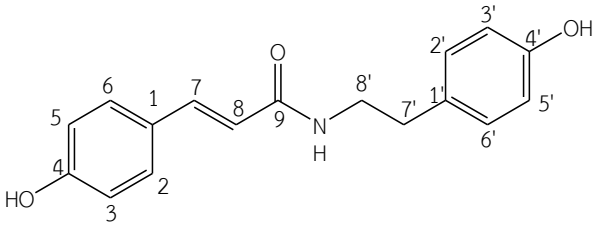

N-trans-coumaroyltyramine [**32**]

Table 11 NMR Spectral data of compound PF-7 (in CD_3OD) and *N-trans*-coumaroyltyramine (in CD_3OD)

Position	Compound PF-7		*N-trans*-coumaroyltyramine [32][a]	
	δ_H (mult., *J* in Hz)	δ_C	δ_H (mult., *J* in Hz)	δ_C
1	-	127.6	-	129.1
2	7.30 (*d*, 8.7)	131.2	7.32 (*d*, 7.5)	132.0
3	6.69 (*d*, 8.7)	117.7	6.71 (*d*, 7.5)	118.1
4	-	160.5	-	162.0
5	6.69 (*d*, 8.7)	117.7	6.71 (*d*, 7.5)	118.1
6	7.30 (*d*, 8.7)	131.2	7.32 (*d*, 7.5)	132.0
7	7.37 (*d*, 15.6)	142.4	7.37 (*d*, 15.5)	143.2
8	6.28 (*d*, 15.6)	119.3	6.31 (*d*, 15.5)	119.8
9	-	169.2	-	168.8
1′	-	129.8	-	132.7
2′	6.69 (*d*, 8.4)	131.6	6.98 (*d*, 8.5)	132.2
3′	6.62 (*d*, 8.4)	117.2	6.64 (*d*, 8.5)	117.7
4′	-	156.9	-	158.4
5′	6.63 (*d*, 8.4)	117.2	6.64 (*d*, 8.5)	117.7
6′	6.69 (*d*, 8.4)	131.6	6.98 (*d*, 8.5)	132.2
7′	2.65 (*t*, 7.2)	35.8	2.68 (*t*, 7.0)	37.2
8′	3.36 (*t*, 7.2)	42.5	3.38 (*t*, 7.0)	44.0

[a]Sipowo *et al*., 2017

2. Bioactivities of compounds isolated from leaves and stems of *Pseuduvaria fragrans*

2.1 Cytotoxic activity

The methanol extract of *P. fragrans* leaves exhibited cytotoxic activity against small cell lung cancer cells (NCl-H 187) with 95.13% inhibition at 50 µg/mL. In this study, the isolated compounds were not tested. The cytotoxicity of the extract might have come from (-)-guaiol [**25**] and (+)-isocorydine [**27**] as previous reports have described their cytotoxic activity (Lu *et al*., 2012; Pan *et al*., 2018; Yang *et al*., 2018). The stem methanol extract showed no cytotoxic activity at 50 µg/mL.

2.2 α-Glucosidase inhibitory activity

The methanol extracts of the leaves and stems of *Pseuduvaria fragrans* were evaluated for α-glucosidase inhibitory activity and shown to exhibit 56.46% and 66.16% inhibition at a concentration of 200 µg/mL, respectively.

The hexane and EtOAc extracts of the leaves exhibited α-glucosidase inhibitory activity with 51.56% and 99.71% inhibition at a concentration of 200 µg/mL, respectively. The hexane and EtOAc extracts of the stems showed 99.46% and 76.96% inhibition of α-glucosidase activity at a concentration of 200 µg/mL, respectively (**Table 12**). An IC_{50} value was determined for the compound that showed more than 50% inhibition at 200 µg/mL (**Table 13**).

Table 12 α-Glucosidase inhibitory activity of extract

Extracts	%Inhibition	
	Leaves (mM)	Stems (mM)
Methanol	56.46	66.16
Hexane	51.56	99.46
EtOAc	99.71	76.96
n-Butanol	NA	NA
aqueous	NA	NA
Acarbose	76.15 (1.55)	76.15 (1.55)

Table 13 IC_{50} Values of compounds PF-1 to PF-7 for α-glucosidase inhibitory activity

compounds	IC_{50} (μM)
(-)-guaiol [**25**]	NA
pseuduvarioside [**26**]	NA
(+)-isocorydine [**27**]	NA
Cyathocaline [**29**]	NA
Isoursuline [**30**]	NA
N-trans-feruloyltyramine [**31**]	3.58±0.13
N-trans-coumaroyltyramine [**32**]	0.58±0.08
Acarbose	985.6±35.04

NA = no inhibitory activity

Seven pure compounds were evaluated. *N-trans*-Feruloyltyramine [**31**] and *N-trans*-coumaroyltyramine [**32**] exhibited α-glucosidase inhibitory activity (IC_{50} values 3.58 and 0.58 μM, respectively) compared with acarbose as the positive control. *N-trans*-Feruloyltyramine [**31**] showed lower α-glucosidase inhibitory activity, probably due to the methoxy group at position 3. A previous study has reported that [**31**] and [**32**] exhibited α-glucosidase inhibitory activity (IC_{50} values 10.62 and 0.42 μM, respectively) (Song *et al*., 2016)

Kinetic studies were done by Linewever-Burk plot (or double reciprocal plot) of the inverted values of velocity (1/V) versus the inverted values of substrate concentration (1/[S]). Acarbose as a positive control (**Figure 62**) exhibited increased K_m value but did not affect the V_{max} value. This indicated that acarbose was a competitive inhibitor. In the present study, *N-trans*-feruloyltyramine [**31**] and *N-trans*-coumaroyltyramine [**32**] were prepared at three concentrations (8.0, 4.0 and 2.0 μM) and (2.0, 1.0 and 0.5 μM), respectively. In the presence of each compound (**Table 14**) slopes of the Lineweaver-Burk plots did not change, but the V_{max} and K_m values altered. These results suggested that each compound was an uncompetitive inhibitor

of this enzyme. The inhibition constants (K_i) of the two cinnamoyl tyramides were calculated using the secondary plots of the inverted values of V_{max} ($1/V_{max}$) versus the inhibitor concentration [I].

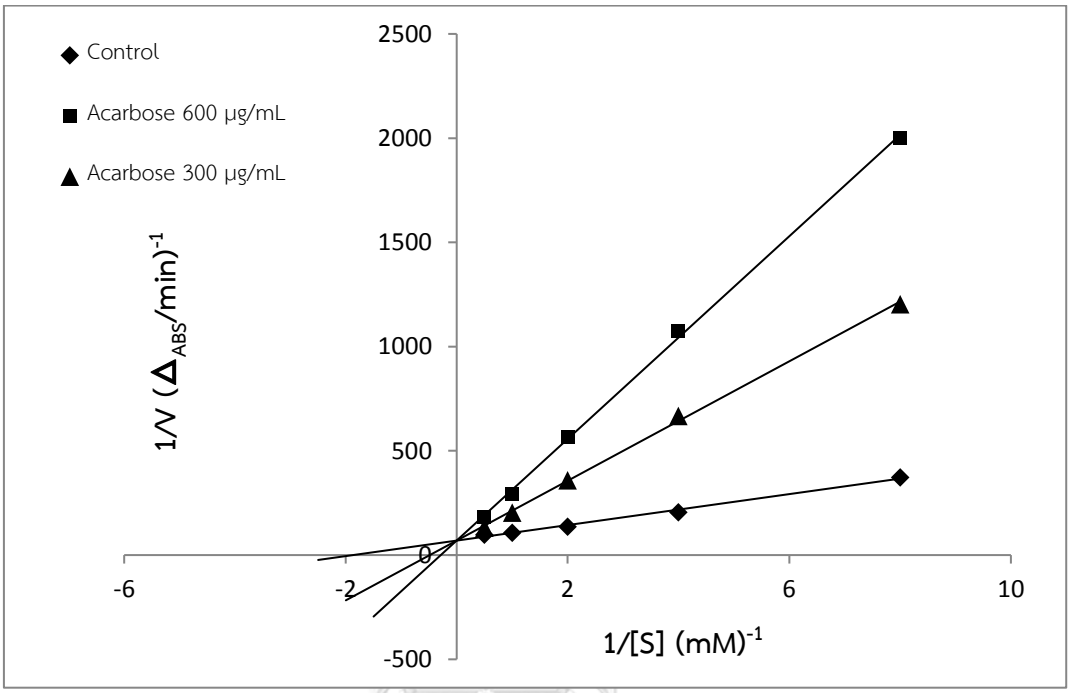

Figure 62 α-Glucosidase inhibition by two concentrations of acarbose

Table 14 Kinetic parameters of α-glucosidase in the presence of *N-trans*-feruloyltyramine [**31**] and *N-trans*-coumaroyltyramine [**32**]

Inhibitors	Dose (µM)	slope	V_{max} ΔA_{405}/min	K_m (mM)	K_i (µM)
None	-	37.15	0.0144	0.53	
N-trans-feruloyltyramine	8.0	36.51	0.0027	0.10	1.83
	4.0	37.56	0.0044	0.16	
	2.0	36.62	0.0072	0.26	
N-trans-coumaroyltyramine	2.0	35.56	0.0018	0.06	0.20
	1.0	34.67	0.0030	0.10	
	0.5	34.55	0.0077	0.27	

The results showed the maximum velocity (V_{max}) value of 0.0144 ΔA_{405}/min for *p*NPG hydrolysis, and the Michaelis-Menten constant (K_m) value of 0.53 mM. **Figures 63-64** show the Linewaver-Burk plots of 1/V value with different *p*NPG concentrations of *N-trans*-feruloyltyramine [**31**] (8.0, 4.0 and 2.0 μM) and *N-trans*-coumaroyltyramine [**32**] (2.0, 1.0 and 0.5 μM). The result showed that the increase of inhibitor concentration reduced the V_{max} value for *N-trans*-feruloyltyramine [**31**]: (0.0027-0.0072) and for *N-trans*-coumaroyltyramine [**32**]: (0.0018-0.0077) and the K_m value for *N-trans*-feruloyltyramine [**31**]: (0.10-0.26) and for *N-trans*-coumaroyltyramine [**32**]: (0.06-0.27). No change was observed for the slope of each line. These results suggested that both compounds were uncompetitive inhibitors of this enzyme. These findings agreed with an earlier report of *N-trans*-coumaroyltyramine [**32**] (Song *et al*., 2016). From the secondary plots, *N-trans*-feruloyltyramine [**31**] (**Figure 65**) (K_i 1.83 μM) and *N-trans*-coumaroyltyramine [**32**] (**Figure 66**) (K_i 0.20 μM) showed higher α-glucosidase inhibitory activity than acarbose (**Figure 67**) (K_i 172.27 μM).

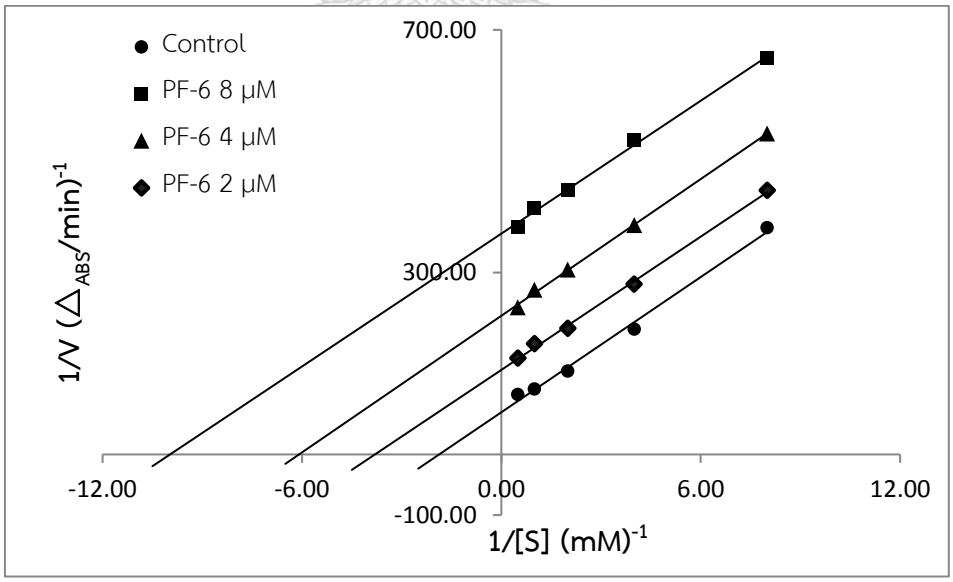

Figure 63 α-Glucosidase inhibition by three concentrations of *N-trans*-feruloyltyramine (PF-6)

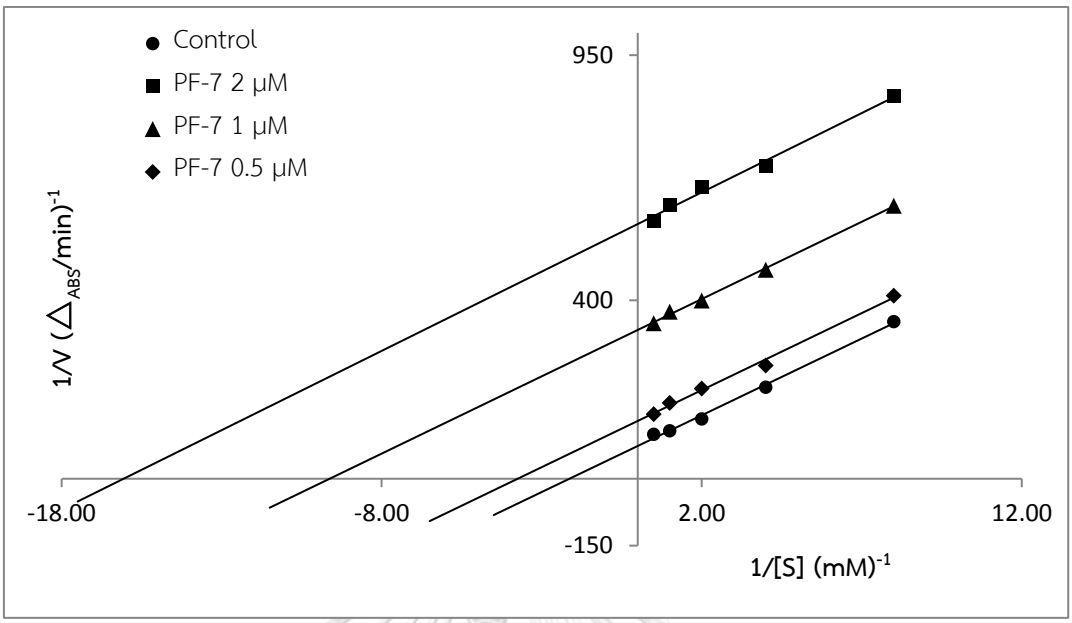

Figure 64 α-Glucosidase inhibition by three concentrations of *N-trans*-coumaroyltyramine (PF-7)

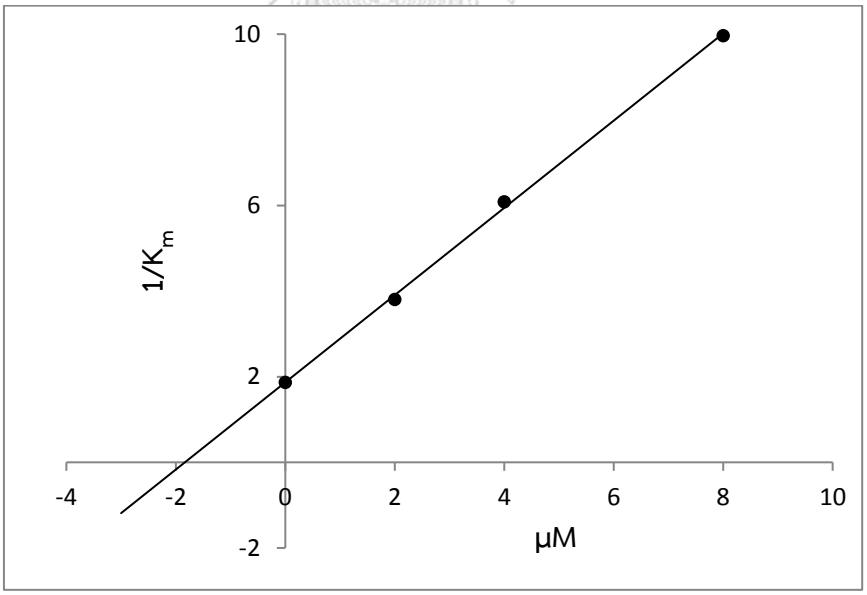

Figure 65 Secondary plot for inhibition constant (K_i) of *N-trans*-feruloyltyramine (PF-6)

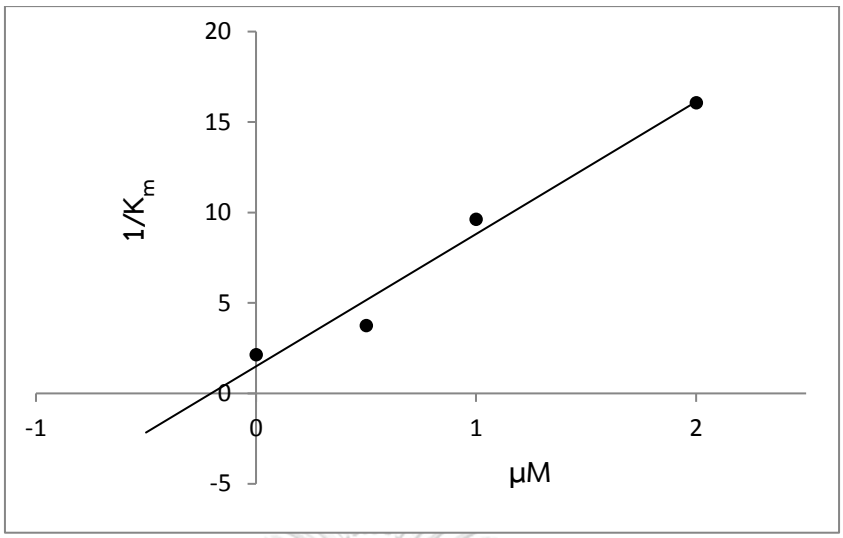

Figure 66 Secondary plot for inhibition constant (K_i) of *N-trans*-coumaroyltyramine (PF-7)

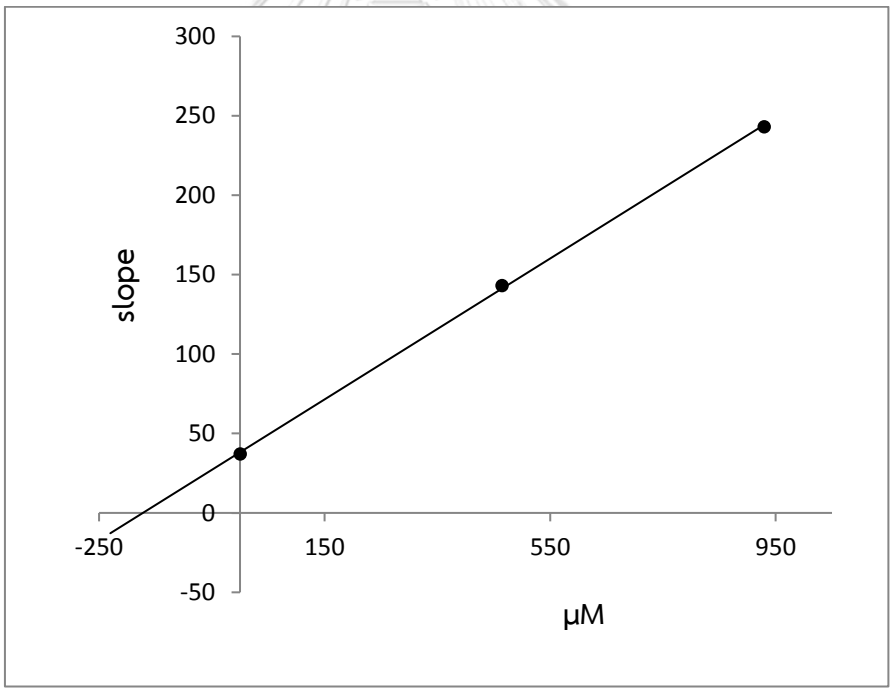

Figure 67 Secondary plot for inhibition constant (K_i) of acarbose

CHAPTER V
CONCLUSION

This study investigated the chemical constituents of the leaves and stems of *P. fragrans* and their α-glucosidase inhibitory activity. Seven compounds were isolated and structurally characterized including one new benzophenone *C*-glycoside, pseuduvarioside [**26**] (PF-2) and six known compounds: (-)-guaiol (PF-1) [**25**], (+)-isocorydine (PF-3) [**27**], cyathocaline (PF-4) [**29**], isoursuline (PF-5) [**30**], *N-trans*-feruloyltyramine (PF-6) [**31**] and *N-trans*-coumaroyltyramine (PF-7) [**32**]. The leaves methanol extract exhibited cytotoxic activity against small cell lung cancer cells (NCl-H 187). This cytotoxicity may have come from (-)-guaiol [**25**] and (+)-isocorydine [**27**], which have been previously studied for this activity. *N-trans*-feruloyltyramine (PF-6) [**31**] and *N-trans*-coumaroyltyramine (PF-7) [**32**] exhibited stronger α-glucosidase inhibitory activity than the positive control (acarbose). The kinetic studies of the activity of both compounds (PF-6 and PF-7) showed their uncompetitve mode of inhibition. This study is the first report of the chemical constituents and α-glucosidase inhibitory activity of this plant.

REFERENCES

Abdel-Mageed, W. M., Bayoumi, S. A., Chen, C., Vavricka, C. J., Li, L., Malik, A., Dai, H., Song, F., Wang, L., Zhang, J., Gao, G. F., Lv, Y., Liu, L., Liu, X., Sayed, H. M., and Zhang, L. (2014). Benzophenone *C*-glucosides and gallotannins from mango tree stem bark with broad-spectrum anti-viral activity. Bioorganic & Medicinal Chemistry, 22, 2236-2243.

Aderogba, M. A., Ndhlala, A. R., Rengasamy, K. R., and Staden, V. J. (2013). Antimicrobial and selected in vitro enzyme inhibitory effects of leaf extracts, flavonols and indole alkaloids isolated from *Croton menyharthii*. Molecules, 18, 12633-12644.

Al-Taweel, A. M., Perveen, S., El-Shafae, A. M., Fawzy, G. A., Malik, A., Afza, N., Iqbal, L. and Latif, M. (2012). Bioactive phenolic amides from *Celtis africana*. Molecules, 17, 2675-2682.

Bakri, Y. M., Talip, M. A., and Azziz, S. S. A. (2017). A mini review on *Alphonsea* sp. (Annonaceae): traditional uses, biological activities and phytochemistry. Journal of Applied Pharmaceutical Science, 7, 200-203.

Beerhues, L., and Liu, B. (2009). Biosynthesis of biphenyls and benzophenones-evolution of benzoic acid-specific type III polyketide synthases in plants. Phytochemistry, 70, 1719-1727.

Benovit, S. C., Silva, L. L., Salbego, J., Loro, V. L., Mallmann, C. A., Baldisserotto, B., Flores, E. M., and Heinzmann, B. M. (2015). Anesthetic activity and bio-guided fractionation of the essential oil of *Aloysia gratissima* (Gillies & Hook.) Tronc. in silver catfish *Rhamdia quelen*. Anais da Academia Brasileira de Ciencias, 87, 1675-1689.

Bhakuni D. S., Tewari, S., and Dhar, M. M. (1972). Aporphine alkaloids of *annona squamosa*. Phytochemistry, 11, 1819-1822.

Birringer, M., Siems, K., Maxones, A., Frank, J., and Lorkowski, S. (2018). Natural 6-hydroxy-chromanols and -chromenols: Structural diversity, biosynthetic pathways and health implications. Royal Society of Chemistry, 8, 4803-4841.

Blanco, O., Castedo, L., Cortesa, D., and Villaverde, M. C. (1991). Alkaloids from *Sarcocapnos saetabensis*. Phytochemistry, 30, 2071-2074.

Chang, K. C., Duh, C. Y., Chen, I. S., and Tsai, I. L. (2003). A cytotoxic butenolide, two new dolabellane diterpenoids, a chroman and a benzoquinol derivative formosan *Casearia membranacea*. Planta Medica, 69, 667-672.

Chatrou, L. W., Pirie, M. D., Erkens, R. H. J., Couvreur, T. L. P., Neubig, K. M., Abbott, J. R., Mols, J. B., Maas J. W., Saunders, R. M. K., and Chase, M. W. (2012). A new subfamilial and tribal classification of the pantropical flowering plant family Annonaceae informed by molecular phylogenetics. Botanical Journal of the Linnean Society, 169, 5-40.

Chatsumpun, N., Sritularak, B., and Likhitwitayawuid, K. (2017). New biflavonoids with alpha-glucosidase and pancreatic lipase inhibitory activities from *Boesenbergia rotunda*. Molecules, 22(11), 1862.

Cheng, X., Wang, D., Jiang, L., and Yang, D. (2008). DNA topoisomerase I inhibitory alkaloids from *Corydalis saxicola*. Chemistry & Biodiversity, 5, 1335-1344.

Choudhary, M. I., Adhikari, A., Rasheed, S., Marasini, B. P., Hussain, N., Kaleem, W. A., and Rahman, Atta-ur. (2011). Cyclopeptide alkaloids of *Ziziphus oxyphylla* Edgw as novel inhibitors of α-glucosidase enzyme and protein glycation. Phytochemistry Letters, 4, 404-406.

Choudhary, M. I., Batool, I., Atif, M., Hussain, S., and Rahman, A. U. (2007). Microbial transformation of (–)-guaiol and antibacterial activity of its transformed products. Journal of Natural Products, 70, 849-852.

Costa, É. R., Louro, G. M., Simionatto, S., Vasconcelos, N. G., Cardoso, C. A. L., Mallmann, V., Silva, R. C. L., Matos, M. F. C., Pizzuti, L., Santiago, E. F., Morel, A. F., Mostardeiro, M. A. and Simionatto, E. (2017). Chemical composition, antitumoral and antibacterial activities of essential oils from leaves and stem bark of *Nectandra lanceolata* (Lauraceae). Journal of Essential Oil Bearing Plants, 20, 1184-1195.

Dang, Y., Gong, H. F., Liu, J. X., and Yu, S. J. (2009). Alkaloid from *Dicranostigma leptopodum* (Maxim) Fedde. Chinese Chemical Letters, 20, 1218-1220.

Doncheva, T., Doycheva, I., and Philipov, S. (2016). Alkaloid chemotypes of *Glaucium flavum* (Papaveraceae) from Bulgaria. Biochemical Systematics and Ecology, 68, 1-5.

Ferreira, M. L., Pascoli, I. C., Nascimento, I. R., Zukerman-Schpector, J., and Lopes, L. M. (2010). Aporphine and bisaporphine alkaloids from *Aristolochia lagesiana* var. *intermedia*. Phytochemistry, 71(4), 469-478.

Forest herbarium, forest and plant conservation research office, department of national parks, wildlife and plant conservation. (2014). Thai plant names Tem Smitinand, revised edition 2014. In (pp. 468). Bangkok: National Buddhist Department Printing.

Forino, M., Tartaglione, L., Dell'Aversano, C., and Ciminiello, P. (2016). NMR-based identification of the phenolic profile of fruits of *Lycium barbarum* (goji berries). Isolation and structural determination of a novel *N*-feruloyl tyramine dimer as the most abundant antioxidant polyphenol of goji berries. Food Chemistry, 194, 1254-1259.

Ghani, S. H. A., Ali, N. A. M., Jamil, M., Mohtar, M., Johari, S. A., Isa, M. M., and Patah, M. F. Z. (2016). Chemical compositions and antimicrobial activity of twig essential oils from three *Xylopia* (Annonaceae) species. African Journal of Biotechnology, 15, 356-362.

Goda, Y., Shibuya, M., and Sankawa, U. (1987). Inhibitors of prostaglandin biosynthesis from *Mucuna birdwoodiana*. Chemical and Pharmaceutical Bulletin, 35, 2675-2677.

He, H., and Lu, Y. H. (2013). Comparison of inhibitory activities and mechanisms of five mulberry plant bioactive components against α-glucosidase. Journal of Agricultural and Food Chemistry, 61, 8110-8119.

Hsieh, P. C., Huang G. J., HO, Y. L., Lin, Y., Huang, S. S., Chiang, Y. T., Tseng, M. C., and Chang, Y. S. (2010). Activities of antioxidants, α-glucosidase inhibitors and aldose reductase inhibitors of the aqueous extracts of four *Flemingia* species in Taiwan. Botanical Studies, 51, 293-302.

Holzbach, J. C., and Lopes, L. M. (2010). Aristolactams and alkamides of *Aristolochia gigantea*. Molecules, 15, 9462-9472.

Jamaludin, R. (1999). Chemical constituents of *Pseuduvaria rugosa* (Masters thesis), University of Malaya, Faculty of Science.

Jiang, Y. G., Wang, C. Y., Jin, C., Jia J. Q., Guo, X., Zhang, G. Z., and Gui, Z. Z. (2014). Improved 1-deoxynojirimycin (DNJ) production in mulberry leaves fermented by microorganism. Brazilian Journal of Microbiology, 45, 721-729.

Joubert, E., Beer, D., Hernández, I., and Munné-Bosch, S. (2014). Accummulation of mangiferin, isomangiferin, iriflophenone-3-*C*-β-glucoside and hesperidin in honeybush leaves (*Cyclopia genistoides* Vent.) in response to harvest time, harvest interval and seed source. Industrial Crops and Products, 56, 74-82.

Justino, A. B., Miranda, N. C., Franco, R. R., Martins, M. M., Silva, N. M. d., and Espindola, F. S. (2018). *Annona muricata* Linn. leaf as a source of antioxidant compounds with *in vitro* antidiabetic and inhibitory potential against α-amylase, α-glucosidase, lipase, non-enzymatic glycation and lipid peroxidation. Biomedicine & Pharmacotherapy, 100, 83-92.

Justino, A. B., Pereira, M. N., Vilela, D. D., Peixoto, L. G., Martins, M. M., Teixeira, R. R., Miranda, N. C., Silva, N.M., Sousa, R. M., Oliveira, A., and Espindola, F. S. (2016). Peel of araticum fruit (*Annona crassiflora* Mart.) as a source of antioxidant compounds with α-amylase, α-glucosidase and glycation inhibitory activities. Bioorganic Chemistry, 69, 167-182.

Kanada, R. M., Simionato, J. I., Arruda, R. F., Santin, S. M. O., Souza, M. C., and Silva, C. C. (2012). *N*-trans-feruloyltyramine and flavonol glycosides from the leaves of *Solanum sordidum*. Revista Brasileira de Farmacognosia, 22, 502-506.

Kimura, T., Nakagawa, K., Saito, Y., Yamagishi, K., Suzuki, M., Yamaki, K., Shinmoto, H., and Miyazawa T. (2004). Determination of 1-deoxynojirimycin in mulberry leaves using hydrophilic interaction chromatography with evaporative light scattering detection. Journal of Agricultural and Food Chemistry, 52, 1415–1418.

Kokotkiewicz, A., Luczkiewicz, M., Pawlowska, J., Luczkiewicz, P., Sowinski, P., Witkowski, J., Bryl, E., and Bucinski, A. (2013). Isolation of xanthone and

benzophenone derivatives from *Cyclopia genistoides* (L.) Vent. (honeybush) and their pro-apoptotic activity on synoviocytes from patients with rheumatoid arthritis. Fitoterapia, 90, 199-208.

Kumar, S., Narwal, S., Kumar, V., and Prakash, O. (2011). α-Glucosidase inhibitors from plants: A natural approach to treat diabetes. Pharmacognosy Reviews, 5, 19-29.

Laprévote, O., Roblot, F., Hocquemiller, R., and Cavé, A. (1988). Alcaloïdes des Annonacées, 87. Azafluorénones de l'Unonopsis spectabilis. Journal of Natural Products, 51, 555–561.

Liu, C., Xiang, W., Yu, Y., Shi, Z. Q., Huang X. Z., and Xu, L. (2015). Comparative analysis of 1-deoxynojirimycin contribution degree to α-glucosidase inhibitory activity and physiological distribution in *Morus alba* L. Industrial Crops and Products, 70, 309-315.

López, J. A., Laurito, J. G., Brenes, A. M., Lin, F. T., Sharaf, M., Wong, L. K., and Schiff, P. L. (1990). Aporphinoid alkaloids of *Guatteria oliviformis* and *G. Tonduzii*. Phytochemistry, 29, 1899-1901.

Lu, P., Sun, H., Zhang, L., Hou, H., Zhang, L., Zhao, F., Ge, C., Yao, M., Wang, T., and Li, J. (2012). Isocorydine targets the drug-resistant cellular side population through PDCD4-related apoptosis in hepatocellular carcinoma. Molecular Medicine, 18, 1136-1146.

Macabeo, A. P. G., Rubio, P. Y. M., Alejandro, G. J. D., and Knorn, M. (2015). An α-glucosidase inhibitor from *Drepananthus philippinensis*. Procedia Chemistry, 14, 36-39.

Mahmood, K., Chan, K. C., Park, M. H., Han, Y. N., and Han, B. H. (1986). An aporphinoid alkaloid from *Pseuduvaria macrophylla*. Phytochemistry, 25, 1509-1510.

Mohammed, A., Koorbanally, N. A., and Islam, M. S. (2016). Anti-diabetic effect of *Xylopia aethiopica* (Dunal) A. Rich. (Annonaceae) fruit acetone fraction in a type 2 diabetes model of rats. Journal of Ethnopharmacology, 180, 131-139.

Moura, N. F. d., Simionatto, E., Porto, C., Hoelzel, S. C. S., Dessoy, E. C. S., Zanatta, N., and More, A. F. (2002). Quinoline alkaloids, coumarins and volatile constituents of *Helietta longifoliata*. Planta Medica, 68, 631-634.

Muller, D., Davis, R. A., Duffy, S., Avery, V. M., Camp, D., and Quinn, R. J. (2009). Antimalarial activity of azafluorenone alkaloids from the Australian tree *Mitrephora diversifolia*. Journal of Natural Products, 72, 1538-1540.

Nafiah, M. A., Chen, J. K. H., Mohammad, S. N. F., Awang, K., Hadi, A. H. A., and Ahmad, K. (2015). Extraction and isolation of alkaloids from the leaves of *Alseodaphne corneri* Kosterm. Malaysian Journal of Chemistry, 15, 27-32.

Nafiah, M. A., Tan, S. P., Khoo, J. H. C., Hasnan, M. H. H., Awang, K., Hadi, A. H. A., and Ahmad, K. (2016). A new aporphine alkaloid from the leaves of *Alseodaphne corneri* Kosterm (Lauraceae). Tetrahedron Letters, 57, 1537-1539.

Ning, X., Shouming, Z., Shouxun, Z., Waterman, P. G., Cunheng, H., and Qitai, Z. (1989). Diterpenes from *Pseuduvaria indochinensis*. Journal of China Pharmaceutical University, 20, 203-207.

Noriega, P., Mosquera, T., Paredes, E., Parra, M., Zappia, M., Herrera, M., Villegas, A., and Osorio, E. (2018). Antimicrobial and antioxidant bioautography activity of bark essential oil from *Ocotea quixos* (Lam.) Kosterm. Journal of Planar Chromatography, 31, 163-168.

O'Brien, J., Wilson, I., Orton, T., and Pognan, F. (2000). Investigation of the Alamar Blue (resazurin) fluorescent dye for the assessment of mammalian cell cytotoxicity European Journal of Biochemistry, 267, 5421-5426.

Okada, K. (2011). The biosynthesis of isoprenoids and the mechanisms regulating it in plants. Bioscience Biotechnology and Biochemistry, 75, 1219-1225.

Okuyama, T., Shibata, S., Hoson, M., Kawada, T., Osada, H., and Noguchi, T. (1986). Effect of oriental plant drugs on platelet aggregation; III. Effect of Chinese drug "xiebai" on human platelet aggregation. Planta Medica, 3, 171-175.

Ortiz, A. A., Suarez, L. E. C., Patiño, G. S., and Ayazo, O. T. (2007). Azafluorenonas en corteza de *Oxandra longipetala* R. E. FR. (Annonaceae). Scientia et Technica, 1, 177-178.

Palazzo, M. C., Wright, H. L., Agius, B. R., Wright, B. S., Moriarity, D. M., Haber, W. A., and Setzer, W. N. (2009). Chemical compositions and biological activities of leaf essential oils of six species of Annonaceae from monteverde, costa rica Records of Natural Products, 3, 153-160

Palmer, T. (1994). Understanding enzymes. Fourth edition. London: Prentice Hall Ellis Horwood.

Pan, J. X., Chen, G., Li, J. J., Zhu, Q. D., Li, J. J., Chen, Z. J., Yu, Z. P., and Ye, L. Y. (2018). Isocorydine suppresses doxorubicin-induced epithelial-mesenchymal transition via inhibition of ERK signaling pathways in hepatocellular carcinoma. American Journal of Cancer Research, 8, 154-164.

Rajamanickam, M., and Rajamanickam, A. (2016). Analgesic and anti-inflammatory activity of the extracts from *Cyperus rotundus* Linn. rhizomes. Journal of Applied Pharmaceutical Science, 6, 197-203.

Ravanelli, N., Santos, K. P., Motta, L. B., Lago, J. H. G., and Furlan, C. M. (2016). Alkaloids from *Croton echinocarpus* Baill.: Anti-HIV potential. South African Journal of Botany, 102, 153–156.

Ren, Y. Y., Zhu, Z. Y., Sun, H. Q. and Chen, L. J. (2017). Structural characterization and inhibition on α-glucosidase activity of acidic polysaccharide from *Annona squamosa*. Carbohydrate Polymers, 174, 1-12.

Seo, G. W., Cho, J. Y., Moon, J. H., and Park, K. H. (2011). Isolation and identification of cinnamic acid amides as antioxidants from *Allium fistulosum* L. and their free radical scavenging activity. Food Science and Biotechnology, 20, 555-560.

Sesang, W., Punyanitya, S., Pitchuanchom, S., Udomputtimekakul, P., Nuntasaen, N., Banjerdpongchai, R., Wudtiwai, B., and Pompimo, W. (2014). Cytotoxic aporphine alkaloids from leaves and twigs of *Pseuduvaria trimera* (Craib). Molecules, 19, 8762-8772.

Shou-Ming, Z., Sholj-Shun, Z., and Ning, X. (1988). Alkaloids From *Pseuduvaria indochinensis*. Phytochemistry, 27, 4004-4005.

Sipowo, R. V. T., Ouahouo, B. M. W., Maza, H. L. D., Ishikawa, H., Nishino, H., Mkounga, P., and Nkengfack, A. E. (2017). Triterpenes and coumaroyltyramide from *Ochthocosmus africanus*. Journal of Diseases and Medicinal Plants, 3, 12-16.

Song, Y. H., Kim, D. W., Curtis-Long, M. J., Park, C., Son, M., Kim, J. Y., Yuk, H. J., Lee, K. W., and Park, K. H. (2016). Cinnamic acid amides from *Tribulus terrestris* displaying uncompetitive alpha-glucosidase inhibition. European Journal of Medicinal Chemistry, 114, 201-208.

Su, Y. C. F., Chaowasku, T., and Saunders, R. M. K. (2010). An extended phylogeny of *Pseuduvaria* (Annonaceae) with descriptions of three new species and a reassessment of the generic status of *Oreomitra*. Systematic Botany, 35, 30-39.

Su, Y. C., Smith, G. J., and Saunders, R. M. (2008). Phylogeny of the basal angiosperm genus *Pseuduvaria* (Annonaceae) inferred from five chloroplast DNA regions, with interpretation of morphological character evolution. Molecular Phylogenetics and Evolution, 48, 188-206.

Taha, H., Arya, A., Khan, A. K., Shahid, N., Noordin, M. I. B., & Mohan, S. (2018). Effect of *Pseuduvaria macrophylla* in attenuating hyperglycemia mediated oxidative stress and inflammatory response in STZ-nicotinamide induced diabetic rats by upregulating insulin secretion and glucose transporter-1, 2 and 4 proteins expression. Journal of Applied Biomedicine. doi:https://doi.org/10.1016/j.jab.2018.05.004

Taha, H., Arya, A., Paydar, M., Looi, C. Y., Wong, W. F., Murthy, C. R. V., Noordin, M. I., Ali, H. M., Mustafa, A. M., and Hadi, A. H. (2014). Upregulation of insulin secretion and downregulation of pro-inflammatory cytokines, oxidative stress and hyperglycemia in STZ-nicotinamide-induced type 2 diabetic rats by *Pseuduvaria monticola* bark extract. Food and Chemical Toxicology, 66: 295-306.

Taha, H., Hadi, A. H., Nordin, N., Najmuldeen, I. A., Mohamad, K., Shirota, O., Nugroho, A. E., Piow, W. C., Kaneda, T., and Morita, H. (2011). Pseuduvarines A and B, two new cytotoxic dioxoaporphine alkaloids from *Pseuduvaria rugosa*. Chemical and Pharmaceutical Bulletin, 59, 896-897.

Taha, H., Looi, C. Y., Arya, A., Wong, W. F., Yap, L. F., Hasanpourghadi, M., Mohd, M. A., Paterson, I. C., and Mohd, A. H. (2015). (6*E*,10*E*) Isopolycerasoidol and (6*E*,10*E*) isopolycerasoidol methyl ester, prenylated benzopyran derivatives from

Pseuduvaria monticola induce mitochondrial-mediated apoptosis in human breast adenocarcinoma cells. Plos One, 10, 1-19.

Ting-Jun M. A., Xi-Cheng, S., and Chang-Xi, J. (2008). Telephenone D, a new benzophenone *C*-glycoside from *Polygala telephioides*. Chinese Journal of Natural Medicines, 8, 9-11.

Uadkla, O., Yodkeeree, S., Buayairaksa, M., Meepowpan, P., Nuntasaen, N., Limtrakul, P., and Pompimon, W. (2013). Antiproliferative effect of alkaloids via cell cycle arrest from *Pseuduvaria rugosa*. Pharmaceutical Biology, 51, 400-404.

Waikedre, J., Vitturo, C. I., Molina, A., Theodoro, P. N., Silva, M. R., Espindola, L. S., Maciuk, A., and Fournet, A. (2012). Antifungal activity of the essential oils of *Callitri*s neocaledonica and C. sulcata heartwood (Cupressaceae). Chemistry & Biodiversity, 9, 644-653.

Wang, S. C., Wang, F., and Yue, C. H. (2015). Chemical constituents from the petioles and leaves of *Aquilaria sinensis*. Biochemical Systematics and Ecology, 61, 458-461.

Wijeratne, K., Silva, L. B. D., Kikuchi, T., Tezuka, Y., Gunatilaka, A. A. L., and Kingston, D. G. I. (1995). Cyathocaline, an azafluorenone alkaloid from *Cyathocalyx zeylanica*. Journal of Natural Products, 58, 459–462.

Wirasathien, L., Boonarkart, C., Pengsuparp, T., and Suttisri, R. (2006). Biological activities of alkaloids from *Pseuduvaria setosa*. Pharmaceutical Biology, 44, 274-278.

Wu, X. D., Cheng, J. T., He, J., Zhang, X. J., Dong, L. B., Gong, X., Song, L. D., Zheng, Y. T., Peng, L. Y., and Zhao, Q.S. (2012). Benzophenone glycosides and epicatechin derivatives from *Malania oleifera*. Fitoterapia, 83, 1068-1071.

Yang, X., Zhu, J., Wu, J., Huang, N., Cui, Z., Luo, Y., Sun, F., Pan, Q., Li, Y., and Yang, Q. (2018). (-)-Guaiol regulates autophagic cell death depending on mTOR signaling in NSCLC. Cancer Biology & Therapy, 19, 1-9.

Yin, Z., Zhang, W., Feng, F., Zhang, Y., and Kanga, W. (2014). α-Glucosidase inhibitors isolated from medicinal plants. Food Science and Human Wellness, 3, 136-174.

Zerbe, P., and Bohlmann, J. (2015). Plant diterpene synthases: Exploring modularity and metabolic diversity for bioengineering. Trends in Biotechnology, 33, 419-428.

Zhang, Y., Qian, Q., Ge, D., Li, Y., Wang, X., Chen, Q., Gao, X., and Wang, T. (2011). Identification of benzophenone *C*-glucosides from mango tree leaves and their Inhibitory effect on triglyceride accumulation in 3T3-L1 adipocytes. Journal of Agricultural and Food Chemistry, 59, 11526-11533.

Zhao, C. G., Yao, M. J., Yang, J. W., Chai, Y. L., Sun, X. D., and Yuan, C. S. (2014). A new benzopyran derivative from *Pseuduvaria indochinensis* Merr. Natural Product Research, 28, 169-173.

APPENDIX

				A average					B average	B-A	% inhibition
blank	0.053	0.051	0.053	0.052	0.895	0.883	0.881	0.886		0.834	
A 20 mg/ml	0.052	0.055	0.053	0.053	0.192	0.185	0.188	0.188		0.135	83.82
A 10 mg/ml	0.051	0.057	0.054	0.054	0.244	0.259	0.237	0.247		0.193	76.89
A 5.0 mg/ml	0.053	0.054	0.057	0.054	0.510	0.519	0.542	0.524		0.469	43.70
A 2.5 mg/ml	0.057	0.051	0.053	0.054	0.694	0.697	0.685	0.692		0.639	23.40
A 1.25 mg/ml	0.052	0.051	0.053	0.052	0.753	0.777	0.796	0.775		0.723	13.21

				B average					A average	B-A	% inhibition
blank	0.051	0.050	0.049	0.050	0.728	0.725	0.719	0.724		0.674	
A 20 mg/ml	0.054	0.052	0.054	0.053	0.166	0.173	0.176	0.172		0.119	82.41
A 10 mg/ml	0.054	0.053	0.052	0.053	0.259	0.226	0.219	0.235		0.182	73.00
A 5.0 mg/ml	0.053	0.052	0.053	0.053	0.415	0.440	0.426	0.427		0.374	44.42
A 2.5 mg/ml	0.052	0.051	0.051	0.051	0.552	0.549	0.558	0.553		0.502	25.47
A 1.25 mg/ml	0.050	0.050	0.051	0.050	0.644	0.633	0.616	0.631		0.581	13.80

				B average					A average	B-A	% inhibition
blank	0.048	0.049	0.051	0.049	0.528	0.524	0.536	0.529		0.480	
A 20 mg/ml	0.052	0.051	0.051	0.051	0.146	0.146	0.149	0.147		0.096	80.07
A 10 mg/ml	0.051	0.052	0.051	0.051	0.197	0.194	0.184	0.192		0.141	70.65
A 5.0 mg/ml	0.052	0.051	0.051	0.051	0.323	0.340	0.332	0.332		0.280	41.60
A 2.5 mg/ml	0.051	0.050	0.050	0.050	0.403	0.418	0.412	0.411		0.361	24.80
A 1.25 mg/ml	0.049	0.049	0.049	0.049	0.450	0.483	0.451	0.461		0.412	14.07

Data calculated for IC_{50} of acarbose

				A average					B average	B-A	% inhibition
blank	0.049	0.047	0.048		0.834	0.821	0.778	0.788	0.805	0.757	
PF-6 (20 µM)	0.057	0.059	0.058		0.170	0.170	0.164	0.169	0.168	0.110	85.45
PF-6 (10 µM)	0.053	0.053	0.053		0.224	0.226	0.221	0.220	0.223	0.170	77.60
PF-6 (5 µM)	0.049	0.050	0.049		0.318	0.317	0.313	0.324	0.318	0.269	64.54
PF-6 (2.5 µM)	0.049	0.052	0.051		0.490	0.507	0.499	0.521	0.504	0.454	40.13
PF-6 (1.25 µM)	0.047	0.047	0.047		0.568	0.567	0.613	0.595	0.586	0.539	28.91
PF-6 (0.62 µM)	0.048	0.048	0.048		0.638	0.659	0.624	0.628	0.637	0.590	22.17

				A average					B average	B-A	% inhibition
blank	0.047	0.048	0.047		0.804	0.783	0.784	0.815	0.797	0.749	
PF-6 (20 µM)	0.058	0.058	0.058		0.167	0.166	0.166	0.168	0.167	0.109	85.51
PF-6 (10 µM)	0.054	0.054	0.054		0.217	0.222	0.220	0.225	0.221	0.167	77.74
PF-6 (5 µM)	0.050	0.051	0.051		0.351	0.371	0.369	0.317	0.352	0.301	59.79
PF-6 (2.5 µM)	0.049	0.050	0.049		0.490	0.492	0.469	0.500	0.488	0.439	41.47
PF-6 (1.25 µM)	0.048	0.049	0.049		0.588	0.595	0.575	0.577	0.584	0.535	28.60
PF-6 (0.62 µM)	0.048	0.048	0.048		0.656	0.629	0.614	0.617	0.629	0.581	22.48

				A average					B average	B-A	% inhibition
blank	0.048	0.048	0.048		0.788	0.787	0.778	0.825	0.795	0.746	
PF-6 (20 µM)	0.060	0.059	0.059		0.171	0.172	0.177	0.175	0.174	0.115	84.65
PF-6 (10 µM)	0.057	0.056	0.056		0.219	0.228	0.240	0.254	0.235	0.179	76.03
PF-6 (5 µM)	0.053	0.053	0.053		0.338	0.325	0.317	0.326	0.327	0.274	63.34
PF-6 (2.5 µM)	0.052	0.062	0.057		0.505	0.471	0.486	0.516	0.494	0.437	41.41
PF-6 (1.25 µM)	0.055	0.053	0.054		0.598	0.590	0.569	0.606	0.591	0.537	28.05
PF-6 (0.62 µM)	0.051	0.055	0.053		0.626	0.655	0.635	0.648	0.641	0.588	21.22

Data calculated for IC_{50} of *N-trans*-feruloyltyramine (PF-6) [**31**]

			A average					B average		B-A		% inhibition
blank	0.048	0.050	0.049	0.907	0.907	0.904	0.914	0.908		0.859		
PF-7 (2.00 µM)	0.050	0.054	0.052	0.142	0.145	0.126	0.137	0.137		0.086		90.03
PF-7 (1.00 µM)	0.053	0.056	0.054	0.216	0.205	0.192	0.231	0.211		0.157		81.75
PF-7 (0.50 µM)	0.059	0.055	0.057	0.469	0.503	0.486	0.500	0.490		0.433		49.61
PF-7 (0.25 µM)	0.057	0.056	0.056	0.636	0.690	0.663	0.686	0.669		0.612		28.67
PF-7 (0.125 µM)	0.049	0.056	0.053	0.785		0.756	0.776	0.772		0.720		16.15
PF-7 (0.0625 µM)	0.049	0.054	0.051	0.850	0.828	0.848	0.812	0.835		0.783		8.79

			A average					B average		B-A		% inhibition
blank	0.049	0.049	0.049	0.910	0.906	0.924	0.894	0.909		0.859		
PF-7 (2.00 µM)	0.053	0.051	0.052	0.121	0.126	0.134	0.135	0.129		0.077		91.00
PF-7 (1.00 µM)	0.051	0.050	0.051	0.308	0.325	0.337		0.323		0.272		68.31
PF-7 (0.50 µM)	0.049	0.053	0.051	0.584	0.532	0.551	0.522	0.547		0.496		42.24
PF-7 (0.25 µM)	0.054	0.050	0.052	0.667	0.671	0.666	0.680	0.671		0.619		28.00
PF-7 (0.125 µM)	0.051	0.050	0.050	0.761	0.799	0.780		0.780		0.730		15.10
PF-7 (0.0625 µM)	0.049	0.050	0.049	0.847	0.808	0.829		0.828		0.778		9.42

			A average					B average		B-A		% inhibition
blank	0.046	0.045	0.046	0.905	0.903	0.905	0.921	0.909		0.863		
PF-7 (2.00 µM)	0.047	0.049	0.048	0.135	0.140	0.137	0.142	0.139		0.091		89.51
PF-7 (1.00 µM)	0.047	0.048	0.048	0.205		0.189	0.198	0.197		0.150		82.66
PF-7 (0.50 µM)	0.048	0.048	0.048	0.477	0.452	0.444	0.423	0.449		0.401		53.57
PF-7 (0.25 µM)	0.047	0.047	0.047	0.601	0.607	0.628	0.641	0.619		0.572		33.72
PF-7 (0.125 µM)	0.047	0.046	0.047	0.712	0.698	0.741	0.738	0.722		0.676		21.72
PF-7 (0.0625 µM)	0.047	0.047	0.047	0.793	0.778	0.820		0.797		0.750		13.14

Data calculated for IC_{50} of *N-trans*-coumaroyltyramine (PF-7) [**32**]

	mM								
Control Sub.	2.0		A				B		
Time (min.)			Average					Average	B-A
5	0.047	0.047	0.047	0.128	0.132	0.127	0.135	0.131	0.083
10	0.047	0.048	0.048	0.185	0.192	0.183	0.191	0.188	0.140
15	0.049	0.049	0.049	0.231	0.242	0.229	0.239	0.235	0.186
20	0.048	0.049	0.048	0.277	0.291	0.277	0.286	0.283	0.234
25	0.049	0.049	0.049	0.319	0.337	0.317	0.332	0.326	0.277
30	0.049	0.050	0.050	0.378	0.399	0.398	0.373	0.387	0.337

	mM								
Control Sub.	1.0		A				B		
Time (min.)			Average					Average	B-A
5	0.047	0.046	0.047	0.139	0.136		0.138	0.138	0.091
10	0.048	0.046	0.047	0.195	0.199		0.198	0.197	0.150
15	0.048	0.046	0.047	0.242	0.247		0.245	0.245	0.198
20	0.048	0.046	0.047	0.287	0.296		0.291	0.291	0.244
25	0.048	0.046	0.047	0.326	0.341		0.332	0.333	0.286
30	0.048	0.046	0.047	0.364	0.378		0.371	0.371	0.324

	mM								
Control Sub.	0.5		A				B		
Time (min.)			Average					Average	B-A
5	0.043	0.044	0.043	0.128	0.127	0.129	0.130	0.128	0.085
10	0.045	0.045	0.045	0.176	0.176	0.179	0.179	0.177	0.133
15	0.045	0.045	0.045	0.212	0.213	0.217	0.215	0.214	0.170
20	0.045	0.044	0.044	0.246	0.245	0.251	0.250	0.248	0.204
25	0.045	0.045	0.045	0.276	0.275	0.282	0.279	0.278	0.233
30	0.045	0.044	0.044	0.302	0.300	0.308	0.304	0.304	0.259

	mM								
Control Sub.	0.25		A				B		
Time (min.)			Average					Average	B-A
5	0.045	0.043	0.044	0.117	0.119	0.118		0.118	0.074
10	0.046	0.044	0.045	0.150	0.155	0.154		0.153	0.108
15	0.046	0.044	0.045	0.172	0.178	0.178		0.176	0.131
20	0.046	0.044	0.045	0.192	0.200	0.199		0.197	0.152
25	0.046	0.045	0.045	0.209	0.218	0.217	0.228	0.218	0.173
30	0.046	0.046	0.046	0.222	0.232	0.232	0.243	0.232	0.186

	mM								
Control Sub.	0.125		A				B		
Time (min.)			Average					Average	B-A
5	0.045	0.042	0.044	0.095	0.097	0.099	0.097	0.097	0.053
10	0.046	0.043	0.045	0.115	0.118	0.120	0.118	0.118	0.073
15	0.046	0.043	0.045	0.127	0.131	0.134	0.132	0.131	0.086
20	0.046	0.043	0.045	0.137	0.142	0.146	0.142	0.142	0.097
25	0.047	0.043	0.045	0.145	0.149	0.152	0.150	0.149	0.104
30	0.048	0.043	0.045	0.159	0.164	0.166	0.164	0.163	0.118

Data calculated for control of Linewever-Burk plots

	mM								
Control Sub.	2.0		A				B		
Time (min.)			Average				Average		B-A
5	0.048	0.048	0.048	0.139	0.144	0.140	0.143	0.141	0.094
10	0.050	0.050	0.050	0.203	0.215	0.207	0.212	0.209	0.159
15	0.052	0.051	0.051	0.262	0.276	0.267	0.272	0.270	0.218
20	0.052	0.051	0.051	0.316		0.322	0.329	0.323	0.271
25	0.051	0.049	0.050	0.356		0.362	0.370	0.363	0.313
30	0.051	0.048	0.049	0.404		0.413	0.420	0.412	0.363

	mM								
Control Sub.	1.0		A				B		
Time (min.)			Average				Average		B-A
5	0.046	0.047	0.046	0.136	0.135	0.132	0.133	0.134	0.088
10	0.048	0.051	0.049	0.199	0.197	0.191	0.191	0.194	0.145
15	0.047	0.051	0.049	0.251	0.251	0.242	0.242	0.247	0.198
20	0.048	0.051	0.049	0.300	0.297	0.288	0.288	0.293	0.244
25	0.048	0.050	0.049	0.344	0.341	0.329	0.330	0.336	0.287
30	0.048	0.051	0.049	0.388	0.384	0.371	0.371	0.378	0.329

	mM								
Control Sub.	0.5		A				B		
Time (min.)			Average				Average		B-A
5	0.045	0.044	0.044	0.136	0.132	0.132	0.130	0.132	0.088
10	0.048	0.046	0.047		0.184	0.187	0.180	0.184	0.136
15	0.049	0.050	0.050		0.229	0.229	0.224	0.227	0.177
20	0.050	0.050	0.050		0.268	0.269	0.262	0.266	0.217
25	0.049	0.048	0.048		0.302	0.302	0.295	0.300	0.251
30	0.049	0.048	0.049		0.326	0.328	0.318	0.324	0.276

	mM								
Control Sub.	0.25		A				B		
Time (min.)			Average				Average		B-A
5	0.043	0.044	0.044	0.128	0.130	0.123	0.120	0.125	0.082
10	0.047	0.046	0.047	0.162		0.157	0.153	0.157	0.110
15	0.047	0.048	0.048	0.198		0.187	0.184	0.190	0.142
20	0.046	0.046	0.046	0.215		0.205	0.200	0.207	0.161
25	0.046	0.046	0.046	0.240		0.229	0.222	0.231	0.185
30	0.045	0.046	0.045	0.263		0.253	0.245	0.254	0.208

	mM								
Control Sub.	0.125		A				B		
Time (min.)			Average				Average		B-A
5	0.045	0.045	0.045	0.104	0.105	0.110	0.102	0.105	0.060
10	0.045	0.045	0.045	0.121	0.121	0.132	0.118	0.123	0.078
15	0.048	0.046	0.047	0.140	0.143	0.148	0.136	0.142	0.095
20	0.046	0.048	0.047	0.154	0.155		0.152	0.154	0.107
25	0.045	0.045	0.045	0.165	0.165		0.162	0.164	0.120
30	0.046	0.045	0.046	0.173	0.174		0.172	0.173	0.128

Data calculated for control of Linewever-Burk plots

	mM								
Control Sub.	2.0		A				B		
Time (min.)			Average					Average	B-A
5	0.051	0.050	0.050	0.127	0.128	0.128	0.129	0.128	0.078
10	0.053	0.050	0.052	0.191	0.190	0.186	0.187	0.188	0.137
15	0.053	0.051	0.052	0.242	0.243	0.238	0.241	0.241	0.189
20	0.053	0.051	0.052	0.288		0.284	0.287	0.287	0.234
25	0.053	0.052	0.052	0.332	0.336		0.331	0.333	0.281
30	0.052	0.053	0.053	0.383	0.384		0.381	0.382	0.330

	mM								
Control Sub.	1.0		A				B		
Time (min.)			Average					Average	B-A
5	0.048	0.046	0.047	0.131	0.130	0.129	0.129	0.130	0.082
10	0.050	0.049	0.049	0.189	0.188	0.186	0.186	0.187	0.138
15	0.049	0.050	0.049	0.239	0.238	0.235	0.236	0.237	0.187
20	0.049	0.049	0.049		0.281	0.278	0.280	0.280	0.231
25	0.049	0.049	0.049	0.324	0.322	0.318	0.322	0.322	0.272
30	0.049	0.048	0.048	0.363	0.362	0.357	0.363	0.361	0.313

	mM								
Control Sub.	0.5		A				B		
Time (min.)			Average					Average	B-A
5	0.046	0.046	0.046	0.123	0.127	0.126	0.127	0.126	0.080
10	0.047	0.046	0.047	0.174	0.178	0.176	0.177	0.176	0.129
15	0.048	0.046	0.047	0.215	0.220	0.216	0.219	0.218	0.171
20	0.048	0.047	0.047	0.252		0.251	0.255	0.253	0.205
25	0.048	0.046	0.047	0.285	0.288		0.288	0.287	0.240
30	0.048	0.046	0.047	0.317	0.320	0.313	0.319	0.317	0.270

	mM								
Control Sub.	0.25		A				B		
Time (min.)			Average					Average	B-A
5	0.045	0.045	0.045	0.116	0.120	0.121	0.121	0.120	0.075
10	0.046	0.046	0.046	0.149	0.156	0.156	0.158	0.155	0.109
15	0.046	0.046	0.046	0.179	0.187	0.186	0.189	0.185	0.139
20	0.046	0.046	0.046	0.204	0.212	0.211	0.214	0.210	0.164
25	0.046	0.046	0.046	0.225	0.234	0.233	0.235	0.232	0.186
30	0.046	0.046	0.046	0.245	0.255	0.252	0.255	0.252	0.206

	mM								
Control Sub.	0.125		A				B		
Time (min.)			Average					Average	B-A
5	0.046	0.048	0.047	0.096	0.097	0.100	0.100	0.098	0.051
10	0.047	0.050	0.049	0.120	0.121	0.125	0.126	0.123	0.074
15	0.048	0.049	0.049	0.139	0.139	0.143		0.140	0.092
20	0.047	0.049	0.048	0.151	0.152	0.157		0.153	0.105
25	0.047	0.049	0.048	0.162	0.163	0.168	0.169	0.165	0.117
30	0.047	0.049	0.048	0.171	0.172	0.178	0.178	0.175	0.127

Data calculated for control of Linewever-Burk plots

	µg/mL		mM
Acarbose	600	Sub.	2.0

			A				B		
Time (min.)			Average				Average		B-A
5	0.048	0.051	0.049	0.104	0.103	0.107	0.103	0.104	0.055
10	0.049	0.052	0.051		0.140	0.147	0.133	0.140	0.089
15	0.048	0.050	0.049		0.170	0.173	0.163	0.169	0.120
20	0.049	0.049	0.049		0.199	0.206	0.196	0.200	0.151
25	0.050	0.052	0.051		0.225	0.233	0.223	0.227	0.176
30	0.048	0.051	0.050	0.265	0.252	0.260	0.250	0.257	0.207

	µg/mL		mM
Acarbose	600	Sub.	1.0

			A				B		
Time (min.)			Average				Average		B-A
5	0.050	0.049	0.050	0.086	0.084	0.087	0.084	0.085	0.036
10	0.053	0.051	0.052	0.109	0.108	0.111	0.106	0.108	0.057
15	0.053	0.051	0.052	0.128	0.127	0.131	0.124	0.128	0.076
20	0.053	0.052	0.052	0.144	0.144	0.147	0.143	0.144	0.092
25	0.053	0.052	0.053	0.161	0.160	0.161	0.159	0.160	0.108
30	0.052	0.052	0.052	0.180	0.179	0.180	0.178	0.179	0.127

	µg/mL		mM
Acarbose	600	Sub.	0.5

			A				B		
Time (min.)			Average				Average		B-A
5	0.045	0.046	0.046	0.069	0.064	0.065	0.067	0.066	0.021
10	0.046	0.045	0.045	0.083	0.076	0.076	0.075	0.077	0.032
15	0.046	0.048	0.047	0.098	0.085	0.084	0.083	0.087	0.040
20	0.045	0.046	0.046		0.094	0.092	0.093	0.093	0.048
25	0.045	0.046	0.046		0.101	0.099	0.102	0.101	0.055
30	0.046	0.047	0.047	0.119	0.109	0.106	0.108	0.111	0.064

	µg/mL		mM
Acarbose	600	Sub.	0.25

			A				B		
Time (min.)			Average				Average		B-A
5	0.047	0.047	0.047	0.059	0.059	0.057	0.060	0.059	0.012
10	0.048	0.046	0.047	0.065	0.064	0.063	0.066	0.065	0.018
15	0.048	0.046	0.047	0.073	0.071	0.067	0.071	0.071	0.023
20	0.047	0.046	0.046	0.076	0.074	0.070	0.075	0.074	0.028
25	0.048	0.046	0.047	0.077	0.076	0.077	0.080	0.078	0.031
30	0.048	0.047	0.047	0.081	0.080	0.082	0.086	0.082	0.035

	µg/mL		mM
Acarbose	600	Sub.	0.125

			A				B		
Time (min.)			Average				Average		B-A
5	0.047	0.045	0.046	0.051	0.052	0.053	0.050	0.051	0.006
10	0.048	0.048	0.048	0.055	0.057	0.057	0.054	0.056	0.008
15	0.048	0.048	0.048	0.059	0.060	0.058	0.056	0.058	0.011
20	0.048	0.048	0.048	0.060	0.060	0.063	0.061	0.061	0.013
25	0.047	0.048	0.048	0.061	0.062	0.062	0.064	0.062	0.015
30	0.048	0.047	0.048	0.065	0.066	0.066	0.065	0.065	0.018

Data calculated for acarbose 600 µg/mL of Linewever-Burk plots

	µg/mL		mM
Acarbose	600	Sub.	2.0

			A					B	
Time (min.)			Average					Average	B-A
5	0.050	0.049	0.050	0.089	0.088	0.089	0.092	0.089	0.040
10	0.049	0.051	0.050	0.117	0.119	0.125	0.122	0.120	0.070
15	0.049	0.051	0.050	0.143	0.144	0.146	0.145	0.144	0.095
20	0.049	0.050	0.050	0.165	0.167	0.174	0.169	0.169	0.119
25	0.049	0.050	0.049	0.189	0.192	0.194	0.193	0.192	0.143
30	0.050	0.050	0.050	0.215	0.218	0.219	0.223	0.219	0.169

	µg/mL		mM
Acarbose	600	Sub.	1.0

			A					B	
Time (min.)			Average					Average	B-A
5	0.049	0.056	0.053	0.076	0.078	0.079	0.074	0.077	0.024
10	0.048	0.052	0.050	0.096	0.098	0.098	0.095	0.097	0.047
15	0.047	0.052	0.050	0.110	0.114	0.115	0.111	0.113	0.063
20	0.047	0.052	0.050	0.124	0.129	0.129	0.125	0.127	0.077
25	0.047	0.050	0.048		0.140	0.142	0.138	0.140	0.092
30	0.049	0.048	0.048		0.158	0.158	0.155	0.157	0.109

	µg/mL		mM
Acarbose	600	Sub.	0.5

			A					B	
Time (min.)			Average					Average	B-A
5	0.047	0.048	0.048	0.066	0.065	0.067	0.065	0.066	0.018
10	0.046	0.048	0.047	0.076	0.075	0.079	0.077	0.077	0.030
15	0.048	0.048	0.048	0.088	0.083	0.088	0.084	0.086	0.038
20	0.046	0.048	0.047	0.093	0.091	0.097	0.091	0.093	0.046
25	0.047	0.047	0.047	0.102	0.098	0.105	0.101	0.101	0.055
30	0.046	0.049	0.047	0.110	0.107	0.116	0.109	0.111	0.063

	ug/ml		mM
Acarbose	600	Sub.	0.25

Time			Average					Average	A
5	0.045	0.045	0.045	0.058	0.057	0.059	0.060	0.058	0.013
10	0.046	0.047	0.047	0.064	0.063	0.064	0.067	0.065	0.018
15	0.045	0.045	0.045	0.068	0.068	0.067	0.070	0.068	0.023
20	0.045	0.045	0.045	0.073	0.072	0.072	0.073	0.072	0.027
25	0.046	0.045	0.045	0.076	0.076	0.075	0.077	0.076	0.031
30	0.045	0.045	0.045	0.080	0.080	0.078	0.082	0.080	0.035

	µg/mL		mM
Acarbose	600	Sub.	0.125

			A					B	
Time (min.)			Average					Average	B-A
5	0.045	0.048	0.047	0.054	0.052	0.051	0.052	0.052	0.006
10	0.045	0.047	0.046	0.058	0.060	0.054	0.054	0.057	0.010
15	0.045	0.047	0.046	0.062		0.056	0.056	0.058	0.012
20	0.045	0.047	0.046	0.063	0.063	0.058	0.059	0.061	0.015
25	0.044	0.046	0.045	0.064	0.066	0.060	0.061	0.063	0.017
30	0.045	0.046	0.046	0.068	0.065	0.061	0.063	0.064	0.019

Data calculated for acarbose 600 µg/mL of Linewever-Burk plots

	µg/mL		mM
Acarbose	600	Sub.	2.0

			A					B	
Time (min.)			Average					Average	B-A
5	0.050	0.051	0.050	0.095	0.096	0.094	0.093	0.095	0.044
10	0.051	0.051	0.051	0.128	0.126	0.126	0.126	0.126	0.076
15	0.051	0.051	0.051	0.156	0.154	0.154	0.155	0.155	0.104
20	0.052	0.051	0.051	0.180	0.178	0.179	0.181	0.180	0.128
25	0.051	0.051	0.051	0.205	0.202	0.201	0.207	0.204	0.153
30	0.050	0.050	0.050	0.230	0.224	0.224	0.232	0.227	0.177

	µg/mL		mM
Acarbose	600	Sub.	1.0

			A					B	
Time (min.)			Average					Average	B-A
5	0.047	0.047	0.047	0.079	0.080	0.079	0.077	0.079	0.032
10	0.047	0.048	0.048	0.101	0.101	0.099	0.098	0.100	0.052
15	0.047	0.048	0.047	0.120	0.120	0.116	0.114	0.117	0.070
20	0.047	0.047	0.047	0.135	0.133	0.131	0.129	0.132	0.085
25	0.047	0.047	0.047	0.151	0.147	0.145	0.143	0.147	0.099
30	0.047	0.047	0.047	0.166	0.163	0.160	0.159	0.162	0.115

	µg/mL		mM
Acarbose	600	Sub.	0.5

			A					B	
Time (min.)			Average					Average	B-A
5	0.045	0.046	0.046	0.065	0.067	0.067	0.066	0.066	0.021
10	0.046	0.047	0.046	0.076	0.079	0.078	0.078	0.078	0.032
15	0.046	0.047	0.046	0.086	0.089	0.087	0.088	0.087	0.041
20	0.046	0.046	0.046	0.094	0.097	0.096	0.096	0.096	0.049
25	0.045	0.047	0.046	0.101	0.105	0.103	0.103	0.103	0.057
30	0.046	0.046	0.046	0.109	0.113	0.111	0.112	0.111	0.065

	µg/mL		mM
Acarbose	600	Sub.	0.25

			A					B	
Time (min.)			Average					Average	B-A
5	0.047	0.046	0.047	0.058	0.059	0.058	0.057	0.058	0.011
10	0.047	0.048	0.048	0.065	0.066	0.065	0.064	0.065	0.017
15	0.048	0.048	0.048	0.070	0.070	0.069	0.068	0.069	0.022
20	0.047	0.049	0.048	0.075	0.075	0.073	0.073	0.074	0.026
25	0.048	0.048	0.048	0.079	0.079	0.078	0.076	0.078	0.030
30	0.046	0.048	0.047	0.083	0.083	0.082	0.081	0.082	0.035

	µg/mL		mM
Acarbose	600	Sub.	0.125

			A					B	
Time (min.)			Average					Average	B-A
5	0.046	0.045	0.046	0.053	0.056	0.053	0.052	0.053	0.007
10	0.046	0.047	0.047	0.057	0.059	0.057	0.055	0.057	0.011
15	0.045	0.047	0.046	0.060	0.061	0.059	0.058	0.060	0.014
20	0.045	0.046	0.046	0.063	0.063	0.061	0.060	0.062	0.016
25	0.045	0.046	0.046	0.064	0.065	0.063	0.062	0.064	0.018
30	0.045	0.046	0.046	0.067	0.067	0.065	0.064	0.066	0.020

Data calculated for acarbose 600 µg/mL of Linewever-Burk plots

	µg/mL		mM
Acarbose	300	Sub.	2.0

			A				B		
Time (min.)			Average					Average	B-A
5	0.050	0.048	0.049	0.105	0.105	0.104	0.104	0.104	0.055
10	0.051	0.049	0.050	0.152	0.152	0.150	0.151	0.151	0.101
15	0.051	0.048	0.050	0.196	0.196	0.194	0.194	0.195	0.145
20	0.051	0.049	0.050	0.232	0.233	0.230	0.230	0.231	0.181
25	0.052	0.048	0.050	0.269	0.270	0.267	0.266	0.268	0.218
30	0.051	0.048	0.050	0.296	0.297	0.293	0.303	0.297	0.248

	µg/mL		mM
Acarbose	300	Sub.	1.0

			A				B		
Time (min.)			Average					Average	B-A
5	0.047	0.047	0.047	0.097	0.097	0.100	0.100	0.099	0.052
10	0.047	0.046	0.047	0.128	0.129	0.129	0.129	0.129	0.082
15	0.049	0.046	0.048	0.160	0.160	0.160	0.160	0.160	0.112
20	0.049	0.047	0.048	0.186	0.184	0.185	0.185	0.185	0.138
25	0.048	0.046	0.047	0.206	0.206	0.206	0.206	0.206	0.159
30	0.049	0.047	0.048	0.228	0.229	0.230	0.230	0.229	0.181

	µg/mL		mM
Acarbose	300	Sub.	0.5

			A				B		
Time (min.)			Average					Average	B-A
5	0.049	0.045	0.047	0.075	0.073	0.073	0.076	0.074	0.027
10	0.050	0.051	0.051	0.095	0.094	0.092	0.095	0.094	0.043
15	0.049	0.049	0.049	0.110	0.108	0.107	0.112	0.109	0.061
20	0.049	0.050	0.049	0.123	0.123	0.119	0.126	0.123	0.073
25	0.049	0.051	0.050	0.139	0.138	0.137	0.142	0.139	0.089
30	0.049	0.050	0.050	0.158	0.158	0.155	0.153	0.156	0.106

	µg/mL		mM
Acarbose	300	Sub.	0.25

			A				B		
Time (min.)			Average					Average	B-A
5	0.044	0.047	0.045	0.066	0.064	0.064	0.064	0.065	0.019
10	0.044	0.046	0.045	0.077	0.074	0.073	0.075	0.075	0.030
15	0.045	0.047	0.046	0.083	0.082	0.083	0.083	0.083	0.037
20	0.045	0.047	0.046	0.092	0.088	0.090	0.089	0.090	0.044
25	0.045	0.046	0.045	0.098	0.095	0.096	0.095	0.096	0.051
30	0.046	0.046	0.046	0.107	0.106		0.106	0.107	0.061

	µg/mL		mM
Acarbose	300	Sub.	0.125

			A				B		
Time (min.)			Average					Average	B-A
5	0.044	0.046	0.045	0.057	0.056	0.057	0.058	0.057	0.012
10	0.045	0.045	0.045	0.062	0.061	0.062	0.064	0.062	0.017
15	0.045	0.045	0.045	0.066	0.065	0.066	0.068	0.067	0.021
20	0.045	0.045	0.045	0.070	0.069	0.070	0.071	0.070	0.025
25	0.045	0.045	0.045	0.073	0.073	0.074	0.075	0.074	0.029
30	0.045	0.045	0.045	0.080	0.081	0.077	0.079	0.079	0.034

Data calculated for acarbose 300 µg/mL of Linewever-Burk plots

	µg/mL		mM
Acarbose	300	Sub.	2.0

			A					B	
Time (min.)			Average					Average	B-A
5	0.050	0.050	0.050	0.094	0.093	0.093	0.098	0.095	0.045
10	0.051	0.052	0.051	0.132	0.132	0.132	0.137	0.133	0.082
15	0.052	0.053	0.052	0.166	0.165	0.165	0.168	0.166	0.114
20	0.052	0.052	0.052	0.207	0.206	0.205	0.210	0.207	0.155
25	0.052	0.053	0.052	0.247	0.247	0.244	0.251	0.247	0.195
30	0.052	0.053	0.052	0.280	0.279	0.276	0.283	0.280	0.227

	µg/mL		mM
Acarbose	300	Sub.	1.0

			A					B	
Time (min.)			Average					Average	B-A
5	0.047	0.047	0.047	0.085	0.085	0.087	0.088	0.086	0.039
10	0.048	0.050	0.049	0.112	0.112	0.115	0.117	0.114	0.065
15	0.049	0.051	0.050	0.135	0.135	0.138	0.140	0.137	0.087
20	0.049	0.050	0.050	0.156	0.156	0.159	0.162	0.158	0.109
25	0.049	0.050	0.049	0.185	0.185	0.189	0.193	0.188	0.138
30	0.049	0.050	0.049	0.204	0.203	0.208	0.211	0.206	0.157

	µg/mL		mM
Acarbose	300	Sub.	0.5

			A					B	
Time (min.)			Average					Average	B-A
5	0.047	0.047	0.047	0.073	0.073	0.075	0.075	0.074	0.027
10	0.048	0.048	0.048	0.090	0.090	0.092	0.092	0.091	0.043
15	0.048	0.048	0.048	0.104	0.104	0.106	0.107	0.105	0.057
20	0.048	0.048	0.048	0.116	0.116	0.120	0.119	0.118	0.070
25	0.048	0.048	0.048	0.128	0.127	0.131	0.131	0.129	0.081
30	0.048	0.048	0.048	0.141	0.140	0.144	0.145	0.142	0.095

	µg/mL		mM
Acarbose	300	Sub.	0.25

			A					B	
Time (min.)			Average					Average	B-A
5	0.046	0.048	0.047	0.063	0.063	0.063	0.062	0.063	0.016
10	0.046	0.049	0.047	0.075	0.074	0.073	0.071	0.073	0.026
15	0.047	0.049	0.048	0.081	0.081	0.080	0.079	0.080	0.033
20	0.046	0.049	0.048	0.088	0.088	0.087	0.086	0.087	0.040
25	0.046	0.049	0.048	0.096	0.094	0.093	0.091	0.094	0.046
30	0.047	0.049	0.048	0.101	0.102	0.101	0.100	0.101	0.053

	µg/mL		mM
Acarbose	300	Sub.	0.125

			A					B	
Time (min.)			Average					Average	B-A
5	0.044	0.044	0.044	0.057	0.059	0.058	0.057	0.058	0.013
10	0.045	0.045	0.045	0.063	0.065	0.064	0.063	0.063	0.018
15	0.047	0.045	0.046	0.067	0.069	0.068	0.070	0.069	0.022
20	0.046	0.045	0.046	0.070	0.074	0.072	0.072	0.072	0.027
25	0.046	0.045	0.045	0.074	0.078	0.076	0.074	0.075	0.030
30	0.046	0.045	0.046	0.077	0.081	0.079	0.078	0.079	0.033

Data calculated for acarbose 300 µg/mL of Linewever-Burk plots

	µg/mL		mM
Acarbose	300	Sub.	2.0

			A					B	
Time (min.)			Average					Average	B-A
5	0.049	0.049	0.049	0.101	0.099		0.100	0.100	0.051
10	0.049	0.050	0.050	0.147	0.143		0.145	0.145	0.095
15	0.050	0.051	0.051	0.187	0.181		0.184	0.184	0.133
20	0.051	0.052	0.051	0.225	0.219		0.221	0.222	0.171
25	0.051	0.050	0.051	0.262	0.255		0.256	0.258	0.207
30	0.051	0.051	0.051	0.296	0.288		0.290	0.291	0.240

	µg/mL		mM
Acarbose	300	Sub.	1.0

			A					B	
Time (min.)			Average					Average	B-A
5	0.048	0.047	0.047	0.090	0.088	0.093	0.092	0.091	0.044
10	0.048	0.047	0.048	0.118	0.115		0.119	0.117	0.070
15	0.048	0.047	0.048	0.145	0.140		0.144	0.143	0.095
20	0.049	0.047	0.048	0.169	0.164		0.169	0.167	0.119
25	0.048	0.047	0.047	0.193	0.188		0.192	0.191	0.144
30	0.049	0.047	0.048	0.210	0.204		0.209	0.208	0.160

	µg/mL		mM
Acarbose	300	Sub.	0.5

			A					B	
Time (min.)			Average					Average	B-A
5	0.045	0.047	0.046	0.081	0.080	0.079	0.081	0.080	0.034
10	0.047	0.047	0.047	0.095	0.092	0.092	0.094	0.093	0.046
15	0.047	0.048	0.047	0.110	0.108	0.107	0.108	0.108	0.061
20	0.046	0.048	0.047	0.124	0.121	0.120	0.123	0.122	0.075
25	0.046	0.048	0.047	0.139	0.134	0.133	0.136	0.135	0.089
30	0.046	0.047	0.047	0.147	0.141	0.140	0.143	0.143	0.096

	µg/mL		mM
Acarbose	300	Sub.	0.25

			A					B	
Time (min.)			Average					Average	B-A
5	0.046	0.048	0.047	0.065	0.065	0.066	0.065	0.065	0.018
10	0.047	0.046	0.047	0.074	0.073	0.073	0.076	0.074	0.027
15	0.047	0.047	0.047	0.082	0.081		0.083	0.082	0.035
20	0.046	0.047	0.047	0.088	0.086		0.090	0.088	0.041
25	0.047	0.047	0.047	0.094	0.093		0.096	0.094	0.048
30	0.047	0.047	0.047	0.100	0.099		0.102	0.100	0.053

	µg/mL		mM
Acarbose	300	Sub.	0.125

			A					B	
Time (min.)			Average					Average	B-A
5	0.046	0.048	0.047	0.057	0.058	0.062	0.060	0.059	0.012
10	0.046	0.047	0.047	0.062	0.062	0.067	0.066	0.064	0.018
15	0.046	0.048	0.047	0.066	0.067	0.071	0.070	0.069	0.022
20	0.046	0.048	0.047	0.071	0.071	0.075	0.074	0.073	0.026
25	0.046	0.048	0.047	0.075	0.074	0.079	0.078	0.077	0.030
30	0.046	0.048	0.047	0.078	0.078	0.083	0.082	0.080	0.033

Data calculated for acarbose 300 µg/mL of Linewever-Burk plots

	µM		mM
PF-6	8	Sub.	2.0

			A					B	
Time (min.)			Average					Average	B-A
5	0.049	0.049	0.049	0.070	0.071	0.068	0.070	0.070	0.021
10	0.049	0.049	0.049	0.087	0.091	0.084	0.085	0.087	0.038
15	0.049	0.049	0.049	0.102	0.103	0.099	0.102	0.101	0.052
20	0.049	0.048	0.049	0.115	0.115	0.114	0.115	0.115	0.066
25	0.049	0.049	0.049	0.127	0.128	0.127		0.128	0.079
30	0.048	0.048	0.048	0.140	0.141	0.140		0.140	0.092

	µM		mM
PF-6	8	Sub.	1.0

			A					B	
Time (min.)			Average					Average	B-A
5	0.047	0.046	0.046	0.069	0.071	0.070	0.070	0.070	0.024
10	0.046	0.046	0.046	0.084	0.085	0.084	0.085	0.084	0.038
15	0.047	0.046	0.046	0.097	0.098	0.098	0.099	0.098	0.052
20	0.046	0.046	0.046	0.110	0.108	0.110	0.110	0.109	0.063
25	0.046	0.045	0.046	0.122	0.122	0.122	0.122	0.122	0.076
30	0.047	0.046	0.046	0.134	0.134	0.134	0.132	0.134	0.087

	µM		mM
PF-6	8	Sub.	0.5

			A					B	
Time (min.)			Average					Average	B-A
5	0.044	0.046	0.045	0.067	0.069	0.067	0.069	0.068	0.023
10	0.045	0.047	0.046	0.081	0.082	0.081	0.083	0.082	0.036
15	0.045	0.046	0.046	0.092	0.093	0.093	0.099	0.094	0.049
20	0.045	0.046	0.046	0.102	0.105	0.104	0.108	0.105	0.059
25	0.045	0.045	0.045	0.114	0.114	0.114	0.119	0.115	0.071
30	0.044	0.045	0.045		0.125	0.126	0.125	0.125	0.081

	µM		mM
PF-6	8	Sub.	0.25

			A					B	
Time (min.)			Average					Average	B-A
5	0.045	0.044	0.044	0.068	0.069	0.069	0.066	0.068	0.024
10	0.044	0.044	0.044	0.080	0.080	0.081	0.077	0.080	0.036
15	0.045	0.047	0.046	0.092	0.092	0.092	0.088	0.091	0.045
20	0.044	0.044	0.044	0.100	0.101	0.102	0.098	0.100	0.056
25	0.044	0.044	0.044	0.108	0.108	0.109	0.102	0.107	0.063
30	0.044	0.044	0.044	0.116	0.117	0.119		0.117	0.073

	µM		mM
PF-6	8	Sub.	0.125

			A					B	
Time (min.)			Average					Average	B-A
5	0.043	0.044	0.044	0.071	0.067	0.066	0.065	0.067	0.024
10	0.043	0.044	0.044		0.077	0.076	0.076	0.076	0.033
15	0.043	0.044	0.044		0.087	0.087	0.085	0.086	0.042
20	0.043	0.044	0.043		0.095	0.094	0.094	0.094	0.051
25	0.043	0.043	0.043		0.101	0.101	0.100	0.101	0.058
30	0.043	0.044	0.043		0.105	0.105	0.104	0.105	0.061

Data calculated for *N-trans*-feruloyltyramine (PF-6) [**31**] 8 µM of Linewever-Burk plots

	µM		mM
PF-6	8	Sub.	2.0

			A					B	
Time (min.)			Average					Average	B-A
5	0.053	0.051	0.052	0.070	0.071	0.068	0.068	0.069	0.017
10	0.052	0.052	0.052	0.081	0.083	0.079	0.079	0.081	0.028
15	0.053	0.051	0.052	0.091	0.099	0.088	0.090	0.092	0.040
20	0.053	0.051	0.052	0.106	0.111	0.103	0.105	0.106	0.054
25	0.053	0.051	0.052	0.121	0.126	0.117	0.118	0.120	0.068
30	0.053	0.051	0.052	0.131	0.138	0.129	0.129	0.132	0.080

	µM		mM
PF-6	8	Sub.	1.0

			A					B	
Time (min.)			Average					Average	B-A
5	0.051	0.050	0.050	0.068	0.067	0.067	0.066	0.067	0.017
10	0.050	0.051	0.051	0.078	0.079	0.078	0.077	0.078	0.027
15	0.050	0.051	0.051	0.094	0.092	0.091	0.089	0.092	0.041
20	0.050	0.051	0.051	0.104	0.103	0.103	0.101	0.103	0.052
25	0.050	0.051	0.051	0.119	0.117	0.117	0.115	0.117	0.066
30	0.050	0.051	0.051	0.129	0.129	0.128	0.126	0.128	0.077

	µM		mM
PF-6	8	Sub.	0.5

			A					B	
Time (min.)			Average					Average	B-A
5	0.048	0.048	0.048	0.066	0.067	0.066	0.066	0.066	0.018
10	0.049	0.050	0.049	0.076	0.077	0.075	0.075	0.076	0.027
15	0.048	0.050	0.049	0.089	0.090	0.088	0.089	0.089	0.040
20	0.049	0.050	0.049	0.099	0.100	0.098	0.097	0.098	0.049
25	0.049	0.049	0.049	0.113	0.113	0.111	0.112	0.112	0.063
30	0.049	0.049	0.049	0.124	0.123	0.122	0.122	0.123	0.074

	µM		mM
PF-6	8	Sub.	0.25

			A					B	
Time (min.)			Average					Average	B-A
5	0.046	0.046	0.046	0.066	0.066	0.065	0.065	0.065	0.019
10	0.046	0.046	0.046	0.076	0.076	0.074	0.073	0.075	0.029
15	0.046	0.046	0.046	0.084	0.084	0.083	0.081	0.083	0.037
20	0.046	0.046	0.046	0.093	0.092	0.091	0.088	0.091	0.045
25	0.046	0.046	0.046	0.105	0.105	0.104	0.101	0.104	0.057
30	0.046	0.046	0.046	0.113	0.113	0.112	0.109	0.112	0.066

	µM		mM
PF-6	8	Sub.	0.125

			A					B	
Time (min.)			Average					Average	B-A
5	0.046	0.047	0.046	0.067	0.067	0.064	0.065	0.066	0.019
10	0.046	0.047	0.046	0.076	0.075	0.072	0.072	0.074	0.027
15	0.046	0.046	0.046	0.084	0.083	0.079	0.080	0.081	0.035
20	0.046	0.046	0.046	0.090	0.089	0.086	0.086	0.088	0.041
25	0.046	0.046	0.046	0.099	0.097	0.094	0.094	0.096	0.050
30	0.046	0.047	0.046	0.105	0.103	0.100	0.100	0.102	0.056

Data calculated for *N-trans*-feruloyltyramine (PF-6) [**31**] 8 µM of Linewever-Burk plots

	µM		mM
PF-6	8	Sub.	2.0

			A					B	
Time (min.)			Average					Average	B-A
5	0.055	0.053	0.054	0.069	0.069	0.069	0.075	0.070	0.016
10	0.057	0.059	0.058	0.086	0.083	0.082	0.087	0.085	0.027
15	0.057	0.053	0.055	0.098	0.096	0.093	0.101	0.097	0.042
20	0.058	0.059	0.059	0.112	0.108		0.115	0.112	0.053
25	0.058	0.058	0.058	0.126	0.120		0.126	0.124	0.067
30	0.056	0.051	0.054	0.139	0.132	0.127	0.140	0.134	0.081

	µM		mM
PF-6	8	Sub.	1.0

			A					B	
Time (min.)			Average					Average	B-A
5	0.048	0.048	0.048	0.068	0.068	0.069	0.070	0.069	0.021
10	0.048	0.048	0.048	0.079	0.078	0.082	0.087	0.082	0.034
15	0.048	0.048	0.048	0.090	0.089	0.093	0.099	0.093	0.045
20	0.048	0.048	0.048	0.101	0.100	0.104	0.112	0.105	0.057
25	0.048	0.048	0.048	0.111		0.115	0.124	0.117	0.069
30	0.048	0.047	0.047	0.122		0.125	0.135	0.127	0.080

	µM		mM
PF-6	8	Sub.	0.5

			A					B	
Time (min.)			Average					Average	B-A
5	0.046	0.048	0.047	0.068	0.065	0.065	0.066	0.066	0.019
10	0.048	0.048	0.048	0.081		0.076	0.078	0.078	0.031
15	0.047	0.049	0.048	0.092		0.096	0.099	0.096	0.048
20	0.047	0.049	0.048	0.103		0.106	0.108	0.106	0.058
25	0.047	0.049	0.048	0.118		0.112	0.116	0.116	0.067
30	0.047	0.049	0.048	0.130		0.121	0.124	0.125	0.077

	uM		mM
SE1	8	Sub.	0.25

Time (min.)			Average					Average	A
5	0.048	0.048	0.048	0.067	0.068	0.062	0.066	0.066	0.018
10	0.048	0.048	0.048	0.075	0.075		0.073	0.075	0.027
15	0.047	0.049	0.048	0.085	0.085		0.082	0.084	0.036
20	0.047	0.049	0.048	0.096	0.096		0.092	0.095	0.047
25	0.048	0.048	0.048	0.106	0.106		0.104	0.105	0.057
30	0.047	0.049	0.048	0.115	0.116		0.113	0.115	0.066

	µM		mM
PF-6	8	Sub.	0.125

			A					B	
Time (min.)			Average					Average	B-A
5	0.048	0.048	0.048	0.066	0.067	0.063	0.065	0.065	0.017
10	0.048	0.048	0.048	0.075	0.075	0.071	0.074	0.074	0.026
15	0.048	0.048	0.048	0.093	0.082	0.078	0.081	0.084	0.036
20	0.047	0.048	0.048	0.101	0.090	0.085	0.090	0.092	0.044
25	0.048	0.048	0.048	0.109	0.097	0.092	0.098	0.099	0.051
30	0.048	0.048	0.048	0.116	0.105	0.098	0.104	0.106	0.058

Data calculated for *N-trans*-feruloyltyramine (PF-6) [**31**] 8 µM of Linewever-Burk plots

	µM		mM
PF-6	4	Sub.	2.0

			A					B	
Time (min.)			Average					Average	B-A
5	0.049	0.048	0.049	0.072	0.069	0.067	0.069	0.069	0.021
10	0.051	0.051	0.051	0.095	0.091	0.087	0.088	0.090	0.039
15	0.052	0.051	0.051	0.120	0.113	0.108	0.108	0.112	0.061
20	0.052	0.050	0.051	0.144	0.136	0.128	0.127	0.134	0.083
25	0.052	0.052	0.052	0.170	0.158	0.150	0.151	0.157	0.106
30	0.052	0.053	0.052	0.196	0.180	0.171	0.171	0.180	0.127

	µM		mM
PF-6	4	Sub.	1.0

			A					B	
Time (min.)			Average					Average	B-A
5	0.048	0.046	0.047	0.069	0.067	0.067	0.066	0.067	0.020
10	0.048	0.047	0.047	0.089	0.085	0.084	0.084	0.086	0.038
15	0.048	0.047	0.048	0.109	0.106	0.103	0.103	0.105	0.057
20	0.048	0.047	0.047		0.125	0.123	0.121	0.123	0.076
25	0.048	0.047	0.048		0.146	0.143	0.139	0.143	0.095
30	0.048	0.047	0.048		0.163	0.160	0.157	0.160	0.113

	µM		mM
PF-6	4	Sub.	0.5

			A					B	
Time (min.)			Average					Average	B-A
5	0.046	0.046	0.046	0.069	0.066	0.065	0.064	0.066	0.020
10	0.048	0.048	0.048	0.087	0.084	0.083	0.077	0.083	0.035
15	0.048	0.048	0.048	0.104	0.101	0.099	0.092	0.099	0.051
20	0.048	0.048	0.048	0.123	0.120	0.116	0.107	0.116	0.068
25	0.048	0.048	0.048	0.140	0.138	0.136	0.123	0.134	0.086
30	0.049	0.049	0.049	0.157	0.157	0.153	0.137	0.151	0.102

	µM		mM
Time (min.)	4	Sub.	0.25

			A					B	
Time (min.)			Average					Average	B-A
5	0.046	0.047	0.046	0.064	0.065	0.064	0.067	0.065	0.019
10	0.046	0.046	0.046	0.075	0.074	0.074	0.076	0.075	0.029
15	0.045	0.046	0.046	0.092	0.093	0.092		0.092	0.046
20	0.046	0.047	0.047	0.108	0.107	0.107		0.107	0.061
25	0.046	0.048	0.047	0.115	0.117	0.116	0.119	0.117	0.070
30	0.046	0.047	0.047	0.126	0.126	0.126	0.128	0.127	0.080

	µM		mM
PF-6	4	Sub.	0.125

			A					B	
Time (min.)			Average					Average	B-A
5	0.044	0.045	0.045		0.062	0.064	0.064	0.063	0.019
10	0.045	0.045	0.045	0.072	0.073	0.077	0.077	0.075	0.029
15	0.045	0.045	0.045	0.083	0.086	0.089		0.086	0.041
20	0.045	0.046	0.045	0.089	0.091	0.097	0.096	0.093	0.048
25	0.046	0.046	0.046	0.095	0.099	0.103	0.104	0.101	0.055
30	0.046	0.046	0.046	0.110	0.111	0.114	0.114	0.112	0.066

Data calculated for *N-trans*-feruloyltyramine (PF-6) [**31**] 4 µM of Linewever-Burk plots

	µM		mM
PF-6	4	Sub.	2.0

			A					B	
Time (min.)			Average					Average	B-A
5	0.051	0.050	0.051	0.073	0.075	0.072	0.072	0.073	0.022
10	0.051	0.050	0.050	0.092	0.095	0.090	0.091	0.092	0.042
15	0.051	0.050	0.050	0.111	0.114	0.108	0.109	0.111	0.060
20	0.051	0.050	0.050	0.131	0.134	0.127	0.129	0.130	0.080
25	0.051	0.050	0.050	0.150	0.154	0.146	0.149	0.150	0.100
30	0.051	0.050	0.051	0.171	0.174	0.166	0.168	0.170	0.119

	µM		mM
PF-6	4	Sub.	1.0

			A					B	
Time (min.)			Average					Average	B-A
5	0.049	0.050	0.049	0.073	0.068	0.066	0.067	0.069	0.019
10	0.050	0.051	0.050	0.091	0.084	0.082	0.085	0.086	0.035
15	0.050	0.050	0.050	0.108	0.101	0.101	0.100	0.102	0.052
20	0.053	0.052	0.053	0.126	0.119	0.117	0.117	0.120	0.067
25	0.050	0.051	0.050	0.144	0.136	0.133	0.133	0.136	0.086
30	0.051	0.050	0.051	0.162	0.154	0.150	0.153	0.155	0.104

	µM		mM
PF-6	4	Sub.	0.5

			A					B	
Time (min.)			Average					Average	B-A
5	0.048	0.048	0.048	0.067	0.065	0.066	0.065	0.066	0.018
10	0.050	0.050	0.050	0.083	0.080	0.080	0.079	0.081	0.031
15	0.050	0.050	0.050	0.099	0.095	0.095	0.094	0.096	0.046
20	0.051	0.051	0.051	0.115	0.111	0.110	0.109	0.111	0.060
25	0.050	0.050	0.050	0.130	0.127	0.126	0.123	0.127	0.076
30	0.050	0.049	0.050	0.146	0.142	0.141	0.139	0.142	0.093

	µM		mM
Time (min.)	4	Sub.	0.25

			A					B	
Time (min.)			Average					Average	B-A
5	0.048	0.048	0.048	0.070	0.069	0.067	0.068	0.069	0.020
10	0.050	0.050	0.050	0.084	0.083	0.080	0.081	0.082	0.032
15	0.048	0.050	0.049	0.098	0.099	0.094	0.096	0.097	0.048
20	0.051	0.051	0.051	0.112	0.114	0.109	0.110	0.111	0.060
25	0.049	0.050	0.049	0.123	0.122	0.120	0.122	0.122	0.073
30	0.049	0.050	0.050	0.133	0.134	0.130	0.130	0.132	0.082

	µM		mM
PF-6	4	Sub.	0.125

			A					B	
Time (min.)			Average					Average	B-A
5	0.047	0.048	0.047	0.070	0.067	0.065	0.065	0.067	0.020
10	0.048	0.050	0.049	0.082	0.079	0.078	0.077	0.079	0.030
15	0.049	0.049	0.049	0.094	0.090	0.090	0.088	0.090	0.041
20	0.047	0.051	0.049	0.099	0.099	0.097	0.096	0.098	0.049
25	0.047	0.050	0.049	0.106	0.105	0.104	0.102	0.104	0.056
30	0.047	0.049	0.048	0.116	0.116	0.114	0.111	0.114	0.066

Data calculated for *N-trans*-feruloyltyramine (PF-6) [**31**] 4 µM of Linewever-Burk plots

	µM		mM						
PF-6	4	Sub.	2.0						
			A					**B**	
Time (min.)			**Average**					**Average**	**B-A**
5	0.052	0.050	0.051	0.076	0.071	0.072	0.074	0.073	0.023
10	0.053	0.053	0.053	0.098	0.092	0.093	0.096	0.095	0.042
15	0.053	0.054	0.053	0.121	0.116	0.115	0.119	0.118	0.065
20	0.054	0.053	0.053	0.141	0.137	0.134	0.139	0.138	0.084
25	0.054	0.053	0.053	0.162	0.158	0.154	0.161	0.159	0.105
30	0.054	0.052	0.053	0.184	0.181		0.182	0.182	0.129

	µM		mM						
PF-6	4	Sub.	1.0						
			A					**B**	
Time (min.)			**Average**					**Average**	**B-A**
5	0.049	0.047	0.048	0.072	0.073	0.073	0.072	0.073	0.025
10	0.049	0.049	0.049	0.093	0.094	0.095	0.092	0.093	0.045
15	0.049	0.048	0.049	0.114	0.117	0.119	0.115	0.116	0.068
20	0.050	0.049	0.049	0.133	0.137	0.139	0.134	0.136	0.086
25	0.050	0.048	0.049	0.153	0.159		0.156	0.156	0.107
30	0.050	0.049	0.049	0.171	0.177		0.173	0.174	0.124

	µM		mM						
PF-6	4	Sub.	0.5						
			A					**B**	
Time (min.)			**Average**					**Average**	**B-A**
5	0.047	0.045	0.046	0.070	0.069	0.069	0.068	0.069	0.023
10	0.048	0.048	0.048	0.089	0.088	0.088	0.086	0.088	0.040
15	0.048	0.048	0.048	0.111	0.107	0.109	0.106	0.108	0.060
20	0.048	0.048	0.048	0.128	0.125	0.126	0.123	0.126	0.077
25	0.047	0.048	0.047		0.144	0.145	0.142	0.144	0.096
30	0.047	0.049	0.048		0.160	0.161	0.158	0.160	0.111

	µM		mM						
Time (min.)	4	Sub.	0.25						
			A					**B**	
Time (min.)			**Average**					**Average**	**B-A**
5	0.046	0.047	0.046	0.070	0.071	0.070	0.070	0.071	0.024
10	0.047	0.048	0.048	0.087	0.089	0.089	0.088	0.088	0.040
15	0.047	0.047	0.047	0.105	0.105		0.107	0.105	0.058
20	0.047	0.049	0.048	0.119	0.123		0.123	0.122	0.074
25	0.047	0.046	0.047	0.131	0.133	0.137	0.135	0.134	0.088
30	0.047	0.046	0.047	0.142	0.144	0.149	0.147	0.146	0.099

	µM		mM						
PF-6	4	Sub.	0.125						
			A					**B**	
Time (min.)			**Average**					**Average**	**B-A**
5	0.048	0.047	0.047	0.067	0.069	0.070	0.069	0.069	0.021
10	0.047	0.046	0.047	0.083	0.084	0.084	0.083	0.083	0.036
15	0.048	0.047	0.048	0.094	0.097	0.097	0.097	0.096	0.048
20	0.048	0.047	0.048	0.104	0.107	0.106	0.106	0.106	0.058
25	0.049	0.047	0.048	0.111	0.114	0.114	0.113	0.113	0.065
30	0.048	0.048	0.048	0.121	0.126	0.126	0.126	0.125	0.077

Data calculated for *N-trans*-feruloyltyramine (PF-6) [**31**] 4 µM of Linewever-Burk plots

	µM		mM
PF-6	2	Sub.	2.0

			A					B	
Time (min.)			Average					Average	B-A
5	0.049	0.048	0.049	0.079	0.080	0.087	0.080	0.082	0.033
10	0.049	0.048	0.049	0.109	0.108	0.119	0.126	0.116	0.067
15	0.049	0.048	0.048	0.142	0.140	0.147	0.163	0.148	0.100
20	0.048	0.047	0.048	0.175	0.172	0.181	0.191	0.180	0.132
25	0.049	0.048	0.048	0.209	0.206	0.214	0.230	0.215	0.166
30	0.049	0.047	0.048	0.242	0.239	0.252	0.266	0.250	0.201

	µM		mM
PF-6	2	Sub.	1.0

			A					B	
Time (min.)			Average					Average	B-A
5	0.049	0.047	0.048	0.081	0.079	0.080	0.080	0.080	0.032
10	0.047	0.046	0.047	0.110	0.108	0.108	0.109	0.109	0.062
15	0.047	0.046	0.046		0.138	0.139	0.141	0.139	0.093
20	0.047	0.046	0.046	0.175	0.165	0.164	0.173	0.169	0.123
25	0.048	0.047	0.047	0.209		0.198	0.206	0.204	0.157
30	0.047	0.046	0.046	0.242	0.226	0.226	0.238	0.233	0.186

	µM		mM
PF-6	2	Sub.	0.5

			A					B	
Time (min.)			Average					Average	B-A
5	0.046	0.046	0.046	0.075	0.075	0.076		0.075	0.029
10	0.047	0.047	0.047	0.097	0.099	0.100		0.099	0.052
15	0.047	0.047	0.047	0.123	0.125	0.126	0.133	0.127	0.080
20	0.046	0.046	0.046	0.147	0.147	0.152	0.161	0.152	0.106
25	0.046	0.046	0.046	0.172	0.173	0.179		0.175	0.129
30	0.045	0.046	0.046		0.197	0.205	0.217	0.206	0.161

	µM		mM
PF-6	2	Sub.	0.25

			A					B	
Time (min.)			Average					Average	B-A
5	0.046	0.045	0.046	0.074	0.070	0.072	0.073	0.072	0.027
10	0.047	0.045	0.046		0.088	0.088	0.096	0.090	0.044
15	0.047	0.045	0.046		0.106	0.106	0.113	0.108	0.063
20	0.047	0.045	0.046		0.124	0.125	0.135	0.128	0.082
25	0.046	0.046	0.046		0.143	0.144	0.155	0.147	0.102
30	0.047	0.044	0.045		0.160	0.160	0.173	0.164	0.119

	µM		mM
PF-6	2	Sub.	0.125

			A					B	
Time (min.)			Average					Average	B-A
5	0.045	0.046	0.046	0.071	0.069	0.067	0.067	0.069	0.023
10	0.045	0.046	0.046		0.084	0.081	0.084	0.083	0.037
15	0.045	0.047	0.046		0.091	0.093	0.090	0.091	0.045
20	0.045	0.046	0.046	0.109	0.102	0.100	0.102	0.103	0.057
25	0.045	0.046	0.045		0.115	0.111	0.115	0.114	0.068
30	0.045	0.046	0.046		0.128	0.121	0.129	0.126	0.080

Data calculated for *N-trans*-feruloyltyramine (PF-6) [**31**] 2 µM of Linewever-Burk plots

	µM		mM
PF-6	2	Sub.	2.0

			A					B	
Time (min.)			Average					Average	B-A
5	0.051	0.051	0.051	0.083	0.081	0.079	0.079	0.081	0.030
10	0.051	0.051	0.051	0.109	0.107	0.104	0.105	0.106	0.055
15	0.050	0.052	0.051	0.146	0.144	0.143	0.142	0.144	0.093
20	0.051	0.052	0.051	0.180	0.177	0.175	0.177	0.177	0.126
25	0.050	0.051	0.051	0.211	0.210	0.208	0.209	0.210	0.159
30	0.050	0.051	0.051	0.240	0.239	0.237	0.238	0.238	0.187

	µM		mM
PF-6	2	Sub.	1.0

			A					B	
Time (min.)			Average					Average	B-A
5	0.048	0.050	0.049	0.077	0.076	0.077	0.076	0.077	0.028
10	0.050	0.050	0.050	0.104	0.100	0.102	0.100	0.101	0.051
15	0.050	0.050	0.050	0.128	0.125	0.127	0.126	0.127	0.076
20	0.050	0.050	0.050	0.154	0.152	0.154	0.151	0.153	0.103
25	0.050	0.050	0.050	0.179	0.177	0.180	0.177	0.178	0.128
30	0.049	0.049	0.049	0.209	0.208	0.212	0.209	0.209	0.160

	µM		mM
PF-6	2	Sub.	0.5

			A					B	
Time (min.)			Average					Average	B-A
5	0.048	0.046	0.047	0.076	0.077	0.075	0.077	0.076	0.029
10	0.047	0.046	0.046	0.097	0.100	0.098	0.100	0.099	0.052
15	0.048	0.046	0.047	0.120	0.124	0.121	0.125	0.122	0.075
20	0.049	0.046	0.048	0.145	0.148	0.144	0.150	0.147	0.099
25	0.048	0.046	0.047	0.167	0.173	0.168	0.174	0.170	0.123
30	0.048	0.046	0.047	0.192	0.197	0.192	0.199	0.195	0.148

	µM		mM
PF-6	2	Sub.	0.25

			A					B	
Time (min.)			Average					Average	B-A
5	0.047	0.045	0.046	0.074	0.074	0.073	0.075	0.074	0.028
10	0.048	0.045	0.046	0.093	0.092	0.092	0.095	0.093	0.046
15	0.048	0.045	0.046	0.110	0.110	0.110	0.113	0.111	0.064
20	0.047	0.046	0.046	0.127	0.126	0.127	0.132	0.128	0.082
25	0.047	0.045	0.046	0.140	0.140	0.142	0.146	0.142	0.096
30	0.046	0.045	0.046	0.155	0.156	0.158	0.162	0.158	0.112

	µM		mM
PF-6	2	Sub.	0.125

			A					B	
Time (min.)			Average					Average	B-A
5	0.048	0.047	0.048	0.069	0.069	0.069	0.070	0.069	0.022
10	0.048	0.047	0.048	0.085	0.083	0.085	0.086	0.085	0.037
15	0.048	0.047	0.047	0.095	0.093	0.095	0.097	0.095	0.047
20	0.050	0.049	0.049	0.105	0.103	0.104	0.107	0.105	0.056
25	0.048	0.047	0.047	0.120	0.116	0.118	0.122	0.119	0.072
30	0.048	0.047	0.047	0.128	0.126	0.128	0.131	0.128	0.081

Data calculated for *N-trans*-feruloyltyramine (PF-6) [**31**] 2 µM of Linewever-Burk plots

	µM		mM
PF-6	2	Sub.	2.0

			A					B	
Time (min.)			Average					Average	B-A
5	0.050	0.049	0.049	0.081	0.077	0.075	0.076	0.077	0.028
10	0.050	0.049	0.050	0.112	0.105	0.102	0.102	0.105	0.055
15	0.051	0.049	0.050	0.145	0.136	0.132	0.133	0.136	0.086
20	0.051	0.049	0.050	0.174	0.163	0.158	0.161	0.164	0.114
25	0.051	0.049	0.050	0.207	0.193	0.187	0.190	0.194	0.144
30	0.051	0.049	0.050	0.238	0.221	0.215	0.219	0.224	0.174

	µM		mM
PF-6	2	Sub.	1.0

			A					B	
Time (min.)			Average					Average	B-A
5	0.047	0.048	0.047		0.072	0.071	0.071	0.071	0.024
10	0.047	0.047	0.047		0.096	0.094	0.093	0.094	0.047
15	0.047	0.048	0.047		0.122	0.119	0.119	0.120	0.073
20	0.046	0.047	0.047		0.144	0.141	0.141	0.142	0.095
25	0.046	0.047	0.047		0.170	0.167	0.167	0.168	0.121
30	0.046	0.047	0.047		0.196	0.192	0.193	0.194	0.147

	µM		mM
PF-6	2	Sub.	0.5

			A					B	
Time (min.)			Average					Average	B-A
5	0.044	0.045	0.045	0.075	0.073	0.073	0.073	0.073	0.028
10	0.045	0.047	0.046	0.099	0.095	0.095	0.095	0.096	0.050
15	0.045	0.046	0.046	0.124	0.120	0.120	0.121	0.121	0.076
20	0.046	0.046	0.046	0.145	0.140	0.142	0.142	0.142	0.096
25	0.045	0.046	0.046	0.168	0.162	0.165	0.165	0.165	0.120
30	0.045	0.046	0.046	0.191	0.184	0.188	0.187	0.188	0.142

	µM		mM
PF-6	2	Sub.	0.25

			A					B	
Time (min.)			Average					Average	B-A
5	0.046	0.047	0.047	0.073	0.068	0.068	0.070	0.070	0.024
10	0.048	0.048	0.048	0.092	0.086	0.085	0.090	0.088	0.040
15	0.050	0.048	0.049	0.114	0.104	0.103	0.109	0.108	0.059
20	0.047	0.048	0.048	0.130	0.120	0.118	0.126	0.124	0.076
25	0.048	0.047	0.047	0.149	0.136	0.135	0.145	0.141	0.094
30	0.047	0.047	0.047	0.167	0.152	0.151	0.165	0.159	0.112

	µM		mM
PF-6	2	Sub.	0.125

			A					B	
Time (min.)			Average					Average	B-A
5	0.046	0.045	0.046	0.071	0.070	0.068	0.071	0.070	0.025
10	0.047	0.046	0.046	0.090	0.087	0.086	0.083	0.086	0.040
15	0.047	0.045	0.046	0.103	0.099	0.097	0.100	0.100	0.054
20	0.047	0.045	0.046	0.116	0.111	0.109	0.113	0.112	0.066
25	0.047	0.045	0.046	0.126	0.120	0.118	0.123	0.122	0.076
30	0.046	0.046	0.046	0.137	0.130	0.128	0.133	0.132	0.086

Data calculated for *N-trans*-feruloyltyramine (PF-6) [**31**] 2 µM of Linewever-Burk plots

	µM		mM
PF-7	2	Sub.	2.0

			A					B	
Time (min.)			Average					Average	B-A
5	0.045	0.046	0.045	0.061	0.056	0.057	0.056	0.058	0.012
10	0.047	0.046	0.046	0.071	0.067	0.066	0.065	0.067	0.021
15	0.047	0.046	0.047	0.079	0.074	0.074	0.074	0.076	0.029
20	0.046	0.046	0.046	0.088	0.082	0.081	0.082	0.083	0.037
25	0.046	0.046	0.046	0.096	0.091	0.088	0.090	0.091	0.045
30	0.046	0.046	0.046	0.103	0.099		0.098	0.100	0.053

	µM		mM
PF-7	2	Sub.	1.0

			A					B	
Time (min.)			Average					Average	B-A
5	0.045	0.045	0.045	0.057	0.056	0.056	0.057	0.056	0.011
10	0.046	0.048	0.047	0.066	0.065	0.066	0.066	0.066	0.019
15	0.045	0.047	0.046	0.074	0.073	0.074	0.075	0.074	0.028
20	0.045	0.048	0.047	0.082	0.082	0.081	0.081	0.082	0.035
25	0.046	0.048	0.047	0.089	0.088	0.089	0.089	0.089	0.042
30	0.046	0.047	0.046	0.095	0.093	0.096	0.094	0.094	0.048

	µM		mM
PF-7	2	Sub.	0.5

			A					B	
Time (min.)			Average					Average	B-A
5	0.043	0.043	0.043	0.055	0.055	0.055	0.056	0.055	0.012
10	0.043	0.044	0.043	0.064	0.064	0.065	0.064	0.064	0.021
15	0.043	0.044	0.043	0.070	0.074	0.073	0.073	0.072	0.029
20	0.043	0.044	0.043	0.076	0.081	0.077		0.078	0.035
25	0.043	0.044	0.044	0.085	0.088	0.087	0.087	0.087	0.043
30	0.043	0.044	0.043	0.091	0.090	0.092		0.091	0.047

	µM		mM
PF-7	2	Sub.	0.25

			A					B	
Time (min.)			Average					Average	B-A
5	0.046	0.042	0.044	0.056	0.056	0.056	0.054	0.056	0.011
10	0.047	0.044	0.046	0.067	0.064	0.064	0.062	0.064	0.018
15	0.042	0.044	0.043	0.071	0.072	0.070	0.070	0.071	0.027
20	0.042	0.043	0.043	0.077	0.076	0.077	0.075	0.076	0.033
25	0.042	0.044	0.043	0.085	0.083	0.082	0.081	0.083	0.040
30	0.042	0.044	0.043	0.089	0.087	0.087	0.087	0.088	0.045

	µM		mM
PF-7	2	Sub.	0.125

			A					B	
Time (min.)			Average					Average	B-A
5	0.043	0.046	0.045	0.056	0.057	0.054	0.054	0.055	0.011
10	0.043	0.048	0.046		0.068	0.061	0.061	0.063	0.017
15	0.044	0.046	0.045	0.067	0.073	0.066	0.067	0.068	0.023
20	0.046	0.047	0.046	0.073	0.075	0.073	0.073	0.073	0.027
25	0.046	0.046	0.046	0.078	0.080	0.079	0.080	0.080	0.034
30	0.045	0.044	0.044		0.086	0.083	0.082	0.083	0.039

Data calculated for *N-trans*-coumaroyltyramine (PF-7) [**32**] 2 µM of Linewever-Burk plots

	µM		mM						
PF-7	2	Sub.	2.0						
			A					B	
Time (min.)			Average					Average	B-A
5	0.047	0.047	0.047	0.063	0.063	0.061	0.063	0.063	0.016
10	0.048	0.049	0.048	0.075	0.076	0.073	0.075	0.075	0.026
15	0.048	0.048	0.048	0.086	0.085		0.086	0.086	0.038
20	0.048	0.048	0.048	0.094	0.094		0.094	0.094	0.046
25	0.047	0.048	0.048	0.103	0.104	0.099	0.100	0.102	0.054
30	0.047	0.047	0.047	0.111	0.111	0.107	0.105	0.108	0.061

	µM		mM						
PF-7	2	Sub.	1.0						
			A					B	
Time (min.)			Average					Average	B-A
5	0.045	0.043	0.044	0.062	0.062	0.062	0.061	0.062	0.018
10	0.045	0.043	0.044	0.073	0.072	0.072	0.071	0.072	0.028
15	0.045	0.043	0.044	0.082	0.081	0.081	0.079	0.081	0.037
20	0.045	0.043	0.044	0.091	0.089	0.089	0.088	0.089	0.045
25	0.045	0.044	0.045	0.099	0.097	0.097	0.096	0.097	0.053
30	0.045	0.043	0.044	0.107	0.105	0.105		0.105	0.061

	µM		mM						
PF-7	2	Sub.	0.5						
			A					B	
Time (min.)			Average					Average	B-A
5	0.043	0.044	0.043	0.060	0.061	0.061	0.061	0.061	0.017
10	0.043	0.044	0.043	0.070	0.071	0.070	0.071	0.070	0.027
15	0.043	0.044	0.043	0.078	0.079	0.078	0.079	0.079	0.035
20	0.043	0.043	0.043	0.087	0.087	0.086	0.084	0.086	0.043
25	0.043	0.044	0.043	0.094	0.095	0.093	0.092	0.093	0.050
30	0.043	0.043	0.043	0.101	0.101	0.099	0.099	0.100	0.057

	µM		mM						
PF-7	2	Sub.	0.25						
			A					B	
Time (min.)			Average					Average	B-A
5	0.043	0.045	0.044	0.061	0.060	0.059	0.060	0.060	0.017
10	0.043	0.044	0.043	0.071	0.069	0.068	0.070	0.069	0.026
15	0.042	0.045	0.043	0.079	0.077	0.075	0.077	0.077	0.033
20	0.042	0.044	0.043	0.085	0.084		0.084	0.084	0.041
25	0.043	0.045	0.044	0.093	0.091		0.091	0.091	0.047
30	0.043	0.044	0.043	0.099	0.097		0.097	0.098	0.054

	µM		mM						
PF-7	2	Sub.	0.125						
			A					B	
Time (min.)			Average					Average	B-A
5	0.044	0.045	0.045	0.058	0.059	0.059	0.058	0.058	0.014
10	0.044	0.044	0.044	0.065	0.067	0.066	0.065	0.066	0.021
15	0.044	0.044	0.044	0.072	0.073	0.072	0.071	0.072	0.028
20	0.044	0.046	0.045	0.078	0.079	0.078		0.078	0.033
25	0.045	0.044	0.045	0.084	0.085	0.084		0.084	0.040
30	0.045	0.044	0.044	0.088	0.090	0.089		0.089	0.045

Data calculated for *N-trans*-coumaroyltyramine (PF-7) [**32**] 2 µM of Linewever-Burk plots

	µM		mM
PF-7	2	Sub.	2.0

			A					B	
Time (min.)			Average					Average	B-A
5	0.050	0.047	0.048	0.058	0.058	0.058	0.060	0.059	0.010
10	0.049	0.048	0.049	0.065	0.066	0.064	0.067	0.066	0.017
15	0.049	0.048	0.048	0.073	0.072	0.071	0.074	0.073	0.024
20	0.049	0.047	0.048	0.083	0.081	0.081	0.084	0.082	0.034
25	0.049	0.048	0.049	0.096	0.094	0.092	0.097	0.095	0.046
30	0.049	0.048	0.049	0.106	0.105		0.097	0.103	0.054

	µM		mM
PF-7	2	Sub.	1.0

			A					B	
Time (min.)			Average					Average	B-A
5	0.045	0.047	0.046	0.058	0.057	0.057	0.057	0.057	0.011
10	0.045	0.046	0.046	0.064	0.064	0.064	0.065	0.064	0.019
15	0.045	0.046	0.045	0.072	0.069	0.071	0.072	0.071	0.026
20	0.045	0.046	0.045	0.080		0.079	0.082	0.080	0.035
25	0.045	0.046	0.045	0.088		0.086	0.091	0.089	0.043
30	0.045	0.046	0.045	0.098		0.098	0.102	0.099	0.054

	µM		mM
PF-7	2	Sub.	0.5

			A					B	
Time (min.)			Average					Average	B-A
5	0.043	0.045	0.044	0.060	0.057	0.055	0.059	0.058	0.014
10	0.044	0.045	0.045	0.063	0.064	0.063	0.067	0.064	0.019
15	0.044	0.046	0.045	0.072		0.069	0.074	0.071	0.027
20	0.044	0.046	0.045	0.082	0.078	0.077	0.084	0.080	0.035
25	0.044	0.045	0.045	0.088	0.085	0.085	0.093	0.088	0.043
30	0.043	0.045	0.044	0.098	0.094		0.101	0.097	0.053

	µM		mM
PF-7	2	Sub.	0.25

			A					B	
Time (min.)			Average					Average	B-A
10	0.043	0.045	0.044	0.063	0.065	0.061	0.065	0.064	0.020
15	0.043	0.045	0.044	0.070	0.071	0.068	0.072	0.070	0.027
20	0.043	0.044	0.044	0.079		0.077	0.079	0.078	0.035
25	0.043	0.045	0.044	0.088	0.088	0.085		0.087	0.043
30	0.043	0.045	0.044	0.095	0.097	0.091	0.091	0.094	0.050

	µM		mM
PF-7	2	Sub.	0.125

			A					B	
Time (min.)			Average					Average	B-A
5	0.045	0.046	0.045	0.057	0.055	0.058	0.055	0.056	0.011
10	0.044	0.046	0.045	0.063	0.062	0.059	0.059	0.061	0.016
15	0.044	0.045	0.045	0.068	0.067	0.064		0.066	0.022
20	0.044	0.045	0.044	0.074	0.071		0.069	0.071	0.027
25	0.044	0.045	0.044	0.082	0.079	0.077	0.076	0.079	0.034
30	0.044	0.044	0.044	0.087	0.084	0.081	0.081	0.083	0.039

Data calculated for *N-trans*-coumaroyltyramine (PF-7) [**32**] 2 µM of Linewever-Burk plots

	µM		mM
PF-7	1	Sub.	2.0

			A					B	
Time (min.)			Average					Average	B-A
5	0.047	0.049	0.048	0.062	0.063	0.063	0.071	0.064	0.016
10	0.048	0.050	0.049	0.076	0.077	0.077	0.086	0.079	0.030
15	0.048	0.051	0.050	0.091	0.091	0.092	0.099	0.093	0.044
20	0.048	0.050	0.049	0.107	0.106	0.107	0.115	0.109	0.059
25	0.048	0.047	0.048	0.122	0.120	0.122		0.121	0.073
30	0.048	0.050	0.049	0.135	0.138	0.137		0.137	0.088

	µM		mM
PF-7	1	Sub.	1.0

			A					B	
Time (min.)			Average					Average	B-A
5	0.046	0.049	0.047	0.061	0.060	0.062	0.060	0.061	0.013
10	0.047	0.050	0.048	0.077	0.074	0.076	0.072	0.075	0.026
15	0.047	0.051	0.049	0.093	0.087	0.088	0.084	0.088	0.039
20	0.047	0.052	0.049	0.103	0.101	0.104	0.095	0.101	0.052
25	0.046	0.050	0.048	0.116	0.115	0.118	0.107	0.114	0.066
30	0.047	0.048	0.047	0.135	0.130	0.131	0.120	0.129	0.082

	µM		mM
PF-7	1	Sub.	0.50

			A					B	
Time (min.)			Average					Average	B-A
5	0.045	0.047	0.046	0.060	0.060	0.060	0.059	0.060	0.014
10	0.044	0.045	0.044	0.073	0.072	0.072	0.071	0.072	0.028
15	0.044	0.045	0.045	0.085	0.084	0.084	0.082	0.084	0.039
20	0.044	0.045	0.044	0.098	0.097	0.095	0.094	0.096	0.052
25	0.047	0.044	0.046	0.110	0.109	0.106	0.106	0.108	0.062
30	0.044	0.052	0.048	0.124	0.122	0.129	0.129	0.126	0.078

	µM		mM
PF-7	1	Sub.	0.25

			A					B	
Time (min.)			Average					Average	B-A
5	0.045	0.044	0.044	0.060	0.058	0.058	0.059	0.059	0.015
10	0.047	0.045	0.046	0.073	0.069	0.069	0.070	0.070	0.024
15	0.045	0.045	0.045	0.086	0.079	0.081	0.081	0.082	0.037
20	0.045	0.046	0.046	0.095	0.089	0.093	0.092	0.092	0.047
25	0.045	0.046	0.046		0.099	0.103	0.103	0.102	0.056
30	0.045	0.046	0.045		0.111	0.115	0.115	0.114	0.068

	µM		mM
PF-7	1	Sub.	0.125

			A					B	
Time (min.)			Average					Average	B-A
5	0.045	0.043	0.044	0.059	0.059	0.063	0.058	0.060	0.016
10	0.046	0.044	0.045	0.069	0.068	0.070	0.068	0.069	0.024
15	0.046	0.044	0.045	0.079	0.078	0.083	0.077	0.079	0.034
20	0.049	0.046	0.048	0.091	0.089	0.093	0.087	0.090	0.042
25	0.046	0.044	0.045	0.097	0.095	0.096	0.093	0.095	0.050
30	0.050	0.043	0.047	0.098	0.104		0.102	0.101	0.055

Data calculated for *N-trans*-coumaroyltyramine (PF-7) [**32**] 1 µM of Linewever-Burk plots

	µM		mM						
PF-7	1	Sub.	2						
			A					B	
Time (min.)			Average					Average	B-A
5	0.046	0.045	0.046	0.064	0.065	0.065	0.063	0.064	0.019
10	0.047	0.047	0.047	0.080	0.082	0.082	0.079	0.081	0.034
15	0.047	0.048	0.047	0.097	0.099	0.100		0.098	0.051
20	0.048	0.047	0.047	0.112	0.114		0.110	0.112	0.065
25	0.049	0.047	0.048	0.124	0.126	0.127		0.126	0.078
30	0.048	0.047	0.048	0.140		0.140	0.134	0.138	0.090

	µM		mM						
PF-7	1	Sub.	1.0						
			A					**B**	
Time (min.)			**Average**					**Average**	**B-A**
5	0.045	0.047	0.046	0.063	0.062	0.063	0.064	0.063	0.017
10	0.046	0.048	0.047	0.078	0.078	0.078	0.079	0.078	0.031
15	0.046	0.049	0.047	0.092	0.092	0.093	0.094	0.093	0.045
20	0.047	0.048	0.048	0.107	0.107	0.107		0.107	0.060
25	0.047	0.048	0.047	0.117	0.117	0.117	0.119	0.117	0.070
30	0.046	0.048	0.047	0.132	0.132	0.131	0.134	0.132	0.085

	µM		mM						
PF-7	1	Sub.	0.50						
			A					**B**	
Time (min.)			**Average**					**Average**	**B-A**
5	0.044	0.044	0.044	0.061	0.061	0.062	0.062	0.061	0.018
10	0.044	0.046	0.045	0.075	0.073	0.075	0.076	0.075	0.030
15	0.044	0.045	0.045	0.089	0.088	0.089	0.091	0.089	0.044
20	0.045	0.045	0.045	0.102		0.102	0.103	0.102	0.058
25	0.045	0.045	0.045	0.115	0.113	0.115		0.115	0.070
30	0.044	0.044	0.044	0.123		0.124	0.126	0.124	0.080

	µM		mM						
PF-7	1	Sub.	0.25						
			A					**B**	
Time (min.)			**Average**					**Average**	**B-A**
5	0.043	0.045	0.044	0.061	0.063	0.064	0.062	0.062	0.018
10	0.044	0.045	0.045	0.074	0.076	0.078	0.076	0.076	0.031
15	0.044	0.045	0.044	0.086	0.088	0.090	0.089	0.088	0.044
20	0.044	0.045	0.044	0.098	0.101	0.102	0.102	0.101	0.056
25	0.044	0.046	0.045	0.105	0.109	0.111	0.109	0.108	0.064
30	0.045	0.046	0.045	0.113	0.118	0.118	0.118	0.116	0.071

	µM		mM						
PF-7	1	Sub.	0.125						
			A					**B**	
Time (min.)			**Average**					**Average**	**B-A**
5	0.045	0.044	0.045	0.061	0.061	0.063	0.063	0.062	0.018
10	0.046	0.045	0.046	0.073	0.075	0.076	0.076	0.075	0.029
15	0.045	0.044	0.045	0.079	0.081	0.084	0.083	0.082	0.037
20	0.045	0.045	0.045		0.087	0.089	0.089	0.089	0.044
25	0.045	0.045	0.045		0.097	0.099	0.101	0.099	0.054
30	0.046	0.045	0.045		0.106	0.109	0.107	0.107	0.062

Data calculated for *N-trans*-coumaroyltyramine (PF-7) [**32**] 1 µM of Linewever-Burk plots

	µM		mM
PF-7	1	Sub.	2.0

			A					B	
Time (min.)			Average					Average	B-A
5	0.048	0.047	0.047	0.060	0.060	0.059	0.061	0.060	0.013
10	0.049	0.049	0.049	0.075	0.072	0.072	0.076	0.074	0.025
15	0.049	0.049	0.049	0.084	0.084		0.086	0.085	0.036
20	0.049	0.050	0.049	0.101	0.101	0.098	0.100	0.100	0.050
25	0.050	0.050	0.050	0.119	0.118	0.117		0.118	0.068
30	0.049	0.048	0.049	0.131	0.131	0.125		0.129	0.080

	µM		mM
PF-7	1	Sub.	1.0

			A					B	
Time (min.)			Average					Average	B-A
5	0.046	0.046	0.046	0.057	0.057	0.058	0.058	0.058	0.012
10	0.047	0.048	0.048	0.068	0.067	0.070	0.068	0.068	0.020
15	0.048	0.048	0.048	0.080		0.081	0.080	0.080	0.032
20	0.047	0.049	0.048	0.093	0.095	0.097	0.094	0.095	0.047
25	0.048	0.050	0.049	0.110	0.107	0.110	0.110	0.109	0.061
30	0.048	0.050	0.049	0.125	0.123	0.126	0.126	0.125	0.076

	µM		mM
PF-7	1	Sub.	0.50

			A					B	
Time (min.)			Average					Average	B-A
5	0.045	0.044	0.044	0.056	0.057	0.056	0.056	0.056	0.012
10	0.047	0.045	0.046	0.067	0.068	0.065	0.066	0.067	0.021
15	0.046	0.045	0.046	0.081	0.083	0.078	0.078	0.080	0.034
20	0.046	0.044	0.045	0.095		0.093	0.092	0.093	0.048
25	0.047	0.044	0.046	0.106	0.109	0.102		0.106	0.060
30	0.047	0.044	0.046	0.121	0.124	0.116	0.113	0.118	0.073

	µM		mM
PF-7	1	Sub.	0.25

			A					B	
Time (min.)			Average					Average	B-A
5	0.045	0.045	0.045	0.057	0.059	0.059	0.062	0.059	0.014
10	0.046	0.047	0.046	0.067	0.069	0.066	0.067	0.067	0.021
15	0.045	0.047	0.046	0.077	0.081	0.077	0.076	0.078	0.032
20	0.045	0.047	0.046	0.086	0.094	0.088	0.088	0.089	0.043
25	0.046	0.047	0.047	0.096	0.104	0.096	0.098	0.099	0.052
30	0.046	0.047	0.046	0.108	0.117	0.110	0.112	0.112	0.065

	µM		mM
PF-7	1	Sub.	0.125

			A					B	
Time (min.)			Average					Average	B-A
5	0.045	0.044	0.045	0.055	0.056	0.059	0.058	0.057	0.012
10	0.045	0.044	0.045	0.064	0.065	0.070	0.069	0.067	0.022
15	0.045	0.044	0.044	0.071	0.075	0.075	0.075	0.074	0.030
20	0.044	0.045	0.044	0.079	0.083	0.083		0.081	0.037
25	0.044	0.044	0.044	0.087	0.092	0.091	0.090	0.090	0.046
30	0.044	0.045	0.044	0.094	0.100	0.099	0.102	0.099	0.054

Data calculated for *N-trans*-coumaroyltyramine (PF-7) [**32**] 1 µM of Linewever-Burk plots

	µM		mM
PF-7	0.5	Sub.	2.0

			A					B	
Time (min.)			Average					Average	B-A
5	0.048	0.051	0.050	0.091	0.083	0.088	0.086	0.087	0.037
10	0.049	0.052	0.050	0.130	0.116	0.125	0.125	0.124	0.073
15	0.049	0.054	0.051	0.166	0.147	0.160	0.159	0.158	0.106
20	0.049	0.053	0.051	0.204	0.176	0.195	0.193	0.192	0.141
25	0.049	0.053	0.051	0.241	0.208	0.233	0.228	0.227	0.176
30	0.050	0.052	0.051	0.278	0.239	0.269	0.265	0.263	0.212

	µM		mM
PF-7	0.5	Sub.	1.0

			A					B	
Time (min.)			Average					Average	B-A
5	0.052	0.047	0.049	0.085	0.079	0.081	0.085	0.083	0.033
10	0.051	0.047	0.049	0.116	0.107	0.111	0.119	0.113	0.064
15	0.050	0.048	0.049	0.146		0.137	0.152	0.145	0.097
20	0.049	0.047	0.048	0.175		0.166	0.185	0.175	0.127
25	0.050	0.046	0.048	0.205		0.195	0.217	0.206	0.158
30	0.049	0.047	0.048	0.245	0.214	0.224		0.227	0.180

	µM		mM
PF-7	0.5	Sub.	0.50

			A					B	
Time (min.)			Average					Average	B-A
5	0.049	0.046	0.048	0.085	0.078	0.080	0.084	0.082	0.034
10	0.048	0.046	0.047	0.115	0.104	0.108	0.115	0.110	0.063
15	0.050	0.047	0.048	0.143	0.126	0.133	0.145	0.137	0.088
20	0.049	0.047	0.048	0.171	0.150	0.158		0.160	0.111
25	0.050	0.046	0.048	0.198	0.174	0.184		0.185	0.137
30	0.051	0.048	0.049	0.217		0.200	0.218	0.212	0.162

	µM		mM
PF-7	0.5	Sub.	0.25

			A					B	
Time (min.)			Average					Average	B-A
5	0.046	0.046	0.046	0.081	0.083	0.077	0.078	0.080	0.034
10	0.048	0.046	0.047	0.107	0.109	0.102	0.101	0.105	0.057
15	0.048	0.046	0.047	0.128	0.132	0.123	0.123	0.127	0.080
20	0.049	0.046	0.047	0.151	0.155	0.144	0.145	0.149	0.101
25	0.050	0.045	0.048	0.171		0.164	0.168	0.168	0.120
30	0.048	0.046	0.047	0.178		0.178	0.185	0.180	0.133

	µM		mM
PF-7	0.5	Sub.	0.125

			A					B	
Time (min.)			Average					Average	B-A
5	0.045	0.044	0.045	0.077	0.074	0.072	0.075	0.074	0.030
10	0.045	0.045	0.045	0.088	0.093	0.089	0.085	0.089	0.044
15	0.045	0.045	0.045	0.105	0.099	0.094	0.103	0.100	0.055
20	0.045	0.044	0.045	0.111	0.113	0.118	0.119	0.115	0.070
25	0.045	0.044	0.045	0.126	0.120	0.124	0.126	0.124	0.079
30	0.045	0.045	0.045	0.136	0.130	0.134	0.137	0.134	0.089

Data calculated for *N-trans*-coumaroyltyramine (PF-7) [**32**] 0.5 µM of Linewever-Burk plots

	µM		mM						
PF-7	0.5	Sub.	2.0						
			A					B	
Time (min.)			Average					Average	B-A
5	0.048	0.047	0.048	0.071	0.073	0.072	0.073	0.072	0.024
10	0.048	0.047	0.047	0.092	0.094	0.094	0.095	0.094	0.046
15	0.048	0.048	0.048		0.131	0.131	0.132	0.132	0.084
20	0.047	0.047	0.047		0.167	0.168	0.171	0.169	0.122
25	0.047	0.047	0.047		0.201	0.202	0.204	0.202	0.155
30	0.047	0.047	0.047		0.238	0.240	0.243	0.240	0.194

	µM		mM						
PF-7	0.5	Sub.	1.0						
			A					B	
Time (min.)			Average					Average	B-A
5	0.046	0.047	0.046	0.070	0.070	0.072	0.069	0.070	0.024
10	0.047	0.046	0.047	0.090	0.090	0.093	0.089	0.090	0.044
15	0.047	0.046	0.046	0.119	0.120	0.125	0.119	0.121	0.074
20	0.047	0.046	0.047		0.151	0.157	0.149	0.152	0.106
25	0.046	0.045	0.046		0.182	0.190	0.181	0.184	0.138
30	0.047	0.045	0.046		0.212	0.222	0.210	0.215	0.169

	µM		mM						
PF-7	0.5	Sub.	0.50						
			A					B	
Time (min.)			Average					Average	B-A
10	0.046	0.046	0.046	0.087	0.095	0.095	0.089	0.091	0.045
15	0.046	0.046	0.046	0.103	0.116	0.116	0.108	0.111	0.065
20	0.046	0.046	0.046	0.132	0.146	0.147	0.138	0.141	0.094
25	0.048	0.046	0.047	0.156	0.172	0.173	0.162	0.166	0.119
30	0.048	0.046	0.047	0.182	0.203	0.204	0.191	0.195	0.148

	µM		mM						
PF-7	0.5	Sub.	0.25						
			A					B	
Time (min.)			Average					Average	B-A
5	0.044	0.044	0.044	0.069	0.069	0.069	0.071	0.070	0.026
10	0.044	0.043	0.044	0.085	0.086	0.087	0.083	0.085	0.042
15	0.044	0.043	0.044	0.102	0.102		0.102	0.102	0.058
20	0.044	0.043	0.044	0.129	0.129		0.125	0.128	0.084
25	0.044	0.044	0.044	0.145	0.145	0.148		0.146	0.102
30	0.044	0.043	0.044	0.171	0.171		0.165	0.169	0.125

	µM		mM						
PF-7	0.5	Sub.	0.125						
			A					B	
Time (min.)			Average					Average	B-A
5	0.045	0.045	0.045	0.066	0.067	0.064	0.065	0.066	0.021
10	0.044	0.044	0.044	0.081	0.083	0.080	0.079	0.081	0.036
15	0.045	0.045	0.045	0.094	0.097	0.091	0.093	0.094	0.049
20	0.044	0.045	0.045	0.107		0.103	0.105	0.105	0.061
25	0.044	0.045	0.045	0.115	0.119		0.113	0.115	0.071
30	0.044	0.044	0.044	0.128	0.133	0.124	0.126	0.128	0.084

Data calculated for *N-trans*-coumaroyltyramine (PF-7) [**32**] 0.5 µM of Linewever-Burk plots

	µM		mM
PF-7	0.5	Sub.	2.0

			A					B	
Time (min.)			Average					Average	B-A
5	0.048	0.047	0.048	0.070	0.069	0.074	0.070	0.071	0.023
10	0.048	0.047	0.047	0.101	0.101	0.103	0.101	0.102	0.054
15	0.048	0.048	0.048	0.132	0.129	0.135	0.129	0.131	0.083
20	0.047	0.047	0.047	0.163	0.164	0.164	0.161	0.163	0.116
25	0.047	0.047	0.047	0.204	0.204	0.207	0.201	0.204	0.157
30	0.047	0.047	0.047	0.238	0.238		0.239	0.238	0.192

	µM		mM
PF-7	0.5	Sub.	1.0

			A					B	
Time (min.)			Average					Average	B-A
5	0.047	0.048	0.048	0.067	0.069	0.067	0.067	0.067	0.020
10	0.046	0.050	0.048	0.084	0.091	0.086	0.086	0.087	0.038
15	0.046	0.051	0.048	0.109	0.117	0.114	0.114	0.114	0.065
20	0.047	0.051	0.049	0.137		0.142	0.145	0.142	0.093
25	0.047	0.049	0.048	0.171		0.174	0.177	0.174	0.126
30	0.047	0.050	0.048		0.215	0.201	0.209	0.209	0.160

	µM		mM
PF-7	0.5	Sub.	0.50

			A					B	
Time (min.)			Average					Average	B-A
5	0.045	0.045	0.045	0.067	0.064	0.063	0.067	0.065	0.020
10	0.045	0.045	0.045	0.083	0.078	0.081	0.084	0.082	0.037
15	0.044	0.046	0.045	0.110	0.104	0.105	0.110	0.107	0.062
20	0.045	0.046	0.045	0.131	0.123	0.126	0.144	0.131	0.086
25	0.045	0.046	0.046	0.161	0.140	0.154	0.162	0.154	0.109
30	0.045	0.045	0.045	0.193	0.176	0.183	0.186	0.184	0.139

	µM		mM
PF-7	0.5	Sub.	0.25

			A					B	
Time (min.)			Average					Average	B-A
5	0.045	0.046	0.045	0.070	0.065	0.064	0.064	0.066	0.021
10	0.045	0.045	0.045	0.078	0.079	0.079	0.079	0.079	0.034
15	0.045	0.045	0.045	0.092	0.093	0.093	0.093	0.092	0.048
20	0.046	0.046	0.046	0.114	0.114	0.113		0.114	0.068
25	0.047	0.047	0.047	0.137	0.139	0.135	0.140	0.138	0.091
30	0.048	0.045	0.046	0.158	0.162	0.161	0.162	0.160	0.114

	µM		mM
PF-7	0.5	Sub.	0.125

			A					B	
Time (min.)			Average					Average	B-A
5	0.045	0.046	0.045	0.063	0.059	0.061	0.063	0.062	0.016
10	0.045	0.046	0.046	0.075	0.071	0.071	0.078	0.074	0.028
15	0.046	0.046	0.046	0.085	0.081	0.082	0.086	0.083	0.037
20	0.046	0.046	0.046	0.096	0.092	0.093	0.097	0.094	0.049
25	0.046	0.046	0.046	0.110	0.105	0.108	0.114	0.109	0.063
30	0.046	0.046	0.046	0.124	0.119	0.121		0.121	0.076

Data calculated for *N-trans*-coumaroyltyramine (PF-7) [**32**] 0.5 µM of Linewever-Burk plots

VITA

Mr. Wongvarit Panidthananon was born on May 12, 1979 in Chonburi, Thailand. He received his bachelor's degree of science in Pharmacy in 2003 from the Faculty of Pharmaceutical Sciences, Huachiew Chalermprakiet University, Samutprakarn, Thailand, and his Master's degree of science in Pharmacy in 2008 from the Faculty of Pharmaceutical Sciences, Chiang Mai University, Thailand.

Publication

Panidthananon, W., Chaowasku T., Sritularak B. and Likhitwitayawuid K. (2018). "A new benzophenone C-glucoside and other constituents of Pseuduvaria fragrans and their α-glucosidase inhibitory activity." Molecules 23(7), 1600; https://doi.org/10.3390/molecules23071600.